The role of thioredoxin-interacting protein in corticosterone-impaired neurite outgrowth

By

Azar Aghazadeh Khasraghi

A Thesis submitted to the Faculty of Graduate Studies of The University of Manitoba
in partial fulfilment of the requirements of the degree of

MASTER OF SCIENCE

Department of Pharmacology and Therapeutics

Rady Faculty of Health Sciences

University of Manitoba

Winnipeg

Canada

Abstract

Background: Glucocorticoid is produced in response to stress. Chronic stress is a high risk factor for developing psychiatric disorders. Many studies have shown that chronic stress and chronic treatment with stress hormone corticosterone cause oxidative damage in the brain. Thioredoxin is an oxidoreductase that reduces protein cysteine oxidation. Thioredoxin also facilitates peroxiredoxin-induced scavenging of H_2O_2, preventing protein cysteine oxidation and carbonylation. Trx can also bind to apoptosis signal-regulating kinase 1 (ASK1) and inhibit apoptosis. Thioredoxin-interacting protein (Txnip) is an endogenous thioredoxin inhibitor, promoting protein cysteine oxidation and carbonylation, and activating ASK1 apoptotic signaling. Previously, our laboratory found that chronic corticosterone treatment had no effect on thioredoxin levels, but increased Txnip levels in cultured mouse neurons, indicating that corticosterone may upregulate Txnip and cause oxidative damage to neurons.

Objective: Establishing if chronic corticosterone treatment increases Txnip, causing oxidative protein damage and impairing neurite outgrowth.

Methods and Results: Using immunoblotting analysis we found that although chronic treatment with corticosterone for 5 days had no effect on Trx, this treatment dose-dependently increased Txnip levels in primary cultured mouse cerebrocortical neurons. Using dimedone conjugation, biotin hydrazide conjugation and biotin-switch methods respectively, we also found that chronic corticosterone treatment increased protein cysteine sulfenylation and protein carbonylation, but had no effect on protein cysteine nitrosylation. We also found that chronic corticosterone had no effects on ASK phosphorylation, cell viability. Cultured neurons were stained by microtubule-associated protein 2 antibody using immunocytochemistry to analyze neurite outgrowth. We found

that chronic corticosterone treatment reduced length and number of neurite branches. To determine the role of Txnip in corticosterone-induced neurite damage, Txnip genes were knocked down by CRISPR/Cas9/Txnip sgRNA technique. We found that knocking down Txnip prevented corticosterone-reduced length and number of neurite branches.

Conclusion: Our findings suggest that chronic corticosterone treatment upregulates Txnip, promoting protein oxidative damage and impairing neurite outgrowth; and also suggest that Txnip may be a potential target for the treatment of psychiatric disorders.

Acknowledgements

First and foremost, I would like to thank my advisor Dr. Jun-Feng Wang for his support, patience and guidance. I am thankful for his invaluable guidance and exceptional support in developing my research skills and writing my thesis. Completion of this journey would not have been possible without his assistance.

I am also extremely grateful to Dr. Tiina Kauppinen and Dr. Sari Hannila for accepting to be my thesis committee members. I really appreciate their efforts in monitoring my progress and offering helpful suggestions and constructive feedback.

I want to express my appreciation to Dr. Hua Tan for teaching me lab skills, helping me in conducting experiments and his constant guidance. I want to extend my thanks to my lab mates Dr. Maria Llanes Cuesta and Sushank Acharya for being supportive and kind, and I also appreciate their help and for sharing their experiences with me during my project. I am also immensely grateful to my friends for being by my side and making the difficulty of being away from my family bearable.

I would like to express my appreciation to all of my family, my parents, my sister, my parents-in-law and sisters-in-law for their unconditional love as well as mental and emotional support.

To my dear husband, Faraz, thank you for your patience and support. Your endless love, kindness and continued encouragement have strengthened and motivated me to keep going.

This research is supported by a project grant from the Canadian Institutes of Health Research (CIHR).

Table of contents

List of figures

List of tables

List of abbreviations

Activator protein-1 (AP-1)
Adrenocorticotropic hormone (ACTH)
Antioxidant response element (ARE)
Apoptosis signal-regulating kinase 1 (ASK1)
Ara-C (Cytosine β-D-arabinofuranoside)
B-cell lymphoma 2 (Bcl-2)
Brain-derived neurotrophic factor (BDNF)
Carbohydrate response element (ChoRE)
carbon dioxide (CO_2).
Catalase (CAT)
Cell Counting Kit-8 (CCK-8)
Central nervous system (CNS)
Chronic unpredictable stress (CUS)
Corticotropin-releasing hormone (CRH)
c-Jun N-terminal kinases (JNK)
Cyclic AMP response element binding protein (CREB)
cAMP response element (CRE)
Cysteine thiol nitrosylation (SNO)
Disulfide bond (S-S)
Dithiothreitol (DTT)
Dulbecco's Modified Eagle Medium (DMEM)
Electron transport chain (ETC)
Endoplasmic reticulum (ER)
Ethylene glycol tetraacetic acid (EGTA)
Ethylenediaminetetraacetic acid (EDTA)
Enhanced chemiluminescence (ECL)
Extracellular signal-regulated kinase 1/2 (ERK1/2)
Flavin adenine dinucleotide (FAD)
Free thiol (SH)
Glucocorticoids (GCs)
Glucocorticoid receptor (GR)
Glucocorticoid response elements (GRE)
Glutathione (GSH)
Glutathione disulfide (GSSG)
Glutathione peroxidase (GPx)
Glutathione reductase (GR)
Hank's Balanced Salt Solution (HBSS)
Horseradish peroxidase-conjugated streptavidin (HRP-streptavidin)
Hydrogen peroxide (H_2O_2)
Hydroxyl radical ($HO^{\bullet}$)
Hypothalamic-pituitary-adrenal (HPA)
Interferon γ (IFN γ)

Interleukin-1/2 (IL-1/2)
Interleukin-1 receptor antagonist (IL-1ra)
L-lactate dehydrogenase (LDH)
Magnesium chloride ($MgCl_2$)
Malonaldehyde (MDA)
Mitogen-activated protein kinases (MAPKs)
Mitogen-activated protein kinase kinase kinase (MAP3K)
N-[6-(biotinamido) hexyl]-3-(2-pyridyldithio) propionamide (biotin–HPDP)
Negative glucocorticoid response elements (nGRE)
Nerve growth factor (NGF)
Neurotrophins-3 (NT-3)
Nicotinamide adenine dinucleotide phosphate (NADPH)
Nicotinamide adenine dinucleotide phosphate oxidases (NOXs)
Nitrate (NO_3^-)
Nitric oxide (NO)
Nitrite (NO_2^-)
Nuclear factor-κB (NF-κB)
Nuclear factor of kappa light polypeptide gene enhancer in B-cells inhibitor alpha (IκB-α)
Nuclear factor erythroid 2-related factor 2 (NRF2)
Oxidized NADPH (NADP+)
Paraventricular hypothalamus (PVN)
Peroxiredoxin (Prx)
Phosphate buffer saline (PBS)
Phosphoinositide 3-kinase (PI3K)
Polyvinylidene fluoride (PVDF)
Protein kinase A (PKA)
Protein kinase C (PKC)
Reactive oxygen species (ROS)
Sodium chloride (NaCl)
Sodium dodecyl sulfate (SDS)
Sulfenic acid (SOH)
Sulfinic acid (SO_2H)
Sulfonic acid (SO_3H)
Superoxide anion radical ($O_2^{\bullet}$)
Superoxide dismutase (SOD)
Thioredoxin (Trx)
Thioredoxin Interacting Protein (Txnip)
Thioredoxin reductase (TrxR)
Trichloroethanol (TCE)
Tumor necrosis factor (TNF)
Tyrosine receptor kinase B (TrKB)
Unfolded protein response (UPR)
Water-soluble tetrazolium salt (WST-8)

1-methoxyphenazine methosulfate (MPMS)
4-hydroxynonenal (HNE)
8-oxo-2'-deoxyguanosine (8-oxo-dG)
8-oxo-7, 8-dihydroguanosine (8-oxoGuo)

1 CHAPTER 1: INTRODUCTION

1.1 Physiology of stress

1.1.1 Activation of hypothalamic-pituitary-adrenal (HPA) axis

Stress response to environmental alterations is a physiological mechanism to maintain biological homeostasis [1]. The brain is the main organ that provides conditions for the body to adapt to stressful factors [2]. The physiological response that leads to restoring homeostasis and adaption to environmental changes is produced through stimulation of hypothalamic-pituitary-adrenal (HPA) axis [1, 2]. Figure 1 displays that in stressful situations, the corticotropin-releasing hormone (CRH) is released by parvocellular neurons, located in the paraventricular hypothalamus (PVN), which triggers anterior pituitary cells to produce adrenocorticotropic hormone (ACTH). ACTH enters into blood circulation and reaches its receptors on the adrenal glands and finally results in the production of glucocorticoids (GCs) [3, 4]. Glucocorticoids show an inhibitory impact on the secretion of CRH and ACTH through a negative feedback mechanism, leading to downregulation of HPA axis activation [5]. Although activity of the HPA axis is crucial for keeping physiological balance after facing an acute stressor, prolonged stimulation of the HPA axis has detrimental health effects [6].

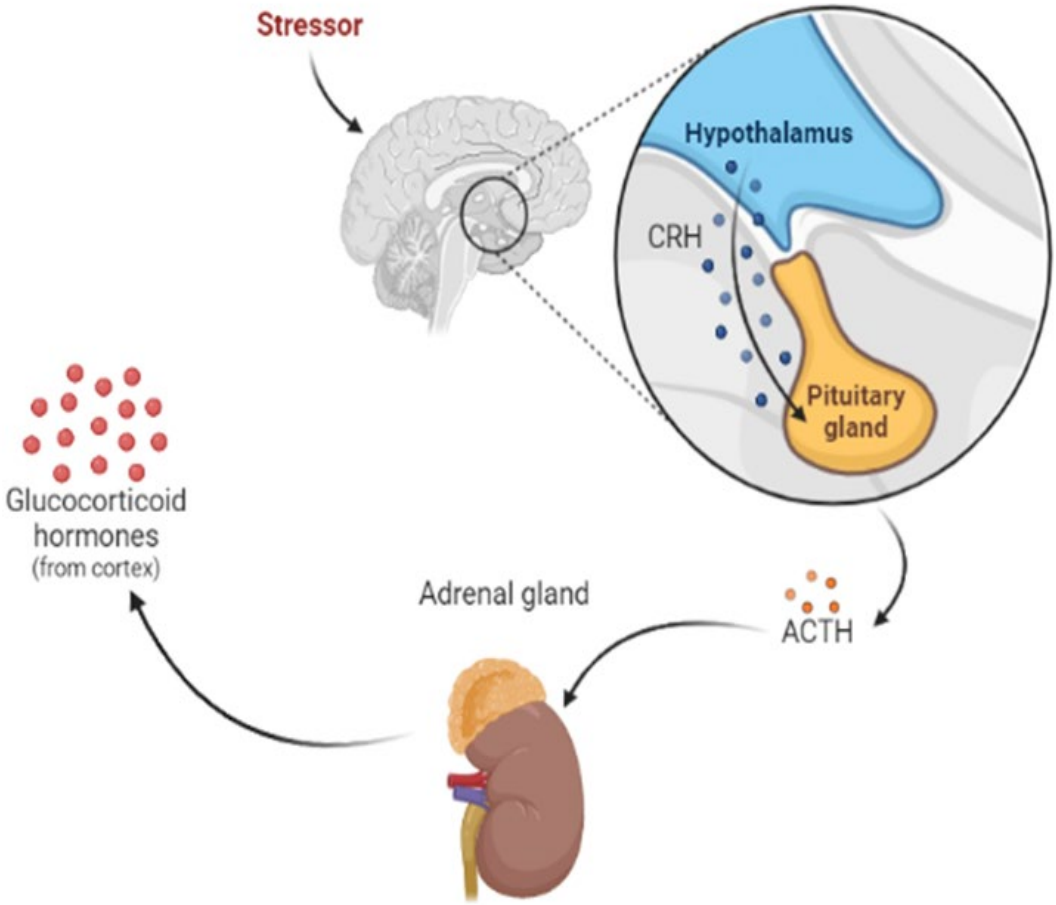

Figure 1. Activation of Hypothalamus-Pituitary-Adrenal (HPA) axis. Exposure to stressful conditions results in release of corticotrophin releasing hormone (CRH) from hypothalamus, which in turn stimulates the anterior pituitary galnds to produce and release adrenocorticotropic hormone (ACTH). ACTH induces secretion of glucocorticoids (GCs) from the adrenal glands. (Created by using www.biorender.com)

HPA axis function is inhibited following increased levels of GCs through negative feedback [7]. Negative feedback not only has the capacity to have a direct influence on PVN and the anterior pituitary gland but also acts indirectly through projection from various brain regions to the PVN [1]. GCs exert negative feedback through suppressing CRH gene transcription and destabilizing CRH mRNA in hypothalamus. Furthermore, in pituitary, GCs reduce the number of CRH receptors, inhibit release of ACTH and transcription of proopiomelanocortin (POMC) [8], which is a prohormone and processed into active peptides including ACTH [7]. Negative feedback effect

of GCs at both levels of hypothalamus and pituitary encompasses fast and delayed mechanisms [8]. Fast feedback involves non-genomic pathways by suppressing release of CRH and ACTH from PVN and pituitary, respectively. Time frame of occurring fast feedback is between milliseconds to minutes. Delayed feedback which lasts hours to days, operates through genomic pathway by inhibiting transcription of CRH in PVN and POMC in pituitary [9, 10]. Glucocorticoids (cortisol in humans and corticosterone in rodents) are synthesized in adrenal cortex. Released ACTH binds to its receptor melanocortin type-2 receptor (MC2R) in adrenal cortex. ACTH binding to MC2R triggers cAMP/protein kinase A (PKA) activation. PKA activity induces phosphorylation and activation of steroidogenic acute regulatory protein (StAR) and hormone-sensitive lipase (HSL) [11]. HSL is responsible for producing cholesterol by hydrolyzing cholesteryl esters [12] and StAR facilitates translocation of cholesterol into mitochondria. In mitochondria, side-chain cleavage cytochrome P450 (P450scc) enzyme catalyzes transformation of cholesterol into pregnenolone. Pregnenolone undergoes series of enzymatic reactions which ultimately result in synthesis and secretion of GCs [11].

GCs maintain body's homeostasis in both basal and stressful situations [13]. GCs are commonly used for their anti-inflammatory and immunosuppressive effects because they inhibit the generation of pro-inflammatory cytokines like TNF-α and IL-1β, and enhance anti-inflammatory cytokines secretion including nuclear factor of kappa light polypeptide gene enhancer in B-cells inhibitor alpha (IκB-α) and Interleukin-1 receptor antagonist (IL-1ra). GCs also show anti-inflammatory effects by preventing nuclear factor-κB (NF-κB) activity [14]. Therefore, GCs protect the body from adverse effects of excessive inflammatory responses [13]. Synthetic GCs such as prednisolone and dexamethasone are prescribed for inflammatory conditions including

obstructive pulmonary disease (COPD), asthma [15], and autoimmune disease like inflammatory bowel disease, rheumatoid arthritis (RA), lupus erythematosus as well as administration as an immunosuppressant in organ transplantation [16].

Excessive production of GC can result in the manifestation of mood disorders; for instance, individuals with an abnormally high level of cortisol who are diagnosed with Cushing syndrome also experience the symptoms of psychiatric diseases such as anxiety, depression, irritability and personality changes [17].

1.1.2 Structure and function of glucocorticoid receptors

GCs exert their pharmacological effects through mineralocorticoid receptor (MR) and glucocorticoid receptor (GR) that function as ligand-activated transcription factors [18]. Liposoluble properties of GCs allow to pass the blood-brain barrier and bind their receptors in the pituitary and hypothalamus to regulate HPA axis function [3]. Since MR has a greater binding affinity for GCs, they are activated even at the lower level of the stress hormones, while GR is stimulated at the high level of GC secretion that occurs in the stress response [17].

GRs are ubiquitously expressed in the brain and peripheral tissues. In central nervous system, GRs are distributed predominantly in the hippocampus, prefrontal cortex, amygdala and PVN of brain [9], and expressed in all cell types including neurons, astrocytes, microglia and oligodendrocytes [19]. Activation of GR participates in the regulation of metabolic and immune processes [9]. GR belongs to the nuclear hormone receptor family. GR consist of 3 main domains including 1) N-terminal transcriptional activation domain, 2) DNA binding domain and 3) C-terminal ligand binding domain. N-terminal transcriptional activation domain engages with components of basal

transcriptional machinery to activate transcription of target genes. There are two zinc finger motifs in DNA binding domain and can bind to glucocorticoid-responsive elements (GREs) in target genes. C-terminal ligand binding domain contains heat shock protein (hsp) binding site. Moreover, DNA binding domain and C-terminal ligand binding domain are also involved in nuclear translocation, receptor dimerization and transactivation [20].

GR exists in cytosol and forms a multiprotein complex that is composed of GR receptor, p23, heat-shock proteins (hsp70 and hsp90) and FK506-binding proteins (FKBP) 51 and 52 (immunophilins) [21]. As shown in Figure 2, upon binding of ligand, GRs undergo conformational alteration, dissociate from heat-shock proteins, then translocate into the nucleus and regulate gene expression. Within nucleus, GR can operate in various mechanisms to regulate gene expression. The first mechanism is transactivation. In this mechanism, two GRs form a dimer (homodimerize). Then DNA binding domains of two GRs bind to the GRE site (consensus sequence: 5′-GGA/TACAnnnTGTTCT-3′) of the targets, which stimulates gene transcription. As an example, gene transcription of enzymes engaged in gluconeogenesis including phosphoenolpyruvate carboxykinase, tyrosine amino transferase and alanine aminotransferase are enhanced upon binding of activated GR to the GRE in promotor regions of these genes. The second mechanism is transrepression. In this mechanism, activated GR binds to the negative GRE (nGRE) (consensus sequence: 5′-CTCC(n)0-2GGAGA-3′) which is different from classic GRE. Binding of GR to nGRE leads to inhibition of gene expression. nGRE exists in promoter region of genes such as POMC (ACTH precursor). Binding of GR to nGRE results in suppressing of POMC gene transcription [20-22]. Third mechanism is transrepression without DNA binding. In this mechanism, targeted genes do not have GRE or other binding sites for GR. Lack of GR binding sites on these genes, results in interaction of activated GR with other transcription factors like NF-

κB and activator protein-1 (AP-1) and preventing expression of genes controlled by these transcription factors [20, 23, 24]. Expression of pro-inflammatory genes like interferon (IFN) γ, interleukin (IL)-1 and IL-2 are mediated by AP-1, and production of cyclooxygenase-2, TNF-α, IL-1β and IL-6 required NF-κB activity [25, 26]. This mechanism mainly mediates GR exerted anti-inflammatory and immunosuppressive effects.

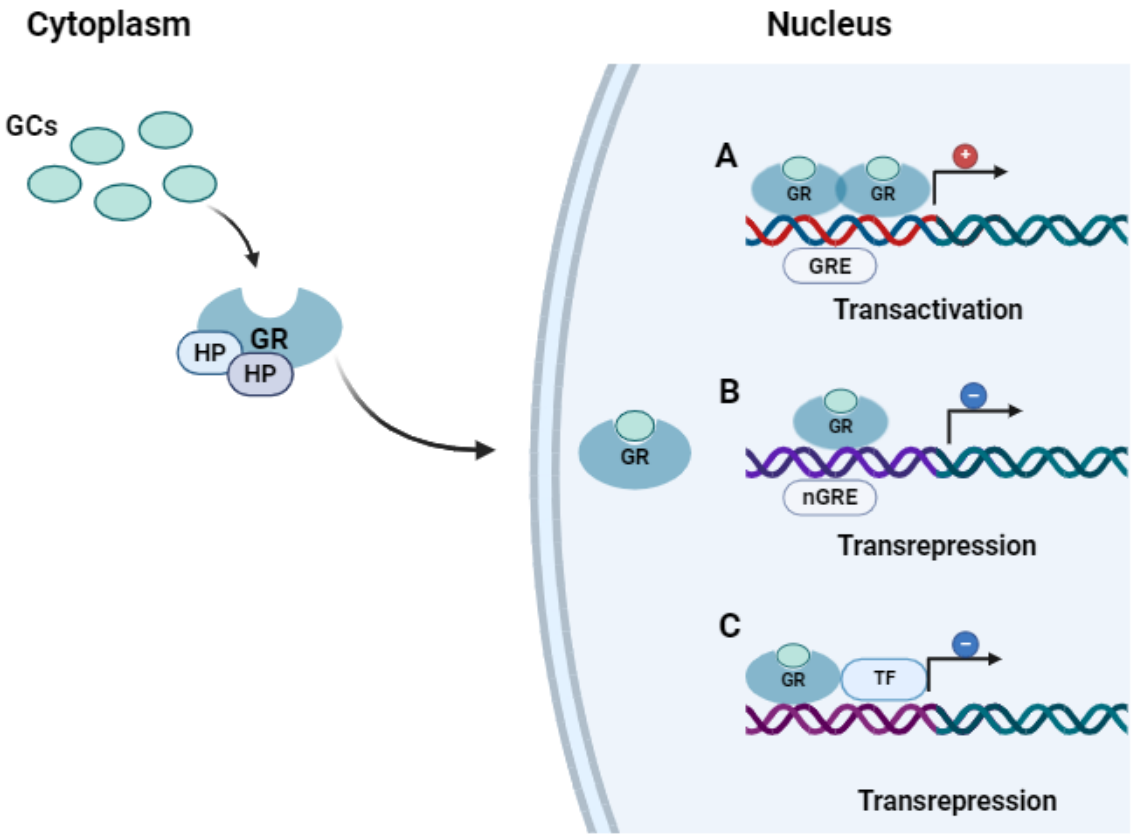

Figure 2. Transrepression and transactivation of glucocorticoid receptor by glucocorticoid. Binding of GCs to GR causes conformational changes and translocation of GR into nucleus. In nucleus GC/GR complex can induce A) transactivation: dimerization of GR and binding to GRE results in gene transcription. B) transrepression: binding of GR to negative GRE (nGRE) inhibits transcription, and C) transrepression: binding of GR to another transcription factor (TF) and binding to a response element different from GRE or nGRE, resulting in inhibition of transcription. GC: Glucocorticoid, GR: Glucocorticoid receptor, HP: Heat shock proteins, GRE: Glucocorticoid response elements, nGRE: negative GRE, TF: Transcription factor, ⊕: Activation, ⊖: Repression. (Created by using www.biorender.com)

1.2 Pathophysiology of chronic corticosterone exposure

1.2.1 Stress, corticosterone and neuroplasticity

1.2.1.1 Chronic stress, chronic CORT treatment and impaired neuroplasticity:

Neuroplasticity is described as the brain's ability to adapt its functioning and structure based on internal or environmental stimuli [27]. Neuronal networks are responsible for cognitive function and social behavior of humans. Facing various experiences and environmental interactions shapes and develops neuronal networks. Morphological changes in the structure of neurons such as dendrites, axons and presynaptic boutons have occurred following exposure to various experiences [28]. Brain development, learning process and environmental interaction induce neuroplasticity [29]. If neuroplasticity results in functional enhancements, it is considered adaptive plasticity, while if the occurrence of neuroplasticity causes functional loss or negative symptoms, it is viewed as maladaptive plasticity [29]. Mechanisms used for adaptation include alteration in neurogenesis, neural network connections and activity of neurochemicals [30].

Chronic stress responses have been associated with remodeling of neuronal architecture and networks in different brain areas including hippocampus, prefrontal cortex and amygdala. Tiny protrusions on the dendrites are called dendritic spines. Dendritic spines facilitate excitatory transmission through increasing synaptic contact surface area [31]. Reduced density of dendritic spine and dendritic loss have occurred through chronic stress exposure [32]. For example, it has been found that exposure to 21 days chronic unpredictable stress (CUS) led to reduction in dendritic spines density and number of mature spines in prefrontal cortex of rats. This stress

exposure also caused a reduction in synaptic protein levels including postsynaptic density protein 95, glutamate receptor 1 and synapsin I protein levels [33]. Exposure to 6 hours/day of restraint stress for 21 days also exhibited a decline in apical dendritic branch number and length and spine density of apical dendrites in rats prefrontal cortex [34]. The results of these studies indicate that chronic stress impairs neuroplasticity.

Research has shown that chronic CORT treatment also impairs neuroplasticity. It has been found that mice receiving CORT 20 mg/kg by oral gavage for 21 days showed a significant decrease in length and branches of dendrites in dentate gyrus of hippocampus [35]. Administration of 40 mg/kg CORT subcutaneously for 3 weeks was found to cause a decline in spines density and length of dendrites in CA1 region and dentate gyrus of hippocampus of rats [36]. Treatment with 40 mg/kg CORT injected subcutaneously for 36 days in mice was also found to reduce hippocampal dendritic branch numbers and spines density [37]. Oral CORT administration for 3 weeks in rats was found to reduce branching in apical dendrites of CA3 hippocampal pyramidal neurons [38]. Oral CORT administration for 28 days in mice reduced total length and dendritic branches of neurons in hippocampus [39]. Also, it has been found that oral administration of CORT for 21 days in mice reduced dendritic spine density in prelimbic cortex, while treatment with RU38486, a GR antagonist, can reverse CORT-induced reduction of dendritic spine density [40]. These results suggest that chronic CORT treatment may target GR receptor and further damage neuroplasticity.

Differentiation of neurons is initiated by formation of neurites which is known as neurite outgrowth. Neurites subsequently develop into axons and dendrites [41]. PC12 is an immortalized cell line derived from rat pheochromocytoma and have an embryonic origin from the neural crest. Exposure of PC12 cells to nerve growth factor (NGF) results in differentiation of PC12 cells to neurons, showing neurite extension and neuronal excitability properties. Therefore, PC12 cells are

phenotypically similar to neuronal cells that are widely used in neurodifferentiation and neurodegeneration studies [42, 43]. Dexamethasone is a synthetic GR agonist. It has been reported that pretreatment of PC12 cells with dexamethasone at 1 μM for one day followed by another 24 hours exposure to 50 ng/ml NGF, reduced length of neurites [44]. Treatment with CORT for 24 hours was also found to decrease length of neurites in PC12 cells [45]. These results suggest that chronic CORT treatment can activate GR receptor and inhibit neurite outgrowth. Taken together, these findings suggest that chronic stress and chronic CORT treatment may reduce dendritic branches and neurite outgrowth, further causing impairment in neuronal plasticity and neural network.

1.2.1.2 Chronic stress, chronic CORT treatment and BDNF signaling:

Neurotrophins play a critical role in facilitating synaptic plasticity within the brain. Neurotrophin family includes brain-derived neurotrophic factor (BDNF), nerve growth factor (NGF); neurotrophins-3 (NT-3) and NT4/5. Neurotrophin receptors are tyrosine kinase receptors and are distributed in locations of nervous system that undergo neuroplasticity [46]. The most well-studied central nervous system (CNS) growth factor is BDNF which is found in several brain regions including thalamus, cortex, hippocampus and amygdala [47]. BDNF is involved in differentiation and survival of neurons and promoting nerve growth during development stage and modulating synaptic transmission and plasticity [47-49]. BDNF expression is mainly regulated by transcription factor cyclic AMP response element binding protein (CREB) activation [49]. CREB participates in expression of genes which are crucial for regulation of survival of neurons, synaptic plasticity and memory [50]. Different protein kinases including protein kinase A (PKA), protein kinase C (PKC) and Ca^{2+}/calmodulin-dependent protein kinase, ERK1/2 kinase and p38 MAPK kinase can

regulate CREB activation by phosphorylating CREB at amino acid serine 133 [51, 52]. Once CREB is phosphorylated by various upstream signaling pathways, it can bind to cAMP response element (CRE) on the promoter of BDNF gene, resulting in expression of BDNF [49]. Bcl-2 is an anti-apoptotic factor and is important for neuronal survival. Transcription factor CREB can also attach to CRE site of Bcl-2 gene and increase Bcl-2 gene expression. It is interesting that NGF and BDNF can also activate CREB and increase Bcl-2 gene expression. Basically, binding of BDNF to TrKB receptor can activate PI3K/Akt signaling, inducing CREB phosphorylation, resulting in Bcl-2 gene expression which promotes neuronal survival [53].

Research has shown that chronic stress and chronic CORT treatment can regulate CREB/BDNF neurotrophic signaling. It has been reported that significant reduction in protein levels of CREB, BDNF and Akt kinase have been found in hippocampus of rats subjected to chronic unpredictable stress for 4 weeks [54]. Administration of chronic unpredictable stressors for 1 and 3 weeks also caused significant decline in mRNA and protein levels of BDNF, CREB and Bcl-2 in rat hippocampus [55]. Exposure to 6 hours/day of chronic restraint stress for 3 weeks induced reduction in the protein levels of BDNF in rats ventral hippocampus and medial prefrontal cerebral cortex [56]. Additionally, it has been reported that BDNF mRNA was reduced in hippocampus and frontal cortex of rats receiving subcutaneous (SC) implant of pellets containing 100 mg of CORT for 21 days [57]. Oral administration of CORT (25 and 100 μg/ml) in drinking water for 14 days led to decline in protein levels of BDNF and phosphorylated CREB in hippocampus of mouse [58]. *In vitro* studies have also shown that 1 day CORT treatment decreased BDNF mRNA and protein levels in cultured mouse hippocampal HT22 cells and SH-SY5Y human neuroblastoma cells [59, 60]. CORT administration has also been found to not only reduce BDNF receptor TrkB protein levels but also reduce phosphorylated CREB, phosphorylated PI3K and phosphorylated

AKT protein levels in cultured mouse neuronal cells [59, 61]. The results of these studies suggest that chronic CORT treatment may induce neuronal growth impairment and cellular damage by inhibiting CREB/BDNF signaling cascade.

1.2.2 Stress, corticosterone and oxidative damage

Oxidative stress happens as a result of excessive generation of reactive oxygen species (ROS) overwhelming endogenous antioxidant defenses [62]. Overproduction of ROS and/or deficiency of antioxidants can cause oxidative stress. Having unpaired electrons makes ROS highly reactive. ROS include superoxide anion radical ($O_2^{\bullet}$), hydrogen peroxide (H_2O_2), and hydroxyl radical ($HO^{\bullet}$), while reactive nitrogen species include nitric oxide (NO), nitrite (NO_2^-) and nitrate (NO_3^-) [62, 63]. Both ROS and reactive nitrogen species are able to cause oxidative damage to biological molecules such as proteins, lipids and nucleic acids. Brain is vulnerable to ROS attack because of its high oxygen intake, rich in unsaturated fatty acids, relatively high levels of redox-active transition metal ions and lower antioxidant defenses [64].

1.2.2.1 ROS production and antioxidants:

There are several pathways that result in ROS production. Mitochondrial electron transport chain (ETC) is the principal origin of ROS generation. In order to generate ATP by oxidative phosphorylation, electrons transfer through mitochondrial membrane protein complexes (I–V) [65, 66]. Due to electron leakage in this process, oxygen molecules can be partially reduced to superoxide mainly through complexes I and III [67-69]. Produced superoxide radicals can be converted into hydrogen peroxide in mitochondrial matrix and intermembrane space by Cu/Zn superoxide dismutase (SOD1) and Mn superoxide dismutase (SOD2), respectively [70]. Reaction

of hydrogen peroxide with transition metal ions like Fe^{2+} and superoxide through Haber-Weiss and Fenton reaction can result in production of extremely reactive hydroxyl radicals [71, 72].

There are several extramitochondrial pathways generating ROS. One of the main extramitochondrial sources leading to ROS generation is nicotinamide adenine dinucleotide phosphate oxidases (NOXs). NOXs are integral membrane protein complexes which consist of different subunits. This enzyme is responsible for transferring electrons to molecular oxygen and subsequently results in formation of superoxide radicals. NOX exists in both phagocytic and non-phagocytic cells and has different isoforms. Among those isoforms, it has been found that NOX2 is expressed in neurons and microglia of hippocampus and cortex of brain. Under normal physiological conditions, ROS is essential for neural stem cell biology, differentiation and mature neuron functioning [73]. Research showed that preventing ROS production through pharmacological and genetic manipulation strategies adversely influences neurogenesis and regeneration of neural stem cells [74]. Overactivation of NOX under pathologic conditions results in excess production of superoxide which overwhelms antioxidant capacity and dysregulates redox balance [73].

Endoplasmic reticulum (ER) stress can also generate ROS. Protein folding procedure occurs within ER with the assistance of chaperones and various enzymes. Exposing hydrophobic amino acid residues in misfolded proteins enhances protein aggregation. Accumulation of aggregated misfolded proteins stimulates ER stress activating unfolded protein response (UPR). Activity of enzymes such as isomerase and ER oxidoreductin 1 during UPR results in generation of ROS [75].

There are various enzymes within peroxisomes including urate oxidase, xanthine oxidase, D-amino acid oxidase, acyl CoA oxidases and D-aspartate oxidase which can generate various types

of ROS depending on the chemical reaction they involve [76]. For example, under normal oxygen levels, xanthine oxidase is responsible for metabolism of xanthine to uric acid via facilitating oxygen molecules reduction to superoxide anions. In addition, under the same condition, oxidation of xanthine oxidase through transferring electrons from flavin adenine dinucleotide to molybdenum (Mo) cofactor results in generation of superoxide anions. However, in low oxygen level condition, oxygen molecules get reduced to hydrogen peroxide via reaction with fully reduced flavin adenine dinucleotide. Another process within peroxisome leading to generation of hydrogen peroxide is the β-oxidation of fatty acids facilitated by acyl-CoA oxidase [77]. Redox reactions are dependent on transition metals such as Cu^{2+}, $Fe^{2/3+}$ and Mn^{2+} to transfer electrons among different molecules. However, transition metals can also be involved in reactions leading to production of more reactive ROS such as hydroxyl radicals [72].

Antioxidant systems keep the balance of ROS levels by neutralizing generated ROS. As shown in Figure 3, enzymatic antioxidants encompass catalase (CAT), superoxide dismutase (SOD), glutathione peroxidase (GPx) and glutathione reductase. SODs reduce superoxide to hydrogen peroxide in the presence of transition metals such as copper, manganese or zinc. Catalase catalyzes reduction of hydrogen peroxide and produces water and oxygen. Also, conversion of hydrogen peroxide to water can be facilitated by the activation of GPx. In this reaction, GPx neutralizes hydrogen peroxide by using glutathione (GSH). GSH provides electron to hydrogen peroxide catalyzed by GPx. Subsequently, GSH is oxidized and converted to disulfide glutathione (GSSG). GSSG is reduced back to GSH catalyzed by glutathione reductase relying on the presence of NADPH [72]. Non-enzymatic antioxidants like glutathione, vitamin C, carotenoids, β-carotene, vitamin E, zinc, selenium and taurine are also critical in restoring ROS balance in the body [78, 79]. Excessive free radicals generation including reactive oxygen and nitrogen species (ROS/RNS)

in neurons subsequently induces neuronal oxidative damage to biological molecules such as DNA, lipids and proteins [62, 80, 81].

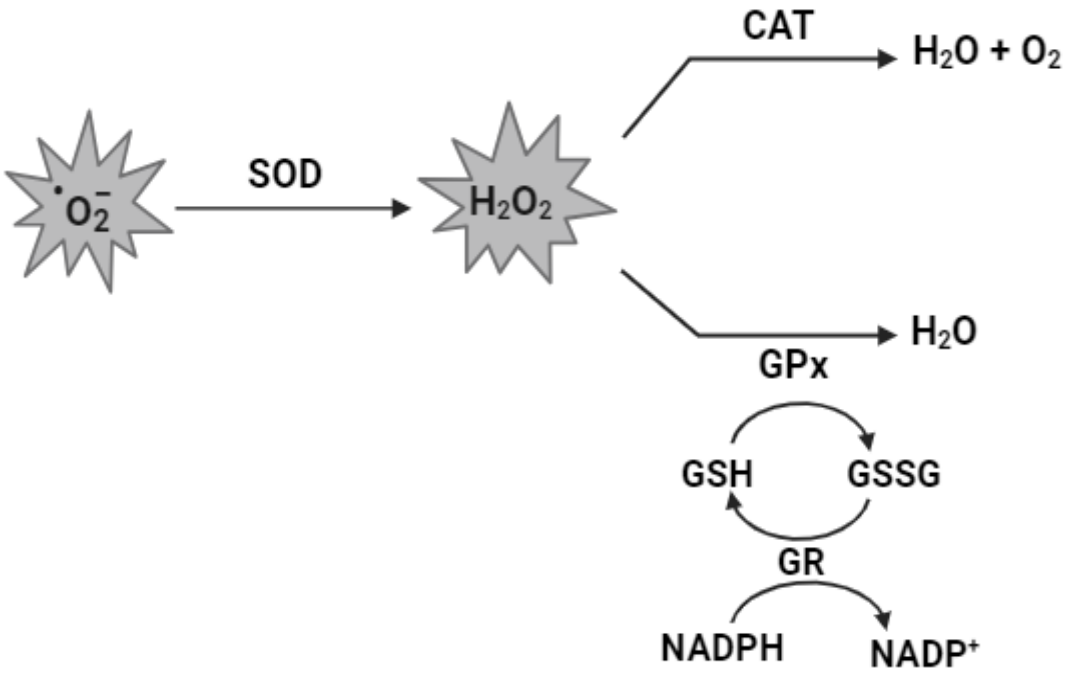

Figure 3. Major cellular antioxidant defense. Superoxide ($^{\cdot}O_2^-$) is converted to hydrogen peroxide (H_2O_2) by superoxide dismutase (SOD). Catalase (CAT) converts H_2O_2 to water (H_2O) and oxygen (O_2). Glutathione peroxidase (GPx) can also convert H_2O_2 to H_2O by using glutathione (GSH). Subsequently, GSH is oxidized and converted to disulfide glutathione (GSSG). GSSG is reduced back to GSH by glutathione reductase (GR) in the presence of nicotinamide adenine dinucleotide phosphate (NADPH).
$^{\cdot}O_2^-$: Superoxide, H_2O_2: Hydrogen peroxide, H_2O: Water, O_2: Oxygen molecule, SOD: Superoxide dismutase, CAT: Catalase, GPx: Glutathione peroxidase, GSH: Glutathione, GSSG: Glutathione disulfide, GR: Glutathione reductase, NADPH: Nicotinamide adenine dinucleotide phosphate, $NADP^+$: Oxidized NADPH. (Created by using www.biorender.com)

DNA oxidation is oxidative damage of deoxyribonucleic acid, which is caused by hydroxyl radicals through attacking deoxyribose, pyrimidine or purine bases of DNA structure [79]. Various lesions can occur in the DNA structure, such as abasic sites (AP sites, located throughout the DNA which have no pyrimidine or purine bases), DNA strand breaks, bases or sugar ring oxidation. The most frequently studied DNA oxidation product is 8-oxo-2'-deoxyguanosine (8-oxo-dG). 8-oxo-

7, 8-dihydroguanosine (8-oxoGuo) is also indicating RNA oxidative damage [82, 83]. Lipid peroxidation is ROS-induced oxidation of polyunsaturated fatty acids. Since neuronal cell membrane is enriched with polyunsaturated fatty acids, they are sensitive to lipid peroxidation [84]. Lipid peroxidation of cell membrane leads to production of 4-hydroxynonenal (HNE) and malonaldehyde (MDA) [79]. Damages to neuronal cell membranes by lipid peroxidation result in decreasing membrane fluidity, altering membrane permeability, reducing membrane-bound enzyme activity and inducing membrane receptor malfunction [85]. Protein oxidation is ROS-induced covalent modification of protein amino acids. Protein oxidation can occur in protein backbone and cause breakage in peptide bonds. Side chain amino acids of protein can also undergo oxidation that results in generation of various protein oxidative modifications such as protein sulfenylation, disulfidation, sulfinylation, sulfonylation, carbonylation, nitrosylation and others. [86]. Also, products of lipid peroxidation (such as MDA and HNE) can lead to protein oxidation which results in generation of carbonylated proteins by introducing carbonyl group to amino acids including proline, arginine and lysine [87].

1.2.2.2 Chronic stress, chronic CORT treatment and ROS production:

There are a number of studies that have explored the effect of chronic exposure to stress and long-term treatment with CORT on ROS production in brain tissues and neuronal cells. Study on mice exposed to 2 hours of chronic restraint stress daily for 8 weeks showed significant rise in the level of ROS in their hippocampus and frontal cortex [88]. It has also been observed that restraint stress for 2 hours per day over 2 weeks caused significant elevation in ROS and MDA levels in the hippocampus of mice [89]. Moreover, another study reported that rats exposed to restraint stress for 6 hours not only showed increased CORT concentration in serum but also showed increased

NADPH oxidase activity and MDA levels in cerebral cortex [90]. These results indicate that chronic stress may release CORT, resulting in ROS production and lipid oxidative damage. Moreover, it has been found that administration of restraint stress for 2 weeks upregulated protein levels of NADPH oxidase subunits, p67phox and p47phox, in mouse hippocampus [89]. Excessive ROS levels have also been observed in hippocampus and frontal cortex of mice subjected to chronic unpredictable mild stress for 4 weeks [91]. Research showed that subjecting to 6 hours/day of chronic restraint stress for 3 weeks significantly increased nitrite and nitrate (NO metabolites) in the brain of rats. Same exposure time to restraint stress in rats caused reduction in the brain mitochondrial complexes activity specifically complex I-II and II-III [92]. Moreover, it has been demonstrated that activity of mitochondrial complexes including complex I, III and IV declined significantly in cerebellum and cerebral cortex of rats exposed to chronic mild stress for 40 days [93]. These findings indicate that chronic stress may impair mitochondrial function, causing increase in ROS production.

Similar findings have been also found with chronic CORT treatment. It has been reported that CORT administration at 1μM for 14 days increased ROS levels in cultured rat hippocampal and cortical neurons. Administering CORT for 24 hours also elevated the levels of ROS in HT22 cells and SH-SY5Y cells [89]. Moreover, SC injection of 0.5 mg/kg CORT for 2 weeks in rats elevated serum levels of superoxide [94]. Higher levels of ROS have also been observed in the hippocampus of female mice after 21 days treatment with daily oral administration of CORT at 20 mg/kg [95]. Treatment of hippocampal slice cultures with GR agonist dexamethasone at 50 μM showed higher levels of ROS [96]. Treatment with 50 μM dexamethasone for 24 hours was also found to decrease expression of genes associated with electron transport chain in murine neural stem cells [97]. Also, expression of NADPH oxidase subunits (p67phox and p47phox) increased significantly in SH-

SY5Y cells following 24 hours treatment with CORT [89]. These results indicate that chronic or excessive CORT treatment may activate GR receptor, further causing mitochondrial dysfunction and NADPH oxidase activation, resulting in ROS production.

1.2.2.3 Chronic stress, chronic CORT treatment and antioxidants:

Numerous studies have observed antioxidant system insufficiency related to chronic stress exposure and chronic CORT treatment in animal models and cultured neuronal cells. Exposure to chronic unpredictable stress for 4 weeks negatively affected antioxidant capacity including a decline in glutathione peroxidase and catalase activity in the brain of rats [98]. It has also been reported that 6 weeks of chronic unpredictable stress led to significant decrease in the levels of reduced glutathione and enzymatic activity of catalase and SOD in mouse brain [99]. Significant decline in reduced glutathione contents and total antioxidant capacity as well as enzymatic activity of SOD and glutathione peroxidase was observed in hippocampus and frontal cortex of mice subjected to 2.5 hours/day of restraint stress for 5 days [100]. Moreover, significant reduction of antioxidant enzymes including superoxide dismutase and glutathione peroxidase have been observed in rats exposed to SC administration of 10 mg/kg CORT for 3 days [101]. Treatment with daily intraperitoneal (i.p) administration of 20 mg/kg CORT for 3 weeks led to decline in the levels of reduced glutathione in striatum, frontal cortex and hippocampus of mice [102, 103]. Also, significant reduction in catalase was reported in hypothalamus of rats subjected to one week of treatment with i.p injection of dexamethasone [104]. *In vitro* studies have also shown that CORT treatment can downregulate antioxidant defense. It has been found that incubation of PC12 cells with CORT at 200 μM for 2 days caused decline in glutathione peroxidase and SOD enzyme activities and in reduced glutathione levels [105]. Treatment with CORT at 300 μM for one day

was also found to decrease catalase, SOD and glutathione peroxidase enzyme activities and reduced glutathione levels in cultured Neuro-2a cells [106], while one day treatment with 125 μM CORT decreased SOD protein level in cultured PC12 cells [87]. These findings recommend that chronic stress, chronic CORT treatment or excessive CORT treatment leads to deficiency of antioxidant defense and further increase in ROS, which may result in progression of oxidative damage to biomolecules such as DNA, proteins and lipids.

1.2.2.4 Chronic stress, chronic CORT treatment and oxidative damage:

ROS overproduction along with antioxidant deficiency can result in oxidative damage. Malondialdehyde (MDA) is generated due to lipid peroxidation. Research has reported elevation in MDA levels in rat frontal cortex and hippocampus following exposure to chronic unpredictable stress [63, 98]. Additionally, research has also shown exposure to chronic restraint stress results in elevation of MDA levels in frontal cortex and hippocampus of rats [100, 107, 108]. These observations indicate that chronic stress can cause lipid peroxidation in rat brain. 8-hydroxy-2-deoxyguanosine (8-OHdG) is marker of DNA oxidation, while the marker of protein oxidation is protein carbonyl. It has been reported that 4 hours/day restraint stress for 3 weeks increased 8-OHdG levels and protein carbonyl levels in brain of rats [107, 108], suggesting that chronic stress also causes DNA oxidation and protein oxidation in rat brain.

Similar findings have been observed with CORT treatment. It has been found that daily oral administration of 10, 20 and 40 mg/kg CORT for 3 weeks showed significant elevation in MDA and protein carbonyl levels in the brain of rats [107]. Also, carbonyl protein and MDA levels increased in brain of mice treated with 20 mg/kg CORT daily for 3 weeks [109]. Daily SC administration of 20 mg/kg CORT for 3 weeks also caused significant elevation in MDA levels in

mouse striatum, frontal cortex and hippocampus [102, 103]. Furthermore, treatment of cultured rat pheochromocytoma PC12 cells with CORT at 125 μM for 1 day showed increase in protein carbonyl levels [87]. These findings indicate that chronic stress, long-term treatment with CORT and excessive CORT treatment can lead to oxidative damage to lipid and protein which can ultimately cause cellular dysfunction.

1.3 Thioredoxin

1.3.1 Trx structure and function

Trx is a low molecular weight protein which was first discovered in E. coli. Later, it is identified in both prokaryotes and eukaryotes. Mammalian Trx has two primary isoforms, Trx1 and Trx2. Trx1 has a molecular weight of 12 kDa and is found in cytosol, while Trx2 is present in mitochondria with a molecular weight of 15.5 kDa [110-112]. Trx has a conserved dithiol active site (-Trp-Cys-Gly-Pro-Cys-Lys-) in which cysteine residues provide antioxidant defense [110]. Five cysteine residues have been found in cytosolic Trx structure. There is an active disulfide bond between Cys32 and Cys35. The other cysteine residues are present in positions 62, 69, and 73 [113]. Proteomic study indicated a non-active disulfide bond existing in cytosolic Trx structure between other cysteines [114]. However, these cysteine residues can be subjected to post-translational modifications such as nitrosylation and glutathionylation to regulate intracellular signaling pathways [115, 116]. Trx is a disulfide thiol oxidoreductase and reduces ROS-induced protein cysteine oxidation. As shown in Figure 4, once oxidized cysteine is reduced by Trx, Trx cysteine thiols are oxidized. In order to regenerate reduced form of Trx, Thioredoxin reductase (TrxR) and NADPH, components of redox system, transfer electrons from NADPH to oxidized Trx. Therefore, Trx redox system activity maintains intracellular redox homeostasis [110, 111,

117-121]. Trx can not only reduce cysteine oxidative modification but also facilitate peroxiredoxin-induced ROS scavenging and block apoptosis signal-regulating kinase 1 (ASK1) apoptotic signaling.

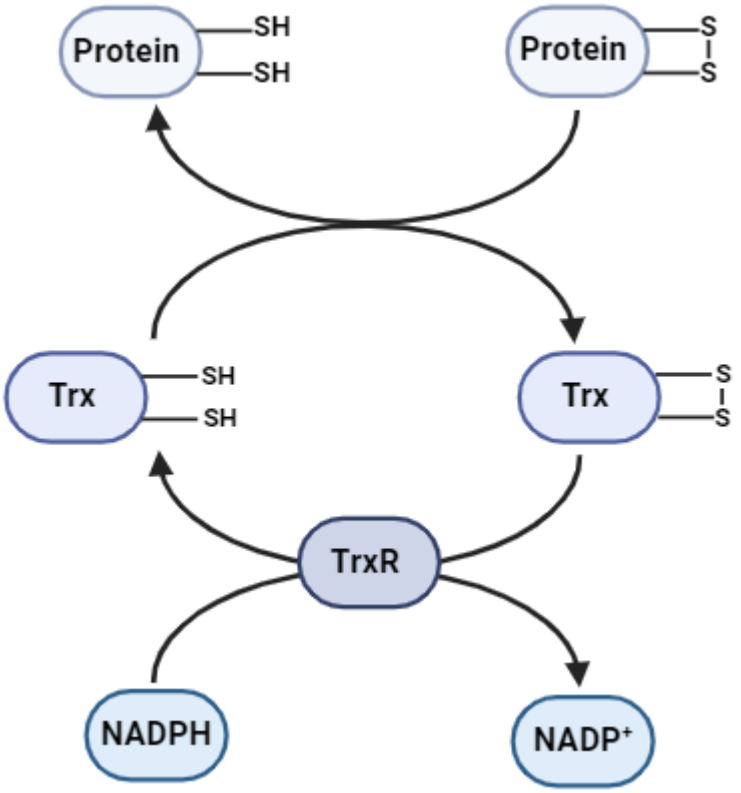

Figure 4. Reduction of oxidized protein by thioredoxin. Trx reduces cysteine thiol protein oxidation and gets oxidized. TrxR reduces oxidized Trx by transferring electrons from NADPH to oxidized Trx.
SH: Free thiol, S-S: Disulfide bond, Trx: Thioredoxin, TrxR: Thioredoxin reductase, NADPH: Nicotinamide adenine dinucleotide phosphate, NADP+: Oxidized NADPH. (Created by using www.biorender.com)

1.3.1.1 Trx reduces cysteine oxidative modification:

Cysteine residue redox-sensitivity and nucleophilicity enable it to be involved in redox defense, signaling, structural stability, enzymatic catalysis and metal binding. Cysteine has a thiol group (-SH) which makes it highly vulnerable to oxidation by H_2O_2 or NO radical [122, 123]. Exposure to

H_2O_2 or NO radicals induces diverse modifications to proteins cysteine thiol such as formation of nitrosothiols (Pr-SNO), sulfenic (Pr-SOH), sulfinic (Pr-SO_2H), and sulfonic (Pr-SO_3H) acids, and disulfide bonds (Pr-S-S-Pr). These modifications can affect signaling pathways [122]. As shown in Figure 5, in the presence of H_2O_2, cysteine thiol is oxidized and forms sulfenic acid. Sulfenylation is an intermediate oxidation state. Reaction of sulfenic acid with another cysteine thiol leads to creation of disulfidation. Under excessive amounts of H_2O_2, sulfenic acid can be over-oxidized, resulting in formation of sulfinic and sulfonic acids. Nitrosothiol can be produced by the attack of NO radical to cystine thiol [124]. Among protein cysteine oxidative modification, nitrosylation, sulfenylation and disulfidation are reversible while higher state oxidation such as sulfinylation and sulfonylation are irreversible. Reversible protein oxidation plays a crucial role not only in cell signaling but also in maintaining redox balance. Both reversible and irreversible protein oxidation can lead to redox imbalance and subsequently cause oxidative damage to cells [123]. Research has revealed that nitrosylation of cysteine residues also impacts protein functions [125]. It has been reported that nitrosylation of apolipoprotein E (ApoE) isoforms (ApoE2 and ApoE3) causes conformational alteration in the structure of ApoE isoforms. These changes reduce binding affinity to low-density lipoprotein (LDL) receptors which is an essential step in lipid metabolism process [126]. Our laboratory previously has identified that vesicular neurotransmitter transporters including vesicular acetylcholine transporter, vesicular glutamate transporter and vesicular monoamine transporter, are susceptible to nitrosylation. This modification can reduce their ability to take up acetylcholine, glutamate and dopamine, respectively [125]. Cysteine oxidative modifications including nitrosylation and sulfenylation can be converted to reduced forms by Trx through disulfide exchange mechanism (Figure 6) [127, 128].

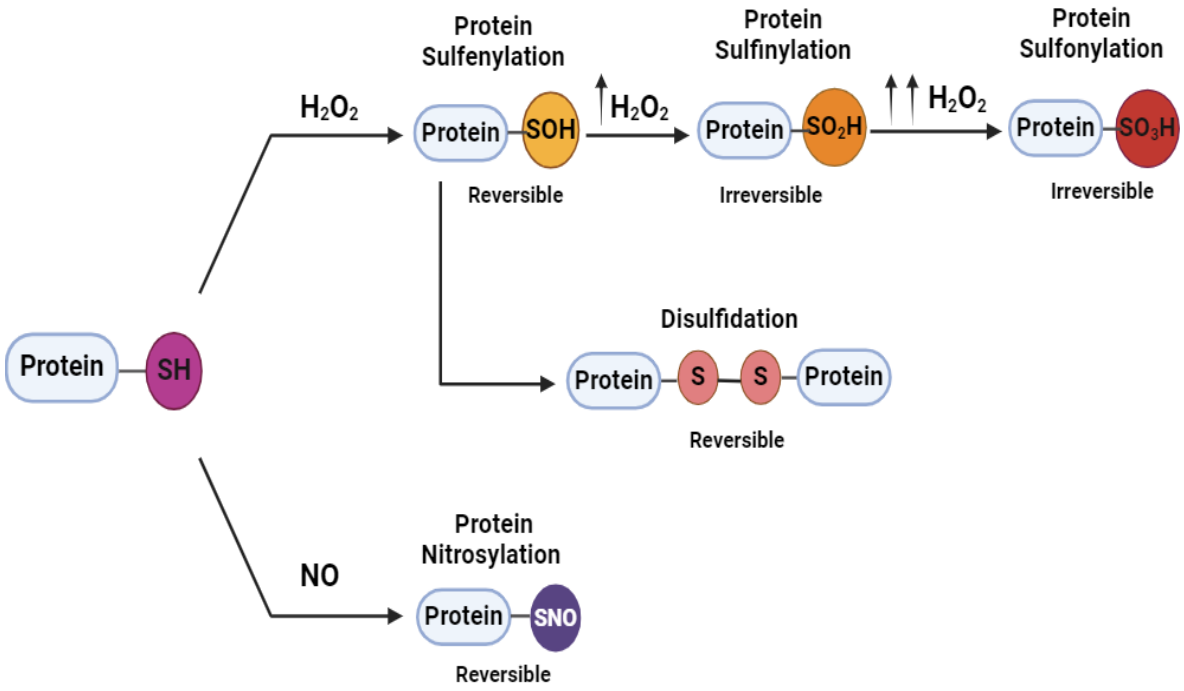

Figure 5. Protein cysteine thiol oxidation with H_2O_2 and NO. Exposure of protein cysteine thiols to H_2O_2 results in formation of sulfenic (Pr-SOH) acid, which can be further oxidized to sulfinic acid (Pr-SO_2H) and sulfonic acid (Pr-SO_3H). Reaction of sulfenic acid with another cysteine thiol leads to disulfidation (Pr-S-S-Pr). Exposure to NO radicals induces formation of nitrosothiols (Pr-SNO).
H_2O_2: Hydrogen peroxide, NO: Nitric oxide, SH: Free thiol, S-S: Disulfide bond, SOH: Sulfenic acid, SO_2H: Sulfinic acid, SO_3H: Sulfonic acid, SNO: Cysteine thiol nitrosylation. (Created by using www.biorender.com)

1.3.1.2 Trx reduces oxidized peroxiredoxin:

Peroxiredoxin (Prx) belongs to a thiol-dependent peroxidase enzymes family and has the ability to detoxify hydrogen peroxide and lipid hydroperoxide [129]. Prx contains two cysteine residues Cys47 (peroxidatic cysteine) and Cys170 (resolving cysteine) [130]. Prx can reduce H_2O_2 to water. First, peroxidatic cysteine donates one electron to H_2O_2, and then it is oxidized to sulfenic acid (Prx-Cys-SOH). Second, resolving cysteine reacts with the sulfenylated cysteine of Prx (Prx-Cys-S_2), forms a disulfide bond, and donates another electron to H_2O_2, which converts H_2O_2 to water. Oxidized Prx (disulfide form) is regenerated to its reduced state by Trx and obtains its capacity as

a peroxides scavenger [129-133]. Therefore, Trx can facilitate Prx-mediated scavenging of H_2O_2 and other peroxides. Because H_2O_2 can react with superoxide and transition metal ions such as Fe^{2+}, and generate hydroxyl radicals that can further cause protein carbonylation [72], Trx can also prevent production of protein carbonylation (Figure 6).

1.3.1.3 Trx inhibits apoptosis signal-regulating kinase-1 (ASK1) activity:

ASK1 is a member of the mitogen-activated protein kinase kinase kinase (MAP3K) family [134]. Various triggers can result in activation of ASK1 including oxidative stress, H_2O_2, endoplasmic reticulum stress and proinflammatory cytokine tumor necrosis factor (TNF) [134-138]. Activation of ASK1 results in initiation of downstream MAPK signaling cascades through phosphorylation of c-Jun N-terminal kinases (JNK) and p38 kinase, resulting in cell apoptosis [137, 139]. ASK1 is residing in both cytosol and mitochondria [140]. Trx could bind to ASK1 and suppress ASK1 kinase activity [137] (Figure 6). Trx reduced state is essential for inhibiting ASK1 activity [141]. Oxidative stress condition stimulates conversion of reduced Trx to oxidized Trx, resulting in dissociation of ASK1 from Trx, inducing ASK1 autophosphorylation at Thr845 and ASK1 activation [142]. Activated ASK1 forms a complex by recruiting TNF-α receptor-associated factor 2 (TRAF2 and TRAF6) which enhances ASK1 phosphorylation. Activated ASK1 phosphorylates JNK/p38 and initiates MAPK signaling cascades [143, 144]. Activation of these pathways leads to secretion of inflammatory cytokines, differentiation, and apoptosis [145].

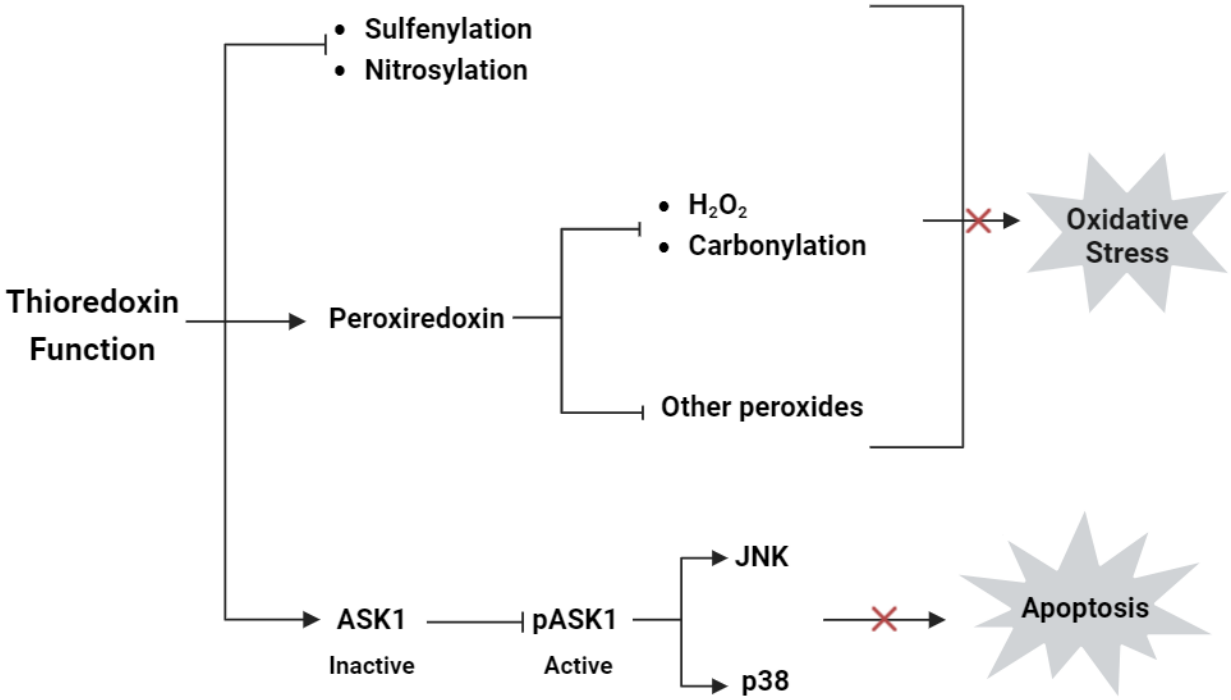

Figure 6. Thioredoxin function. Trx can convert cysteine oxidative modifications including nitrosylation and sulfenylation to their reduced forms. Trx can also facilitate Prx-mediated scavenging of H_2O_2 and other peroxides by reducing oxidized Prx and subsequently preventing H_2O_2 accumulation. H_2O_2 accumulation could lead to protein carbonylation. Finally, binding of Trx to ASK1 inhibits autophosphorylation and activation of ASK1 and subsequently inhibits phosphorylation of JNK/p38, thus preventing ASK1-induced apoptosis.
H_2O_2: Hydrogen peroxide, ASK1: Apoptosis signal-regulating kinase 1, pASK1: phosphorylated ASK1, JNK: c-Jun N-terminal kinases, →: Promotion, ┤: Blocking, × : Inhibition. (Created by using www.biorender.com)

1.3.2 Trx regulation

1.3.2.1 Maintaining Trx at reduced state by Trx reductase (TrxR):

TrxR keeps Trx in reduced form. TrxR is a flavoprotein with homodimeric structure and belongs to pyridine nucleotide-disulfide oxidoreductase family [146, 147]. Molecular weight of each monomer in mammalian TrxR is 55 kDa. Two major isoforms have been identified in mammalians

for TrxR: TrxR1 in cytosol and TrxR2 in mitochondria [148, 149]. Each monomer of TrxR has a flavin adenine dinucleotide (FAD) domain, NADPH binding domain, interface domain and active selenocysteine site at the C-terminal [150, 151]. In order to catalyze reduction of oxidized Trx, first, FAD receives electrons from NADPH and transfers electrons to the redox active disulfide site at the N-terminal. Then electrons move to selenothiol at the C-terminal of another subunit, and from there to oxidized Trx. Finally, reduced Trx can restore oxidized proteins [147, 150].

1.3.2.2 Inhibiting Trx function by thioredoxin interacting protein (Txnip):

Txnip is an endogenous inhibitor for Trx. Txnip gene was initially recognized in HL-60 cells. Due to its responsiveness to 1,25-dihydroxy vitamin-D3, it was first called vitamin-D3 upregulated protein 1 (VDUP-1) [112]. Binding of Txnip to Trx was discovered for the first time by using yeast two-hybrid screening and found to inhibit activity of Trx. Therefore, it is also called thioredoxin binding protein-2 (TBP-2) [152]. Txnip belongs to the family of proteins named α-arrestin with a molecular weight of 46 kDa and consists of 391 amino acids. The gene encoding human Txnip is located on chromosome 1q21.1 with approximately 4174 bp in length and contains 8 exons. Txnip contains two arrestin-like domains: N-terminal containing 10-152 amino acids and C-terminal containing 175-298 amino acids. Two cysteine residues exist in the Txnip structure at positions Cys63 and Cys247 [152]. The existence of two PPXY motifs in the tail at C-terminal domain of Txnip facilitates proteasomal degradation of Txnip through binding of PPXY motif to E3 ubiquitin ligase ITCH [153]. It has been reported that mutation in PPXY motif inhibited Txnip degradation, suggesting critical role of PPXY motif for binding of Txnip to E3 ubiquitin ligase ITCH and facilitating degradation of Txnip [154]. The presence of intramolecular disulfide bonds between Cys63 and Cys247 in Txnip structure provides effective interaction with Trx [152]. Forming of

disulfide bond between Cys247 residue of Txnip and Cys32 residue of Trx leads to inhibition of Trx reducing activity by Txnip. Under normal conditions, Txnip resides in the nucleus. Elevated intracellular ROS upregulates Txnip expression. Subsequently, Txnip moves from nucleus into cytosol and binds to Trx1. Txnip can also translocate into mitochondria to bind to Trx2. Binding of Txnip to active cysteine of Trx (Cys32) prevents reducing activity of Trx [147, 151].

1.3.3 Trx and neuroplasticity

Studies have shown that Trx might be involved in neuronal outgrowth. NGF is a nerve growth factor. It has been reported in PC12 cells that treatment with NGF elevated Trx mRNA and protein levels and that NGF-induced neurite outgrowth was decreased in cells transfected with Trx antisense plasmid in comparison to wild-type. This finding indicates that Trx may mediate NGF-induced neurite growth [155]. It has also been found that, incubation of PC12 cells with recombinant Trx at 1μM for 48 hours induced neurite outgrowth, which is comparable to neurite outgrowth induced by treatment with NGF at 100 ng/ml for 48 hours [156]. Previously, our laboratory has found that knocking out Trx gene or treatment with Trx inhibitor, PX12, decreased the length and the number of neurites in primary cultured mouse cerebral cortical neurons [157]. These results indicate that Trx may produce neurotrophic effect.

Studies have shown Trx can regulate CREB and BDNF neurotrophic signaling. Research has shown that phosphorylated CREB levels were elevated in the hippocampus of Trx transgenic mice compared to wild-type mice [158]. Research has also found that overexpression of Trx not only elevated CRE-driven gene expression but also increased binding between CREB and CRE in human embryonic kidney (HEK) 293 cells [159]. Moreover, previous study in our laboratory showed that treatment of primary cultured mouse cerebral cortical neurons with Trx inhibitor,

PX12, caused significant decrease in phosphorylated CREB levels in primary cultured mouse cerebral cortical neurons [157]. This result implies that Trx can induce CREB activation. Tubby mice can develop photoreceptor degeneration after birth. Trx levels were found lower in these mice. Crossbreeding Tubby mice (Tubby mouse is an animal model of human Usher Syndrome Type 1 in which photoreceptor cells are degenerated progressively) with transgenic Trx mice resulted in generation of Tubby mice with high expression of Trx. Research findings have shown that mRNA and protein levels of BDNF were elevated in retina of transgenic Trx Tubby mice when compared with regular Trx Tubby mice [160], suggesting that Trx can increase BDNF expression. The results of these studies suggested that Trx can upregulate CREB/BDNF neurotrophic signaling.

1.3.4 Stress, chronic CORT treatment and Trx

Research have shown that chronic stress and chronic CORT can regulate Trx antioxidant system. It has been reported that 21 days of exposure to chronic unpredictable mild stress in rats, resulted in lower levels of Trx and higher levels of Trx inhibitor protein Txnip in hippocampus when compared to control rats [161]. Mice exposed to 3 hours of restraint stress daily for 2 weeks exhibited lower levels of Trx in the hippocampus when compared to control group [162].

Our laboratory's previous research has also shown that 28 days exposure to chronic unpredictable stress did not affect Trx protein levels, but elevated Txnip protein levels in mouse hippocampus and frontal cortex [163]. Further, our laboratory found that although treating with 1 μM CORT for 5 days did not affect Trx and TrxR protein levels, it upregulated Txnip mRNA and protein levels in primary cultured mouse cerebral cortical neurons and HT22 mouse hippocampal cells [164]. Our studies suggest that chronic stress and chronic CORT treatment may cause Txnip upregulation,

further inhibiting Trx function. These observations together also indicate that chronic stress and chronic CORT administration could regulate Trx antioxidant system.

1.4 Summary

A number of *in vivo* and *in vitro* studies have been undertaken to prove that chronic stress and prolonged glucocorticoid treatment cause overproduction of ROS, disruption of antioxidant defense and cause development of oxidative damage in rodent brain. Trx antioxidant system has an essential function in maintaining cellular redox homeostasis. Trx is able to reverse protein cysteine oxidation and also facilitate Prx-mediated scavenging of H_2O_2, inhibiting oxidative damage. Trx could also bind to ASK1 and suppress ASK1 apoptotic signaling. Txnip acts as an endogenous Trx inhibitor protein. Previous studies in our laboratory observed that chronic stress and chronic CORT treatment elevated Txnip protein levels. Findings from previous studies in our laboratory suggest that chronic CORT treatment may upregulate Txnip, inhibiting Trx antioxidant defense and leading to oxidative stress and subsequently neuronal damage.

1.5 Hypothesis and overall objectives

HYPOTHESIS: Chronic CORT treatment can increase Txnip expression in cultured neurons, which may increase protein oxidative modifications including sulfenylation, nitrosylation and carbonylation and increase ASK1 phosphorylation, further impairing neuronal outgrowth.

OBJECTIVES: Objectives are to establish if chronic treatment with CORT increases Txnip, causing oxidative damage and impairing neuronal outgrowth.

1. To determine if CORT treatment upregulates Txnip, and increases protein oxidative modification and ASK1 phosphorylation, which causes neuronal damage.

2. To determine if CORT treatment inhibits neurite outgrowth in primary cultured mouse cerebral cortical neurons.

2 CHAPTER 2: MATERIALS AND METHODS

2.1 Cell culture

HT22 cells are immortalized mouse hippocampal neuronal cells and were generously provided by Salk Institute (La Jolla, USA). HT22 cells were cultured in medium consisting of DMEM (Life Technologies Inc, USA), 10% FBS and 1% penicillin/streptomycin and kept in incubator under 5% CO_2 at 37°C.

Primary cortical cell cultures were conducted as previously described [165]. Embryos with 15-17 days of gestation were extracted from CD1 pregnant mice, and cerebral cortices were separated from embryos. Blood vessels and meninges were removed and cortices were collected and put into a tube with chilled 1x Hank‘s Balanced Salt Solution (HBSS) dissection media. To dissociate neurons, cortices were then minced finely and placed in 0.25% trypsin at 37°C for 15 minutes. After trypsinization, cortices were incubated for 15 minutes in DNAse (1 mg/ml) at 37°C. Termination of enzymatic digestion was done with addition of Dulbecco's Modified Eagle Medium (DMEM) enriched with 20% fetal bovine serum (both purchased from Life Technologies Inc, USA), and then supernatant was discarded. 1 ml neurobasal media (Life Technologies Inc.) supplemented with 2% N21-MAX (R&D System, USA), 1× GlutaMAX and 1% penicillin/streptomycin (both purchased from Life Technologies Inc, USA) was added to cerebral cortical tissue and triturated through pipetting. Supernatant containing neuronal cells was transferred and resuspended in 9 ml of enriched Neurobasal media. After cell counting, plates which were coated with poly-D-lysine (50µl/ml) were used for culturing cells. Cells were placed in incubator under 5% carbon dioxide (CO_2) at 37°C. Half of media was removed from each well at 2 days *in vitro* (DIV) and replaced with fresh supplemented Neurobasal media containing Ara-

C (Cytosine β-D-arabinofuranoside) at concentration of 1 μM for overnight. Half of media was changed twice per week and treatment with CORT started at 7 DIV for 5 days. Dimethyl sulfoxide (DMSO) was used to dissolve CORT, therefore DMSO was used as vehicle. In both vehicle and CORT-treated cells, concentration of DMSO in the media was maintained at 0.1%.

2.2 Protein isolation

After removing media, chilled phosphate buffer saline (PBS) was used to wash cells for twice. 75 μl of chilled lysis buffer (recipe is presented in table 2-1) was added to each well. Then, cells were detached by scraper from each well, collected into 1.5 ml microcentrifuge tube and maintained on ice for 1 hour. Samples were vortexed briefly. Then, samples were centrifuged at 4°C, 10,000 g for 10 minutes. After supernatant was transferred into 1.5 ml tubes, protein concentrations in samples were quantified with bradford protein assay [127]. In this method, bovine serum albumin (BSA) standards were prepared at the following concentrations: 0.5, 1, 2, 4, 8 mg/ml. Then, 5 μl from each sample was diluted in 45 μl PBS (1/10 dilution). 10 μl of standards or samples were added to 96-well plate in triplicates. Then, 200 μl of 1X Bradford reagent (Bio-Rad Protein Assay Dye Reagent , Bio-Rad, USA) were added to each well. The 96-well plate was incubated at room temperature for 10 minutes on an orbital shaker. The absorbance at 595 nm was determined using a microplate reader (Thermo Fisher Scientific Inc, Canada) and protein concentration of each sample was calculated based on the BSA standard curve.

Table 2-1 Recipe of lysis buffer

Lysis buffer	HEPES (pH 7.5) 20 mM
	Nonidet P-40 1%
	EGTA 0.1 mM
	EDTA 0.5 mM
	MgCl2 30 mM
	NaCl 250 mM
	Glycerol 20%
	Protease inhibitor cocktail 1×

2.3 Immunoblotting analysis

First, protein concentration of all samples was set at the same concentration of 1 µg/µl. Then, equal volume of protein samples and loading buffer (recipe is presented in table 2-2) were mixed and heated at 95°C for 5 minutes. Then, samples were put on ice for 5 minutes. Samples were loaded on 12% SDS polyacrylamide gel (containing 2,2,2-Trichloroethanol (TCE)) and conducted electrophoresis at 120V for 90 minutes. Following electrophoresis, SDS polyacrylamide gels with TCE were exposed to UV light resulting in reaction of TCE with proteins and generating fluorescent proteins. Subsequently, proteins in activated gel were transferred to polyvinylidene fluoride (PVDF) membranes (Millipore, Billerica, MA). Transferring process was carried out on ice under 220 mA for 120 minutes. After transferring, stain-free images were taken from PVDF membranes by ChemiDoc MP imager (Bio-Rad, Dreieich, Germany) to track total protein loaded in each lane. Membranes were blocked with 5% non-fat milk in TBS-T (recipe is presented in table 2-2) for 60 minutes at room temperature. Then blots were kept in primary antibodies overnight on the orbital shaker at 4°C. Primary antibodies used in this study are presented in the table 2-3. After incubation for 24 hours, membranes were rinsed 4 times, 10 minutes each time, with 1x TBS-T solution. Then, appropriate secondary antibody was prepared with 5% non-fat milk in TBS-T.

Blots were kept in secondary antibody for 2 hours at room temperature on orbital shaker. Blots were rinsed using TBS-T for 4 times, 10 minutes for each time. To visualize immunoreactive bands, membranes were exposed to enhanced chemiluminescence (ECL) and followed by imaging using Bio-Rad ChemiDoc MP imager. Quantification of band density was conducted utilizing Image Lab software (Bio-Rad, Germany).

Table 2-2 Immunoblotting buffers recipes

Loading Buffer	Tris-HCl (pH 6.8) 100mM Glycerol 20% Dithiothreitol (DTT) 200 mM Sodium dodecyl sulfate (SDS) 4% Bromophenol blue 0.2%
TBS-T	Tween-20 0.1% Tris-HCl (pH 7.4) 10mM

Table 2-3 Primary and secondary antibodies used in immunoblotting

Primary Antibody	**Company**	**Dilution ratio**
Anti-ASK1 rabbit polyclonal antibody	Cell Signaling Technology	1:1000
Anti-phosphorylated ASK1 rabbit polyclonal antibody	Cell Signaling Technology	1:1000
Anti-Txnip rabbit monoclonal antibody	Abcam Inc.	1:1000
Anti-Trx1 rabbit monoclonal antibody	Cell Signaling Technology	1:3000
Secondary Antibody	**Company**	**Dilution ratio**
HRP conjugated goat anti-rabbit IgG secondary antibody	Jackson ImmunoResearch	1:3000

2.4 Detection of protein sulfenylation by dimedone conjugation method

Sulfenylated protein levels in primary cultured neurons were determined by performing dimedone conjugated assay [164]. Primary cultured cerebral cortical neurons were rinsed with PBS and then digested with 0.25% trypsin at 37°C. Termination of trypsinization process was done by adding DMEM containing 10% fetal bovine serum mixed with 5% dimedone 1M. After cell suspensions were centrifuged for 5 minutes at 1000 g, supernatant was discarded and 1 ml ice-cold PBS was used to resuspend cell pellets. Then the cell suspensions were collected into microcentrifuge tubes and centrifuged at 4°C for 5 minutes at 10,000 g. After removing supernatant, dimedone conjugated assay lysis buffer (recipe is presented in table 2-4) was utilized to resuspend cell pellets. Samples were vortexed and maintained for 30 minutes on ice. Samples were centrifuged at 10,000 g for 10 minutes at 4°C, Bradford protein assay was used for protein concentration determination. Detection and analysis of sulfenylated proteins were done by loading 10 µg of protein to 12% SDS gel followed by immunoblotting using antibody against sulfenic acid (1:5000, Millipore) [164].

Table 2-4 Dimedone conjugated assay lysis buffer

Lysis buffer	Dimedone 2 mM
	N-ethylmaleimide 10 mM
	Iodoacetamide10 mM
	Citric acid 3 mM
	Sodium phosphate dibasic12 mM
	SDS 0.01%
	EDTA 10 mM
	Catalase 200 units/ml
	Triton-X 0.1%

2.5 Detection of protein carbonylation by biotin hydrazide conjugation method

Biotin hydrazide conjugation method was used for determination of carbonylated proteins [166]. Cells were lysed in a buffer consisting of N-Morpholino-ethanesulfonate 20 mM in water with pH adjusted to 5.5 (MES buffer). After measurement of protein level, all sample protein concentrations were adjusted to the same concentration at 0.5 µg/µl. Then, same volume from each sample was transferred into 1.5 ml tubes and biotin hydrazide was added at 10% of sample volume. To facilitate protein carbonyl labeling with biotin hydrazide, samples were kept at 37°C for 2 hours with gentle agitation during incubation. Immunoblotting was conducted by resolving 15 µl of each sample into 12% SDS gel. Detection of carbonylated proteins was conducted by using horseradish peroxidase-conjugated streptavidin (HRP-streptavidin).

2.6 Detection of protein nitrosylation by biotin-switch assay method

Protein nitrosylation was identified utilizing biotin-switch assay as described in our previous study [125]. In this method, in first step, free thiol of cysteine in samples was blocked with alkylating buffer consisting of 40mM NEM in HEN buffer (HEN buffer recipe is presented in table 2-5). Therefore, 50 µl of protein samples that contain 50 µg protein were incubated with 200 µl of alkylating buffer at 50°C for 40 minutes. After addition of prechilled acetone (1ml) to each sample, they were kept for 20 minutes at -20°C followed by centrifuging at 15,000 g for 15 minutes. After discarding supernatant, pellet was resuspended using 5 µl of 1% SDS in HEN buffer.

250 µl of ascorbate at 50 mM was added to convert nitrosylated cysteine thiols into free thiols that were tagged by adding 15 µl of N-[6-(biotinamido) hexyl]-3-(2-pyridyldithio) propionamide (biotin–HPDP) at 4 mM. Biotinylation reaction of the mixture was facilitated by keeping it for 60 minutes at room temperature. To detect proteins labeled with biotin, 15 µl of samples were

transferred into 12% SDS/PAGE for immunoblotting analysis using polyclonal antibody against biotin (1:2000, Sigma, MO, USA).

Table 2-5 HEN buffer recipe

HEN buffer	HEPES pH 7.7 250 mM Neocuproine 0.1 mM EDTA 1 mM

2.7 Measurement of cell viability by Cell Counting Kit-8

To measure cell viability, 30,000 cells were seeded in each well of 96-well plate. The final volume of supplemented neurobasal media in each well was 100 µl. Cell Counting Kit-8 (CCK-8) (Cayman chemical) was employed for determining cell viability by measuring the activities of dehydrogenases in cells. CCK-8 kit contains the water-soluble tetrazolium salt (WST-8) and the electron-transport mediator 1-methoxy PMS (MPMS). In the presence of MPMS, dehydrogenases in viable cells are able to reduce WST-8 to formazan. Formazan is a yellow-colored product. The quantity of formazan, is measured by a spectrophotometer, is directly correlated to the quantity of viable cells. 10µl of water-soluble tetrazolium salt (WST-8) was transferred to cells, followed by 4 hours incubating at 37°C. The absorbance was recorded at 450nm microplate reader spectrophotometer.

2.8 Measurement of cell viability by anlalyzing lactate dehydrogenase release

Cell viability was also measured by analyzing L-lactate dehydrogenase (LDH) release [167]. In response to cellular plasma membrane damage, LDH is released from cytoplasm to the extracellular environment (culture medium). In this method, released LDH from damaged cells

oxidize lactate and generate NADH. Then, NADH reduces iodonitrotetrazolium chloride (INT) to yellow-colored soluble product formazan which can be detected by spectrophotometry. First, extracellular LDH was measured. 50µl of supernatant from each well was transferred into 96 well plates.The next step was adding 50µl of "Assay Reagent" and mixing it with existing supernatant in each well. "Assay Reagent" is composed of equal amount of "Buffer A", "Buffer B" and 10% of 1-methoxyphenazine methosulfate (MPMS). "Buffer A" consists of 4 mM INT in 0.2 M Tris-HCl, pH 8.2 and "Buffer B" consists of 320 mM lithium lactate, 6.4 mM NAD in 0.2 M Tris-HCl buffer. Then, samples with "Assay Reagent" were kept at room temperature for 1 hour. 96-well plate was protected from light. After one hour incubation, 50µl of 1M acetic acid was added to each to stop reaction. Optical density (OD) values for absorbance were recorded at 490nm utilizing a spectrophotometer. Second, total LDH was measured. 10× "Lysis Solution" was added to each well at 10% of the volume in each well and homogenized for approximately 3 minutes. "Lysis Solution" consists of 9% Triton X-100 in water. Then 50µl of lysate from each well was transferred into 96-well plate, and incubated with "Assay Reagent" at room temperature for 60 minutes. After incubating for 1 hour, 50µl of 1M acetic acid was added to stop reaction. OD values for absorbance were also recorded at 490nm. LDH release was calculated by measuring the ratio of LDH release/total LDH.

2.9 Immunocytochemistry

Cerebral cortical neurons were cultured on 35 mm coverslip dishes to measure neurite outgrowth. First, PBS was utilized to rinse cells for 3 times and then cells were incubated with PFA fixing solution (4% (v/v) paraformaldehyde in 1× PBS) at room temperature for 20 minutes. Then cells were gently rinsed with PBS for 3 times again. Triton X-100 at 0.1% prepared in PBS was added

and incubated for 150 minutes at room temperature to facilitate permeabilization of cells. Non-specific protein bindings were blocked by adding 10% goat serum to cells and incubating at room temperature for 1 hour.

Purity of cultured neurons was assessed at 12 DIV. As shown in table 2-6, primary antibodies including anti-neuronal nuclei (NeuN) rabbit monoclonal antibody, anti-glial fibrillary acidic protein (GFAP) mouse monoclonal antibody, and anti-ionized calcium binding adaptor molecule 1 (Iba1) rabbit polyclonal antibody were employed as markers for neurons, astrocytes and microglia, respectively. After fixation and permeabilization of neurons, primary antibodies were added to cells and incubated for overnight at 4°C. Then, cells were rinsed with PBS for 10 minutes (repeat 3 times). Then fluorescent secondary antibodies Alexa-Fluor 488 goat anti-mouse IgG was used for detecting GFAP, Alexa-Fluor 488 goat anti-rabbit IgG used for detecting Iba1 and Alexa-Fluor 568 goat anti-rabbit IgG was used for detecting NeuN (presented in table 2-7) were prepared in 10% goat serum was added and kept at room temperature for 60 minutes. Images were taken at 20X magnification by Carl Zeiss Fluorescent microscope.

To analyze neurite outgrowth, after performing fixing and permeabilizing, cells were incubated with microtubule-associated protein 2 (MAP2) rabbit monoclonal antibody for 24 hours at 4°C. Next day, PBS was used to rinse cells for 10 minutes (repeat 3 times). Then conjugated secondary antibody Alexa-Fluor 488 goat anti-rabbit IgG (presented in table 2-7) in 10% goat serum was added and kept at room temperature for 1 hour. Fluorescent microscope (Carl Zeiss) was used to capture images at 20X magnification. MAP2 stained neurons were traced and classified into primary, secondary and tertiary branches (Figure 7). The length and number of primary branches, and total number and length of branches including primary, secondary and tertiary branches were quantified semi-manually using the NeuronJ plugin of ImageJ

"(https://www.imagescience.org/meijering/software/neuronj)" [157]. A total number of 40 neurons from 3 cultured dishes per group were analyzed and the experiment was repeated twice.

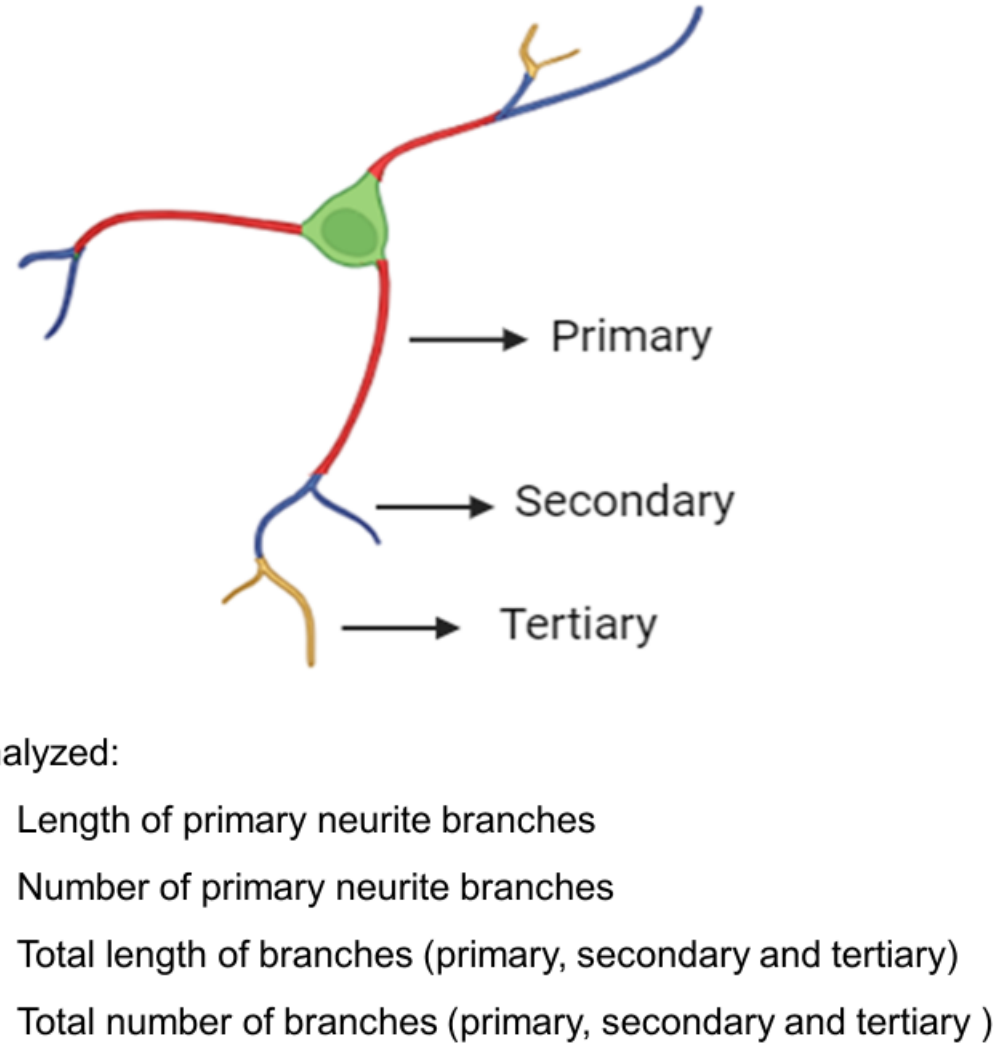

Figure 7. Measurement of neurite outgrowth using MAP2 staining
Neurite branches and length were quantified semi manually using the NeuronJ plugin of ImageJ and labeled as primary, secondary and tertiary. Total length of branches represents the sum of length of primary, secondary and tertiary neurite branches. Total number of branches represents the sum of the number of primary, secondary and tertiary neurite branches. (Created by using www.biorender.com)

Table 2-6 Primary antibodies used in immunocytochemistry

Primary Antibody	Company	dilution ratio
Anti-neuronal nuclei (NeuN) rabbit monoclonal antibody	Cell Signaling Technology	1:500
Anti-glial fibrillary acidic protein (GFAP) Mouse monoclonal antibody	Cell Signaling Technology	1:500
Anti-ionized calcium binding adaptor molecule 1 (Iba1) rabbit polyclonal antibody	Wako Pure Chemical Industries Ltd	1:500
anti microtubule-associated protein 2 (MAP2) rabbit monoclonal antibody	Abcam Inc	1:500

Table 2-7 Secondary antibodies used in immunocytochemistry

Secondary Antibody	Company	Dilution ratio
Alexa-Fluor 488 goat anti-mouse IgG	Thermo Fisher Scientific Inc, Canada	1:500
Alexa-Fluor 488 goat anti-rabbit IgG	Thermo Fisher Scientific Inc, Canada	1:500
Alexa-Fluor 568 goat anti-rabbit IgG	Thermo Fisher Scientific Inc, Canada	1:500

2.10 Knocking down of Txnip gene by CRISPR/Cas9

CRISPR/Cas9 technology was used to knock down Txnip in primary cultured neurons. Primary cultured mouse cortical neurons were placed in 6-well plates and cultured in incubator under 37ºC, 5% CO_2. Txnip single guide RNAs (sgRNAs) or scrambled sgRNAs, and CRISPR/Cas9 All-in-One lentivector pLenti-U6-sgRNA-SFFV-Cas9-2A-Puro (ABM Inc Richmond, BC, Canada) were used to knock down Txnip. The plasmid vectors were packaged by University of Manitoba

Lentiviral Core Service. As shown in Figure 8, Txnip sgRNA includes a complementary sequence to the Txnip gene and a binding sequence to RNA-guided DNA endonuclease Cas9. Once Txnip sgRNA binds to Cas9 and forms a ribonucleoprotein complex, Txnip sgRNA guides Cas9 to Txnip gene and then Cas9 cleaves Txnip gene.

To knock down Txnip gene in primary cultured neurons, at 1 DIV media was discarded and then 700 µL of neurobasal media was added to each well. Transfection was initiated by adding 3 µL of lentiviral particles containing Txnip sgRNA or scrambled sgRNA to each well followed by 24 hours incubation at 37ºC, 5% CO_2. At 2 DIV, 1.3 ml of neurobasal media with N21-MAX supplement was added to each well and maintained in incubator under 5% CO_2 at 37ºC for another 48 hours. The lentivector used contained the antibiotic puromycin resistant gene as a selection marker. Therefore, to select transfected cells, neurons were treated with 1µg/ml puromycin for 72 hours. Neurons containing the lentivector survive, while those lacking the plasmid die after puromycin treatment.

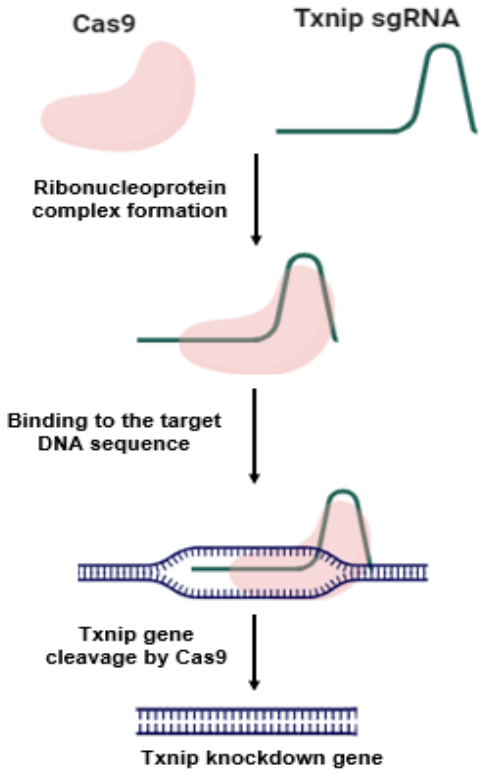

Figure 8. CRISPR/Cas9/Txnip sgRNA Principle
Txnip sgRNA binds to Cas9 and forms ribonucleoprotein complex. Txnip sgRNA guides Cas9 to make a double-stranded break in Txnip gene, inducing impairments in Txnip gene expression. (Created by using www.biorender.com)

2.11 Statistical analysis

In this project, all analyses were performed utilizing SPSS version 24.0. Data obtained from experiments were displayed as means ± SEM. One-way analysis of variance (ANOVA) with Tukey post hoc was performed to assess variation between multiple means. Student's t-test was carried out to determine whether there was a difference among two groups, with significance considered as a p-value less than 0.05.

3 CHAPTER 3: RESULTS

3.1 To determine if CORT treatment upregulates Txnip, and increases protein oxidative modification and ASK1 phosphorylation, which causes neuronal damage.

3.1.1 To determine purity of cultured neurons.

Experiments were performed in primary cultured mouse cerebral cortical neurons. In primary neuronal culture, neurons extend neurites in the first 7 days. Differentiation into mature neurons and synaptic connections formation begin between 7-14 DIV. Therefore, cultured neurons were treated with CORT at 7 DIV for 5 days, and collected in 12 DIV. Half of the media was replaced every other day. Purity of cultured neurons was assessed at 12 DIV by using immunocytochemistry with specific antibodies against NeuN, GFAP and Iba1. NeuN was used as a marker of neurons, GFAP as a marker of astrocytes and Iba1 as a marker for microglia. As presented in Figure 9, the results revealed a high purity of neuronal cells, as indicated by the presence of NeuN staining, which accounted for 96% of the total cell population. This finding suggests that the majority of cells in our culture are mature neurons, which is desirable for study. Additionally, lack of Iba1 staining and the low presence of GFAP staining (4% of the total cell population) indicated undetectable level of microglia and minimal contamination of astrocytes, supporting the neuronal enrichment in our culture. These results highlight the success of our culturing protocol in generating a predominantly neuronal population, providing a solid foundation for subsequent experimental analyses, and ensuring accurate interpretation of our findings.

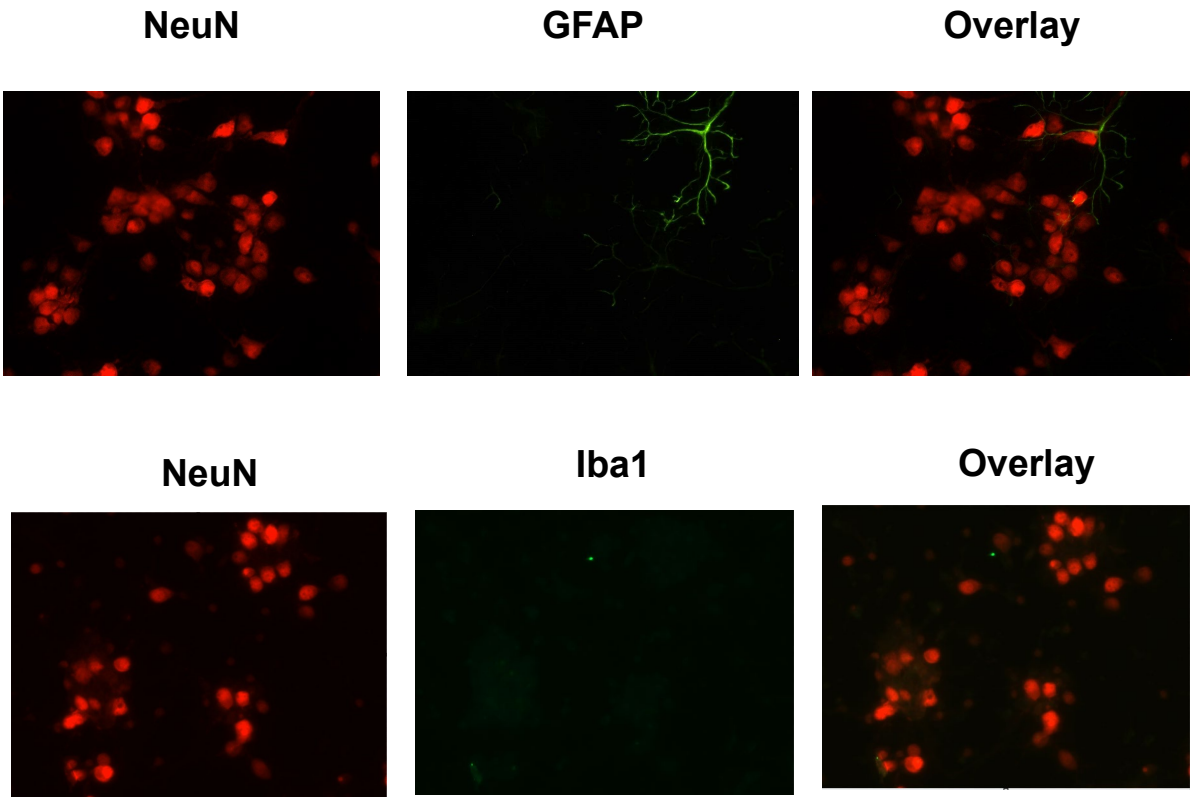

Figure 9. Purity of cultured mouse primary cerebral cortical neurons
Purity of cultured neurons was measured using immunocytochemistry at 12 DIV with anti-NeuN, anti-GFAP and anti-Iba1 antibodies. 96% of cells were enriched with NeuN staining (neurons), and 4% was GFAP staining (astrocytes).

3.1.2 The effect of CORT on Trx and Txnip protein levels

To determine if CORT treatment can upregulate Txnip protein levels on primary cultured neurons and decrease Trx protein levels in these cells, first we analyzed the effect of CORT treatment on Trx and Txnip protein levels. We treated cultured neurons with DMSO as vehicle (CTL) and CORT 1μM at 7 DIV for 5 days. At 12 DIV protein levels of Trx and Txnip were quantified by immunoblotting analysis. No significant changes were found in Trx levels in cultured neurons treated with 1 μM CORT for five days ($p=0.367$, $N=6$) (Figure 10-A). However, we observed that CORT treatment significantly elevated Txnip protein levels in cultured neurons ($p<0.05$, $N=6$)

(Figure 10-B). This finding indicates that the administration of CORT leads to an upregulation of Txnip expression in the neurons.

In addition to this experiment, we also conducted a dose-response analysis on primary cultured mouse cerebral cortical neurons. CORT at concentrations of 0.01, 0.1 and 1 μM or vehicle used to treat cultured neurons at 7 DIV for 5 days. Our findings revealed that increasing concentrations of CORT led to proportional elevation in Txnip protein levels ($p<0.05$, N=6) (Figure 11).

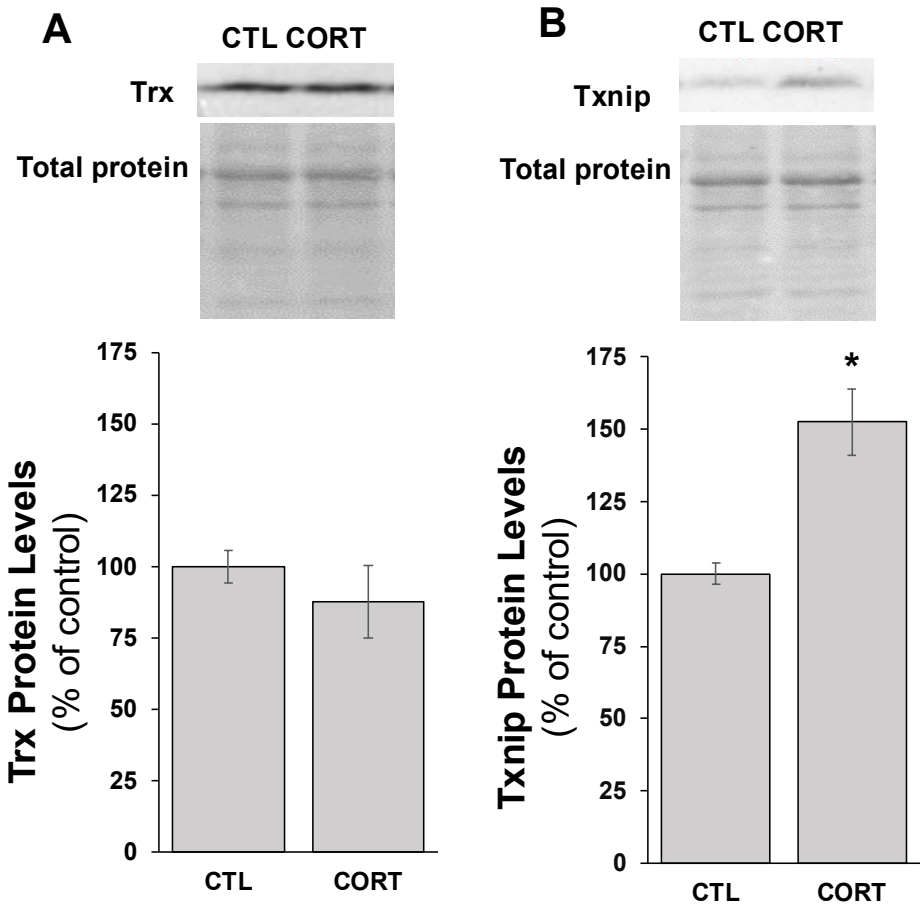

Figure 10. The effect of CORT on Trx and Txnip protein levels in primary cultured mouse cerebral cortical neurons

A) Trx protein levels, B) Txnip protein levels. Primary cultured mouse cerebral cortical neurons were treated with 1 μM CORT or vehicle as a control (CTL) at 7 DIV for 5 days. At 12 DIV, protein levels of Trx and Txnip were measured by conducting immunoblotting analysis. Blot stain free for total protein used as a normalization control. * indicates $p<0.05$ using Student-T test, when comparing CORT treated group with control. Findings are presented as mean ± SEM (N=6).

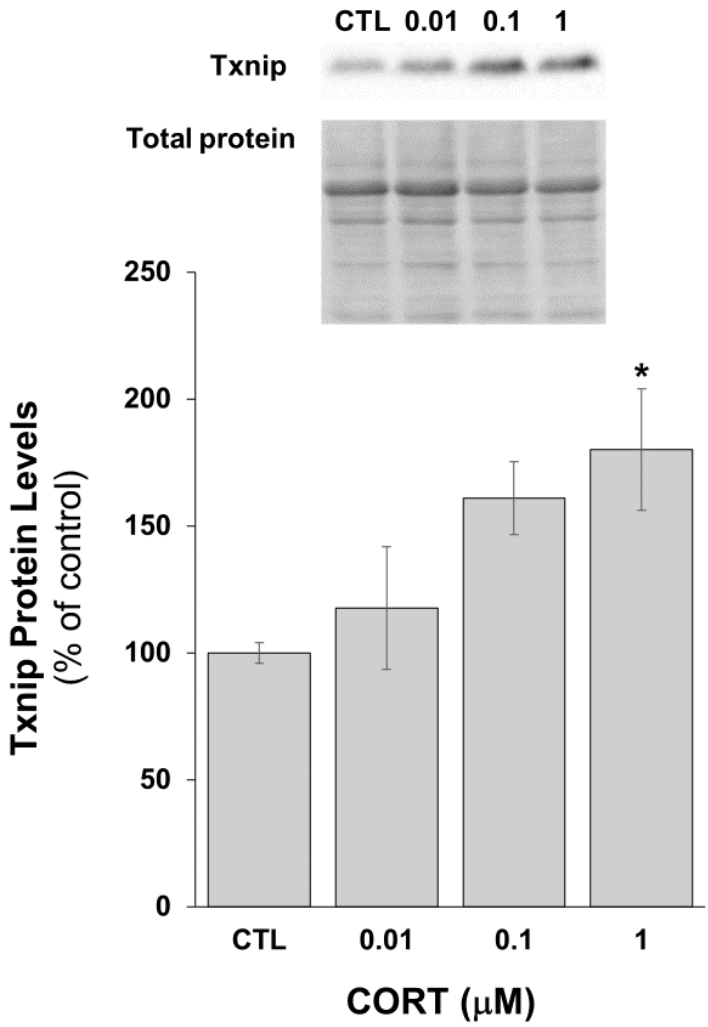

Figure 11. The effect of CORT on Txnip protein levels in primary cultured neurons
Primary cultured mouse cerebral cortical neurons were treated with 0.01, 0.1 and 1 μM CORT and vehicle (CTL) at 7 DIV for 5 days. At 12 DIV, protein levels of Txnip were assessed by conducting immunoblotting analysis. Blot stain free for total protein used as a normalization control. Data analysis was carried out using one-way ANOVA with Tukey's post-hoc. * indicates $p<0.05$ when comparing CORT treated group with control. Findings are presented as mean ± SEM (N=6).

3.1.3 The effect of CORT treatment on protein cysteine oxidative modifications

3.1.3.1 Establishing the methods for measurement of protein sulfenylation, carbonylation and nitrosylation using HT22 hippocampal cells

Txnip can suppress Trx-reducing activity, which can enhance protein oxidation such as protein sulfenylation, nitrosylation and carbonylation. Since CORT treatment elevated Txnip protein levels in primary cultured neurons, it may further enhance protein oxidation in these cells.

Cysteines are vulnerable to hydrogen peroxide (H_2O_2) and nitric oxide ($NO^{\bullet}$) attacks that induce cysteine sulfenylation and nitrosylation, respectively. H_2O_2 can also react with cellular iron ions to form hydroxyl radical ($HO^{\bullet}$) that induces protein carbonylation. First, in order to establish methods for protein sulfenylation, carbonylation and nitrosylation analysis, we assessed H_2O_2 effect on protein sulfenylation and protein carbonylation; and the effect of NO donor S-nitrosoglutathione (GSNO) on protein nitrosylation in HT22 mouse hippocampal cells. Protein sulfenylation was analyzed using dimedone conjugation method [164]. As shown in Figure 12-A, sulfenylated thiols first react with dimedone which results in formation of irreversible dimedone-derivatized proteins. These proteins are subsequently loaded on 12% SDS gel, transferred to membranes and analyzed by immunoblotting utilizing dimedone conjugated anti-sulfenic acid antibody. To perform this method, HT22 cells were treated with 250 and 500 μM H_2O_2 for 60 minutes. We found that treatment with H_2O_2 at 500 μM significantly elevated sulfenylated protein levels in HT22 cells ($p<0.05$, N=6) (Figure 12-B). Protein carbonylation was determined by biotin hydrazide conjugation method [166]. Biotin hydrazide was used to label carbonylated proteins. As shown in Figure 13-A, biotin-labeled hydrazide conjugated proteins (carbonylated proteins) were loaded on 12% SDS gel, then transferred to the membrane, and identified by using horseradish

peroxidase-conjugated streptavidin (HRP-streptavidin). HT22 cells were subjected to receive 1 and 2 mM H_2O_2 for 1.5 hours. We observed that treatment with H_2O_2 at 1 and 2 mM significantly elevated carbonylated protein levels in HT22 cells ($p<0.05$, N=5) (Figure 13-B). Protein nitrosylation was analyzed by conducting biotin-switch method [125]. As shown in Figure 14-A, unmodified thiols in cysteine were first alkylated with NEM irreversibly (thiols which are modified in response to oxidation cannot be alkylated by NEM). This step was followed by using ascorbate to reduce nitrosylated thiols to free thiols. Regenerated free thiols were labeled with biotin-HPDP. Biotinylated proteins (nitrosylated proteins) were measured by conducting immunoblotting and detected with an anti-biotin antibody. HT22 cells were treated with different GSNO concentrations (40 and 80 μM) for duration of 30 minutes. We found that treatment with GSNO at 80 μM caused significant elevation in nitrosylated protein levels in HT22 cells ($p<0.05$, N=6) (Figure 14-B).

3.1.3.2 The effect of CORT on protein sulfenylation, carbonylation and nitrosylation in primary cultured mouse cerebral cortical neurons

The effect of CORT on protein sulfenylation, carbonylation and nitrosylation in primary cultured mouse cerebral cortical neurons was assessed. Cultured neurons were treated with DMSO as vehicle (CTL) and CORT 1μM at 7 DIV for 5 days. At 12 DIV, protein sulfenylation was measured using dimedone conjugation method, protein carbonylation was measured using biotin hydrazide conjugation method and protein nitrosylation was measured using biotin-switch method. Our results showed that chronic treatment with CORT significantly elevated sulfenylated protein levels ($p<0.05$, N=6) and carbonylated protein levels ($p<0.05$, N=6), but it did not affect nitrosylated protein levels ($p=0.285$, N=4) (Figure 15-A, 15-B and 15-C).

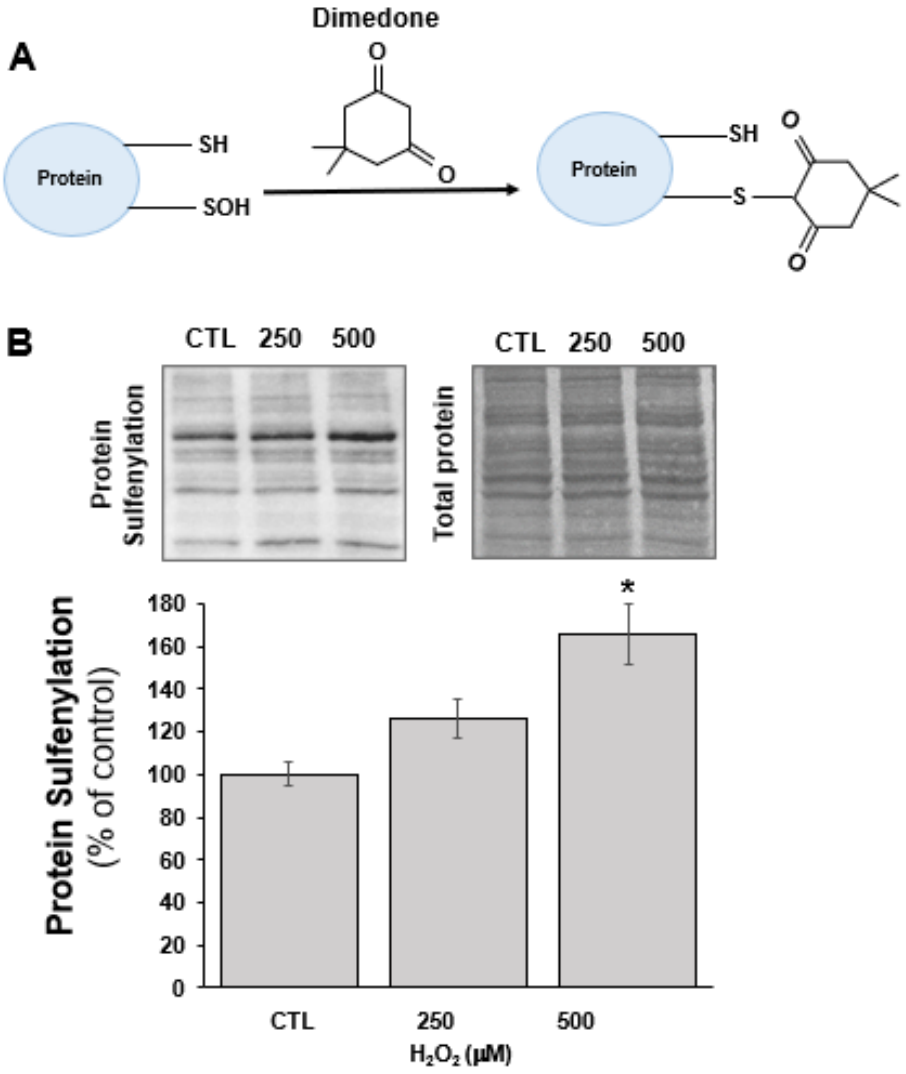

Figure 12. The effect of H_2O_2 on protein sulfenylation in HT22 mouse hippocampal cells
(A) Sulfenylated proteins were detected by using dimedone conjugation method and analyzed by conducting immunoblotting. (B) HT22 cells were treated with 250 and 500 µM H_2O_2 for 60 minutes to induce protein sulfenylation. Coomassie blue staining of the membrane was used to assess equal protein loading. Data analysis was carried out using one-way ANOVA with Tukey's post-hoc. * indicates $p<0.05$ when comparing H_2O_2 treated cells with control. Findings are presented as mean ± SEM (N = 6).

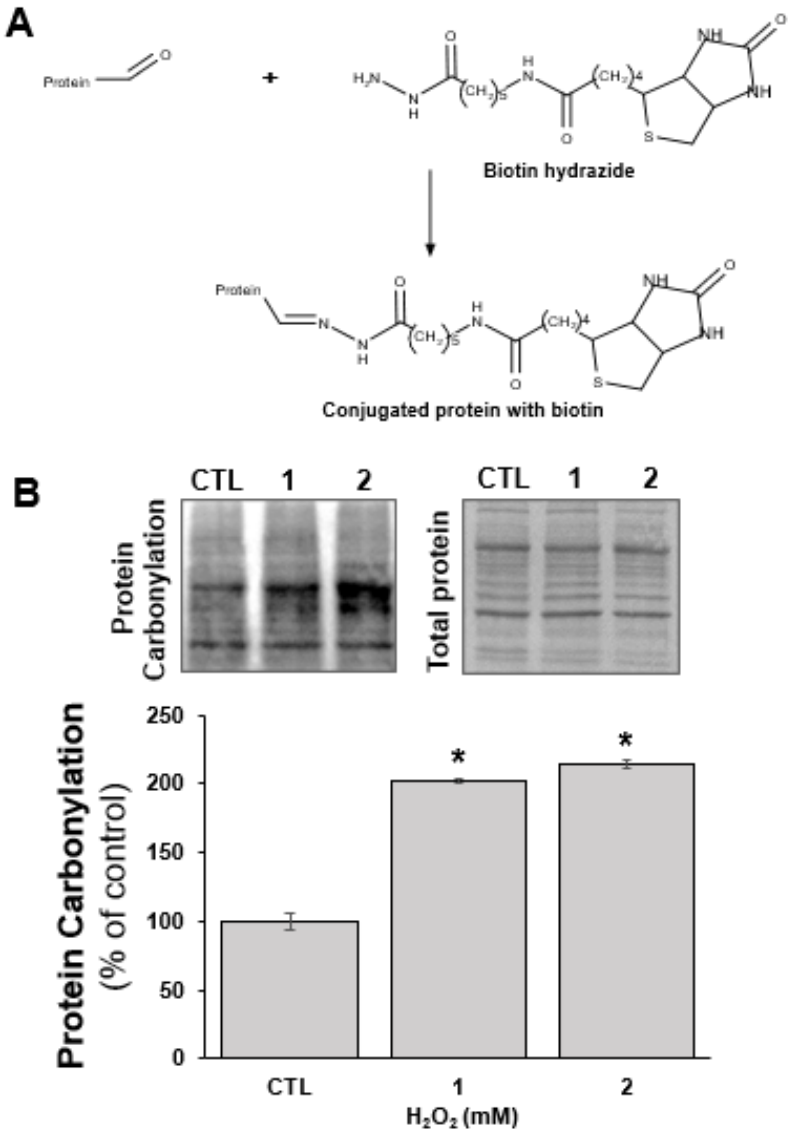

Figure 13. The effect of H_2O_2 on protein carbonylation in mouse HT22 hippocampal cells
(A) Carbonylated proteins were measured by using biotin hydrazide conjugation method and analyzed by conducting immunoblotting (chemical structure was created by using Marvin 19.27.0, 2019, ChemAxon, www.chemaxon.com). (B) HT22 cells received 1 and 2 mM H_2O_2 for 90 minutes to induce protein carbonylation. Coomassie blue staining of the membrane was used to assess equal protein loading. Data analysis was carried out using one-way ANOVA with Tukey's post-hoc. * indicates $p<0.05$ when comparing H_2O_2 treated cells with control. Findings are presented as mean ± SEM (N = 5).

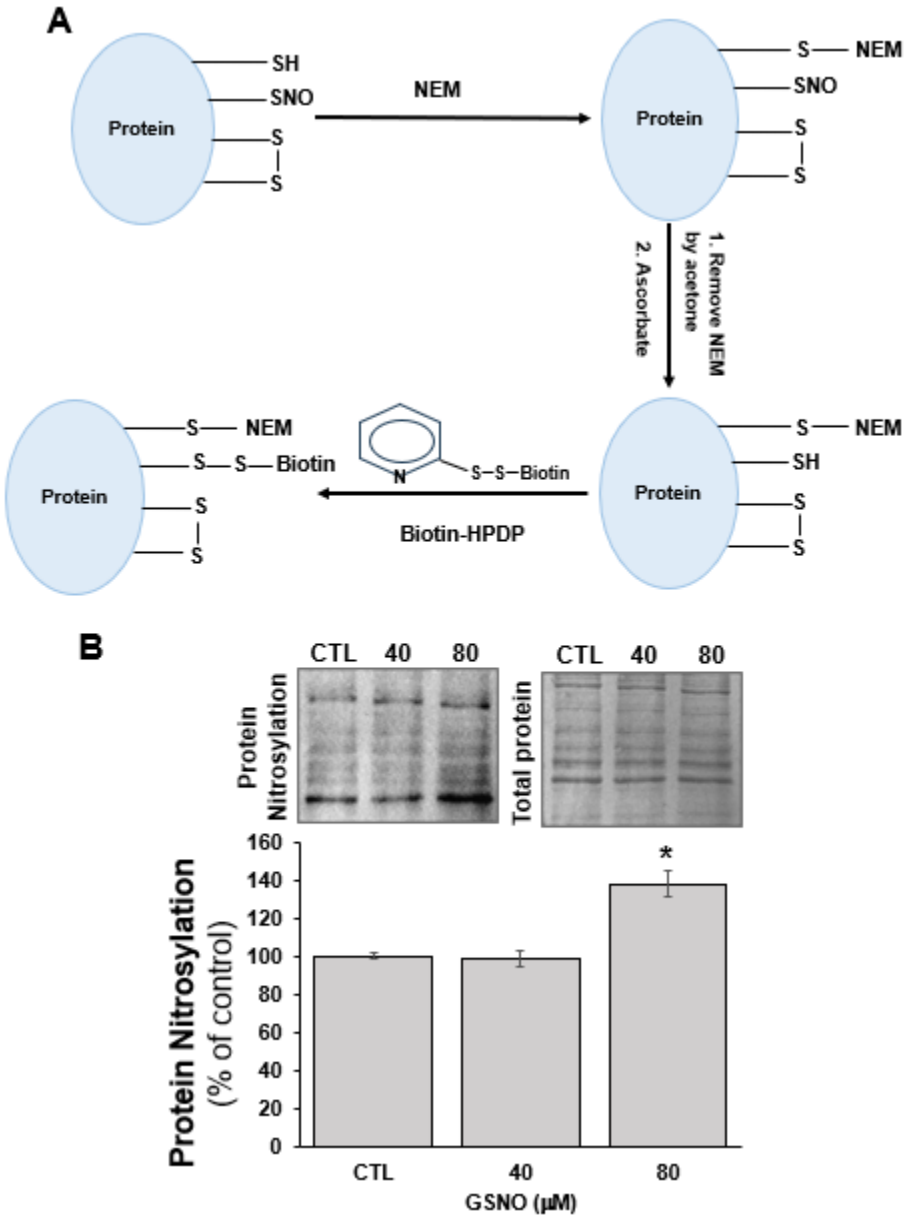

Figure 14. The effect of GSNO on protein nitrosylation in mouse HT22 hippocampal cells
(A) Nitrosylated proteins were detected by using biotin-switch method and analyzed by conducting immunoblotting. (B) HT22 cells were treated with 40 and 80 μM GSNO for 30 minutes to induce protein nitrosylation. Coomassie blue staining of the membrane was used to assess equal protein loading. Data analysis was carried out using one-way ANOVA with Tukey's post-hoc. * indicates $p<0.05$ when comparing GSNO treated cells with control. Findings are presented as mean ± SEM (N = 6).

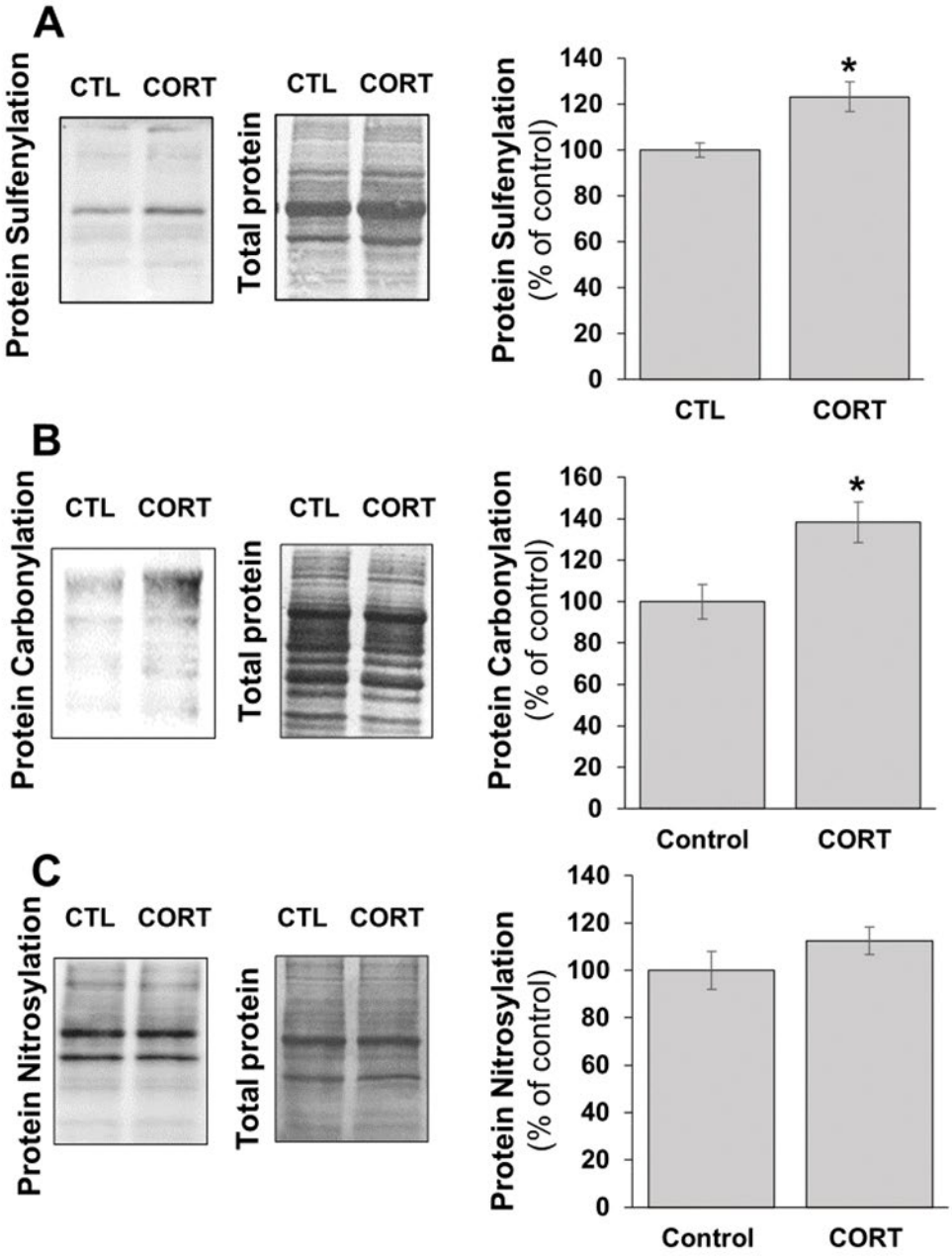

Figure 15. The effect of CORT on protein sulfenylation, carbonylation and nitrosylation in primary cultured mouse cerebral cortical neurons

Primary cultured mouse cerebral cortical neurons were treated with vehicle as control (CTL) or 1 μM CORT at 7 DIV for 5 days. At 12 DIV, A) protein sulfenylation was measured using dimedone conjugation method, B) protein carbonylation was measured using biotin hydrazide conjugation method and C) protein nitrosylation was measured using biotin-switch method. * indicates $p<0.05$ using Student-T test, when comparing CORT treated group with control. Findings are presented as mean ± SEM (N=4-6).

3.1.4 The effect of CORT on ASK1 phosphorylation

Trx at reduced state can bind to ASK1 and inhibit ASK1 activity. Elevated Txnip can bind to Trx leading to release of ASK1. Dissociated ASK1 is activated through autophosphorylation. To understand if CORT-upregulated Txnip can affect ASK1 phosphorylation, CORT at 1μM or vehicle was administered to primary cultured mouse cerebral cortical neurons at 7 DIV for 5 days. First, the total ASK1 was evaluated by conducting immunoblotting analysis. We observed that CORT treatment did not affect ASK1 protein levels ($p=0.852$, $N=6$) (Figure 16-A). Second, phospho-ASK1 protein levels were analyzed using immunoblotting with phospho-ASK1 antibody. Then the same membrane blot was stripped and reprobed with total ASK1 antibody. Phosphorylated ASK1 protein levels were analyzed by measuring the ratio of phosphorylated ASK1/total ASK1 levels. We found that CORT treatment did not affect the protein levels of phosphorylated ASK1 ($p=0.918$, $N=6$) (Figure 16-B).

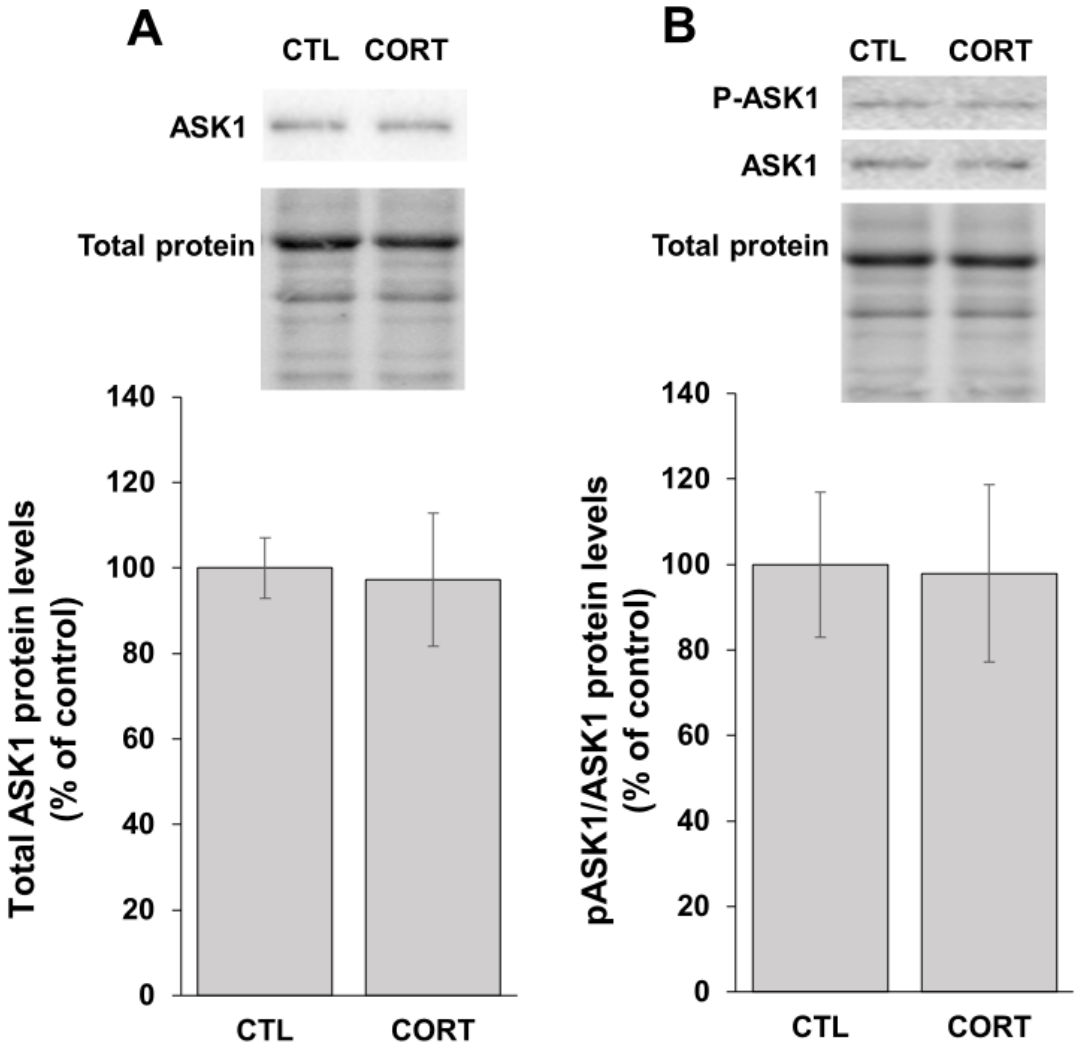

Figure 16. The effect of CORT on phosphorylation of ASK1 (pASK1) in primary cultured mouse cerebral cortical neurons

Primary cultured mouse cerebral cortical neurons were treated with vehicle as control (CTL) or 1 μM CORT at 7 DIV for 5 days. At 12 DIV, protein levels of ASK1 and pASK1 were measured by conducting immunoblotting analysis. Blot stain free for total protein served as a normalization control. A) Total ASK1 protein levels, B) p-ASK/ ASK1 protein levels using same membrane for analyzing ASK1 and p-ASK1. $p>0.05$ using Student-T test, when comparing CORT treated group with control. Findings are presented as mean ± SEM (N=6).

3.1.5 The effect of CORT on cell viability

Measurement of cell viability was carried out by utilizing CCK-8 (Cell Counting Kit-8) assay and lactate dehydrogenase (LDH) release assay. To measure cell vibility by CCK-8, in the presence of an electron mediator, 1-methoxy PMS, dehydrogenases in viable cells reduce WST-8 to form formazan dye which is a yellow-colored soluble product in the culture medium. The quantity of formazan, measurable by a spectrophotometer, is directly correlated to the quantity of viable cells. Rotenone is a mitochondrial complex I inhibitor, thus it can induce cell death. Rotenone was used as a positive control in the CCK-8 assay. Primary cultured mouse cerebral cortical neurons were treated with 1 μM CORT at 7 DIV for 5 days or with 40 μM rotenone at 12 DIV for 4 hours. At 12 DIV, we measured cell viability using CCK-8. We found that although rotenone treatment caused significant decrease in cell viability ($p<0.05$, N=8), CORT treatment did not affect cell viability ($p=0.828$, N=8) (Figure 17-A). Cell viability was also evaluated by performing lactate dehydrogenase (LDH) release assay. In response to damage to cellular plasma membrane, LDH is released from cytoplasm into culture medium. Antimycin A is a mitochondrial complex III inhibitor, thus it can induce cell death. Antimycin A was used as a positive control in LDH release assay. Cultured neurons were treated with 1 μM CORT at 7 DIV for 5 days or 5 μM antimycin A at 10 DIV for 48 hours. At 12 DIV, we measured cell viability using the LDH release assay. We found that antimycin A treatment caused significant release of LDH ($p<0.05$, N=6), but LDH release appeared to be unaffected by CORT treatment ($p=0.891$, N=6) (Figure 17-B). Our results suggest that chronic CORT treatment does not affect cell viability in primary cultured mouse cerebral cortical neurons.

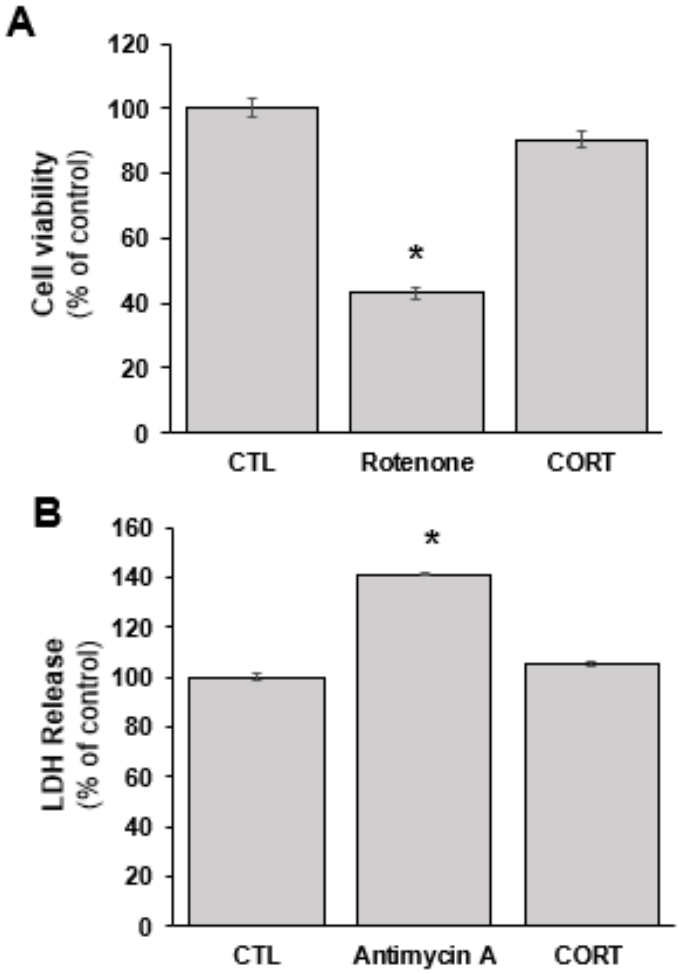

Figure 17. The effect of CORT on cell viability in primary cultured neurons.
A) Primary cultured mouse cerebral cortical neurons were treated with vehicle as control (CTL) or 1 μM CORT at 7 DIV for 5 days or 40μM Rotenone as a positive control for 4 hours at 12 DIV. At 12 DIV, cell viability was measured using CCK8. B) Primary cultured mouse cerebral cortical neurons were treated with vehicle as control (CTL) or 1 μM CORT at 7 DIV for 5 days or 5 μM Antimycin A as a positive control at 10 DIV for 48 hours. At 12 DIV, cell viability was also measured by LDH release assay. Data analysis was carried out using one-way ANOVA with Tukey's post-hoc. * indicates $p<0.05$ as compared to control. Findings are presented as mean ± SEM (N=6-8).

3.2 To determine if chronic CORT treatment inhibits neurite outgrowth in primary cultured mouse cerebral cortical neurons.

3.2.1 The effect of chronic CORT treatment on neurite outgrowth

Chronic treatment with CORT induced protein oxidation in primary cultured neurons, which may further cause impairment in neuronal outgrowth. MAP2 is a neuron-specific cytoskeleton-associated protein. The effect of chronic CORT exposure on neurite outgrowth were measured by using immunocytochemistry with MAP2 antibody. Primary cultured neurons were treated with CORT 1 μM or vehicle at 7 DIV for 5 days. At 12 DIV, MAP2 antibody was used to stain neurite branches and fluorescent microscope was used to take pictures of stained neurites. We found that average length and number of primary neurites in control group were 172.89μm ± 11.22 and 6.55 ± 0.35, respectively. Average total length and number of branches in control group were 355.49μm ± 22.20 and 14.90 ± 0.82, respectively. Our finding showed that treatment with CORT for 5 days induced significant decline in the length and number of primary neurite branches ($p<0.05$, N=40) as well as total number and length of neurite branches ($p<0.05$, N=40) (Figure 18). This finding indicates that chronic CORT treatment can inhibit neurite outgrowth.

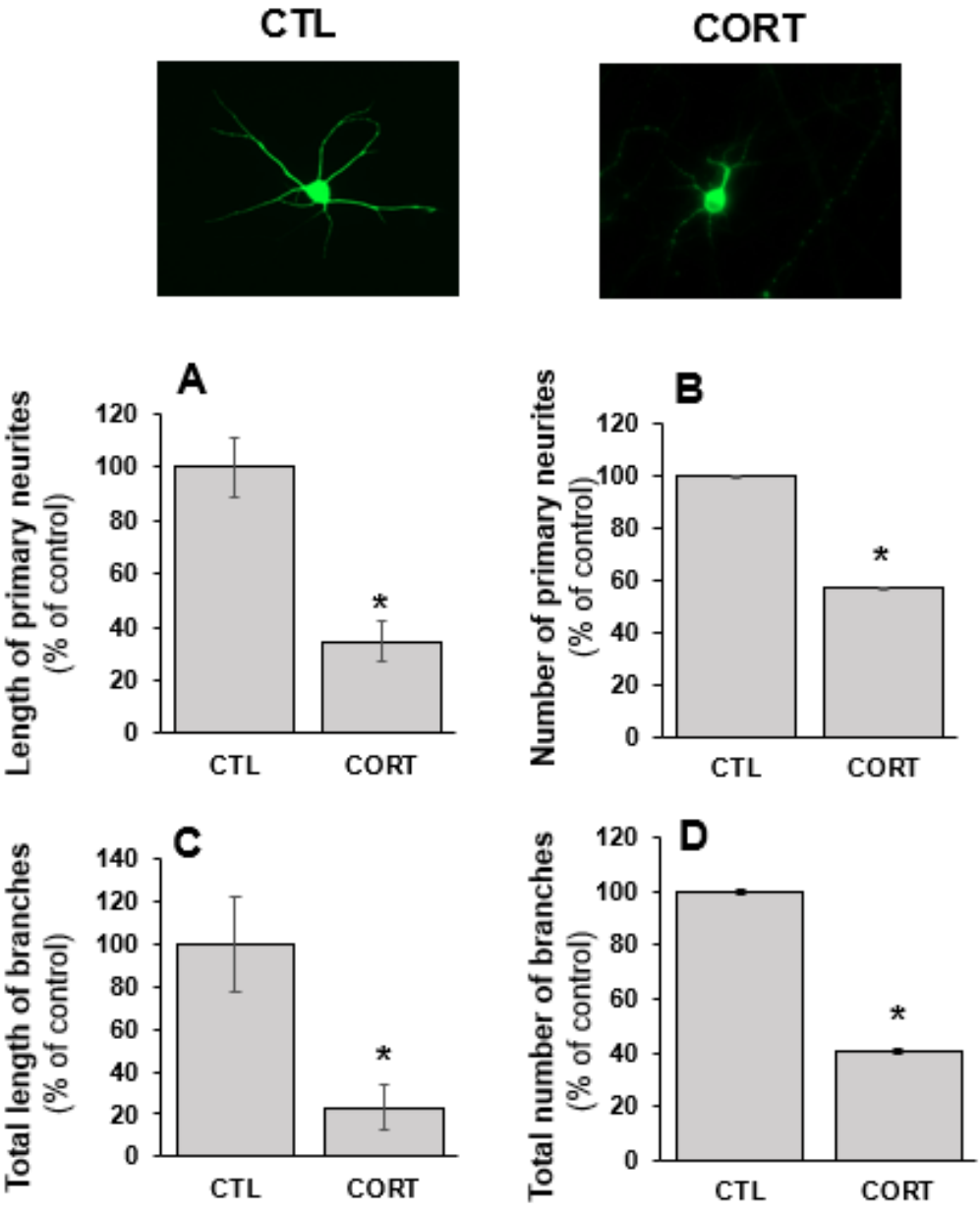

Figure 18. The effect of CORT on neurite outgrowth

Primary cultured mouse cerebral cortical neurons were treated with vehicle as control (CTL) and 1 μM CORT at 7 DIV for 5 days. Neurons were stained by MAP2 antibody using immunocytochemistry at 12DIV. The length (A) and number (B) of primary neurites, and total length (C) and number (D) of branches were quantified. * indicates $p<0.05$ using Student-T test, when comparing CORT treated group with control. Findings are presented as mean ± SEM (N=40).

3.2.2 The effect of Txnip knockdown on CORT-impaired neurite outgrowth

To understand whether Txnip mediates CORT-induced neuronal outgrowth impairment, we knocked down Txnip and then measured neurite outgrowth. Txnip was knocked down by CRISPR/Cas9. At 1 DIV, cells were treated with Txnip sgRNAs/CRISPR/Cas9 or scrambled sgRNAs/CRISPR/Cas9 (SCM). 72 hours after transfection, selection of transfected cells was done by introducing 1μg/ml puromycin to cells. As presented in Figure 19, Txnip protein levels were significantly reduced in Txnip sgRNAs transfected neurons in comparison with scrambled sgRNAs transfected neurons ($p<0.05$, N=5). Then, transfected neurons were treated with CORT 1 μM at 7 DIV for 5 days. At 12 DIV, MAP2 antibody was used to stain neurite branches and fluorescent microscope was used to take pictures of stained neurites. We found that average length and number of primary neurites in SCM transfected neurons were 87.58μm ± 7.27 and 6.40 ± 0.26, respectively. Average total length and number of branches in SCM transfected neurons were 273.97μm ± 20.52 and 19.70 ± 1.09, respectively. As shown in Figure 20, we observed that CORT treatment significantly reduced the number and length of primary neurite branches, and total length and number of neurite branches in SCM transfected primary cultured neurons ($p<0.05$, N=40). However, CORT treatment had no effect on the length ($p=0.999$, N=40) and number of primary neurite branches ($p=0.992$, N=40) when compared to controls in Txnip sgRNA transfected primary cultured neurons as well as total number ($p=0.451$, N=40) and length of neurite branches ($p=0.378$, N=40) when compared to controls in Txnip sgRNA transfected primary cultured neurons. This finding indicates that knocking down Txnip gene can prevent chronic CORT treatment-reduced neurite outgrowth.

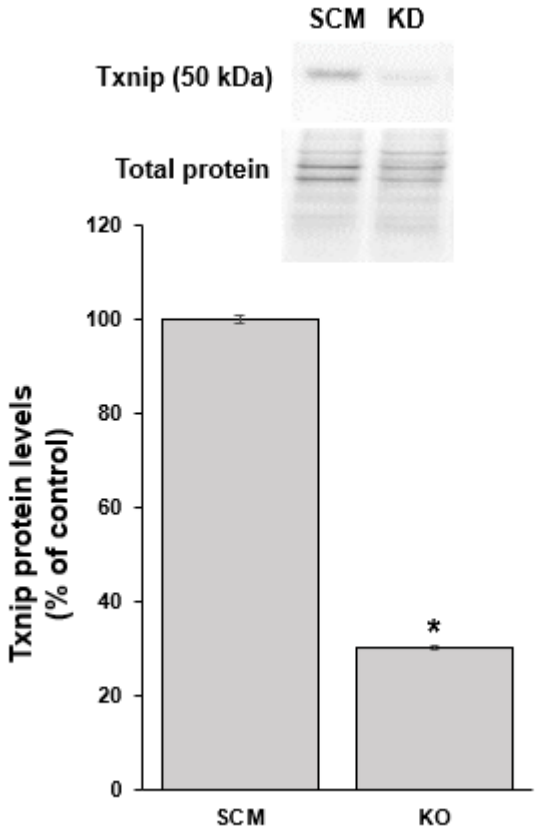

Figure 19. Knocking down of Txnip gene in primary cultured mouse cerebral cortical neurons

At 1DIV, cultured neurons were transfected with Txnip sgRNAs/CRISPR/Cas9 (KD) or scrambled sgRNAs/CRISPR/Cas9 (SCM). At 12 DIV, Txnip protein levels were measured using immunoblotting analysis to analyze knocking down of Txnip gene. Blot stain free for total protein used as a normalization control. * indicates $p<0.05$ using Student-T test, when comparing Txnip KD with SCM. Findings are presented as mean ± SEM (N=5).

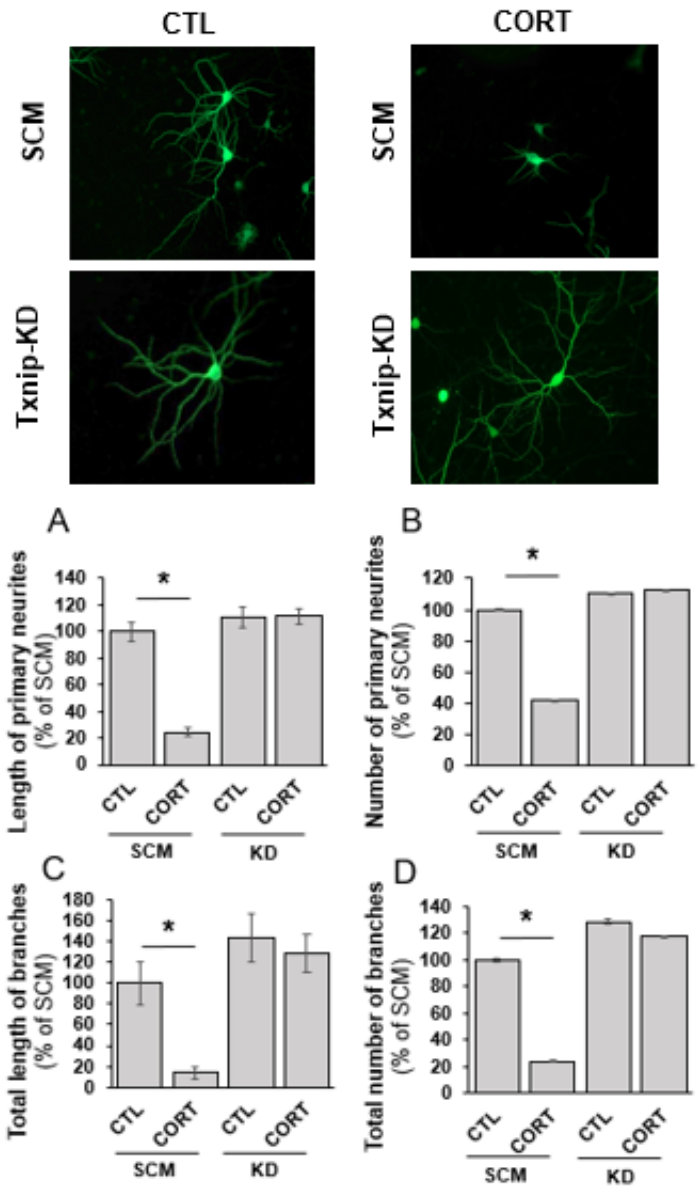

Figure 20. The effect of knockdown Txnip on corticosterone (CORT)-impaired neurite outgrowth in primary cultured mouse cortical neurons

At 1DIV, primary cultured mouse cerebral cortical neurons were transfected with Txnip sgRNAs/CRISPR/Cas9 (KD) or scrambled sgRNAs/CRISPR/Cas9 (SCM). At 7 DIV, cells were treated with vehicle as control (CTL) or 1μM CORT for 5 days. Neurons were stained by MAP2 antibody performing immunocytochemistry at 12DIV. The length (A) and number (B) of primary branches, and total length (C) and number (D) of branches were quantified. Data analysis was performed using one-way ANOVA with Tukey's post-hoc. * indicates $p<0.05$ as compared to SCM-CTL. Findings are presented as mean ± SEM (N=40).

4 CHAPTER 4: DISCUSSION

4.1 Chronic CORT treatment upregulates Txnip

Previously our laboratory has discovered that treatment with 1 μM CORT for 5 days elevated Trx endogenous inhibitor, Txnip protein levels, in primary cultured mouse cerebral cortical neurons and HT22 mouse hippocampal cells [164]. In this present research, we further verified that although CORT treatment elevated Txnip protein levels, it did not affect Trx protein levels in primary cultured mouse cerebral cortical neurons. Furthermore, we also observed that treatment of primary cultured neurons with CORT at 0.01, 0.1 and 1 μM for 5 days dose-dependently increased Txnip protein levels. These findings suggest that Txnip can be elevated following chronic CORT treatment. Studies have found that chronic unpredictable stress exposure for 3-4 weeks in rodents not only led to exhibition of depressive-like behaviors but also elevated Txnip protein levels in hippocampus and frontal cortex [161, 163]. Many studies have shown that exposure of mice and rats to chronic unpredictable stress elevated plasma CORT concentration [168-172]. Taken together, these findings indicate that chronic stress may increase CORT levels, causing Txnip upregulation and depressive-like behaviors. Since Txnip can bind to Trx and inhibit Trx activity, facilitating oxidative stress, our result suggests that chronic CORT treatment may upregulate Txnip, leading to oxidative damage.

Once CORT binds to the glucocorticoid receptor (GR) in the cytoplasm, it induces conformational alteration in GR and results in activation of GR. Subsequently, GR translocate into the nucleus and binds to glucocorticoid response elements (GRE) in DNA, where it can directly control transcription of target genes [129]. Our laboratory previously found that treatment with GR inhibitor RU486 suppressed chronic CORT treatment-upregulated Txnip protein levels in cultured

mouse cerebral cortical neurons, indicating GR may mediate CORT-upregulated Txnip [164]. Our laboratory also observed that treatment with CORT for 5 days not only elevated Txnip protein levels but also increased Txnip mRNA levels, suggesting that CORT may induce Txnip gene expression, further elevating Txnip protein levels.

Txnip gene promoter region has a GRE sequence. It has been reported that treatment of WEHI7.2 murine T-lymphoma cells with synthetic GC dexamethasone elevated Txnip mRNA levels, and that dexamethasone-increased Txnip mRNA can be inhibited by GR antagonist RU486 [173]. Further, when pGL3B vector with Txnip promoter and a luciferase reporter was transfected into WEHI7.2 murine T-cells, dexamethasone treatment was observed to enhance luciferase activity when compared to controls. Deletion and mutation of GRE sequence in Txnip promoter region inhibited dexamethasone treatment-increased luciferase activity [173]. This finding suggests that stimulation of Txnip expression following treatment with dexamethasone is facilitated by presence of GRE in promoter region of Txnip [173]. These findings together indicate that chronic CORT treatment may target GR and facilitate GR binding to GRE site in Txnip promoter region, which increases GRE-driven Txnip gene expression.

Txnip promoter region was also found to contain antioxidant response element (ARE) and carbohydrate response element (ChoRE) sites. Transcription factor Nrf2 can bind to ARE site, while transcription factor MondoA can bind to ChoRE site [174, 175]. Recent studies found that activated MondoA can bind to ChoRE site, which induces ChoRE-mediated Txnip gene expression [175-177]. However, activated Nrf2 was found to bind to ARE site, which inhibits MondoA binding to ChoRE site and then inhibits Txnip gene expression [174]. It has been reported that chronic unpredictable stress for 21 days reduced Nrf2 mRNA and protein levels in rat frontal cortex [178]. Chronic restraint stress for 35 days caused reduction in Nrf2 protein levels in rat

hippocampus [179]. Furthermore, it was also found that treatment of mice with CORT 35mg/ml for 28 days decreased protein levels of Nrf2 in frontal cortex and hippocampus [180]. These results suggest that prolonged exposure to stress or chronic CORT administration may reduce Nrf2 expression, further upregulating Txnip gene expression.

Overall, we observed that chronic CORT treatment did not affect Trx protein levels, but elevated Txnip protein levels in primary cultured mouse cerebral cortical neurons. Since Txnip inhibits activity of antioxidant Trx, this result indicates that chronic CORT treatment may enhance Txnip, further causing oxidative damage. Because Txnip promoter region contains a functional GRE site, chronic CORT treatment may activate GR and elevate GR/GRE binding, upregulating GRE-driven Txnip gene expression. Because Txnip promoter region also contains other gene transcription factor DNA binding sites, chronic CORT treatment may also regulate Txnip expression through GRE-independent mechanisms.

4.2 Chronic CORT treatment increases oxidative protein modification

Txnip is an endogenous Trx inhibitor protein. Trx is a redox protein and can directly reduce oxidative modifications in protein cysteine including protein sulfenylation and protein nitrosylation [181, 182]. Additionally, Trx also reduces oxidized Prx and maintains Prx at an active state. Prx scavenges H_2O_2 that attacks protein cysteines and causes protein sulfenylation [130]. Therefore, Trx can activate Prx and inhibit H_2O_2 accumulation, which indirectly prevents protein sulfenylation. Further, H_2O_2 can also interact with transition ions to produce hydroxyl radicals, which causes protein carbonylation [72]. Therefore, Trx can also prevent protein carbonylation production. Binding of Txnip to Trx active site inhibits enzyme activity of Trx, which may promote protein sulfenylation, protein nitrosylation and protein carbonylation.

In the present study, primary cultured mouse cerebral cortical neurons were treated with CORT at 1 μM for 5 days. We found that 5 days treatment with CORT elevated sulfenylated protein levels and carbonylated protein levels, while it did not affect nitrosylated protein levels. Our result suggests that chronic CORT treatment can induce protein sulfenylation and carbonylation in cultured neurons.

Chronic CORT treatment may elevate Txnip expression, further inhibiting reduction of sulfenylated thiols in protein cysteines and also promoting forming of protein sulfenylation. First, CORT-upregulated Txnip may stimulate Txnip/Trx binding, which attenuates reducing activity of Trx, resulting in accumulation of sufenylated protein. Second, CORT-upregulated Txnip may inhibit Trx activity, which further promotes Prx oxidation and inhibits Prx activity. Inhibited Prx activity can induce H_2O_2 accumulation, promoting protein cysteine sulfenylation [183]. Previous research has observed that 6 hours of chronic restraint stress once a day for 4 weeks increased oxidized Prx protein levels in frontal cortex and hippocampus of mice[184]. Similarly, 7 weeks of chronic unpredictable stress caused elevation in the levels of oxidized Prx in frontal cortex of rats [185]. Oxidized Prx is an inactive form of Prx and can not scavenge H_2O_2. These findings indicate that chronic stress can increase H_2O_2 accumulation by inhibiting Prx activity. Indeed, many studies have shown that chronic restraint stress and chronic unpredictable stress elevated ROS levels in mouse hippocampus and frontal cortex [88, 89, 91]. It has been found that chronic CORT treatment elevated ROS levels in cultured neuronal cells *in vitro* [89, 95]. In this current research, we also observed that treatment of HT22 mouse hippocampal cells with H_2O_2 at 0.5 mM increased sulfenylated protein levels. This finding indicates that CORT- upregulated Txnip may inhibit Trx reducing activity, causing Prx to remain oxidized and at inactive state. Oxidized Prx is unable to neutralize H_2O_2 and induces H_2O_2 accumulation, resulting in generation of protein sulfenylation.

Cysteine residues of proteins contain thiol group that provides it with unique chemical properties. Nucleophilic reactivity, redox activity and having affinity to metals are characteristics of thiol that enable cysteine to be important in protein functioning [186]. Cysteine participates in redox balance, signaling, structural stability, enzymatic catalysis and metal binding [123]. Our result suggests that chronic CORT treatment may induce protein cysteine sulfenylation, and further interrupt cysteine-mediated protein function.

Chronic CORT treatment may elevate Txnip expression, further promoting forming of protein carbonylation. Protein carbonylation is usually generated by highly reactive hydroxyl radical that can attack side-chain amino acids such as threonine, proline, lysine and arginine of protein [187]. Prx is responsible for scavenging H_2O_2 by converting it to water. During this process, redox-active cysteine of Prx becomes oxidized. Oxidized Prx is reduced back to its reduced form by Trx [129]. CORT-increased Txnip may inhibit Trx reducing activity and prevent Prx reduction, causing H_2O_2 accumulation. Accumulated H_2O_2 may further react with metal ions such as Cu^+ and Fe^{2+} to generate hydroxyl radicals that attack proteins and cause protein carbonylation. It has been reported that treatment with H_2O_2 at 0.1-0.3 mM for 24 and 48 hours increased carbonylated protein levels in rat PC12 cells [188]. In this current study, we also observed that treatment of HT22 mouse hippocampal cells with H_2O_2 at 1 and 2 mM for 1.5 hours elevated carbonylated protein levels. This result implies that CORT-increased Txnip may inhibit Prx and increase H_2O_2 accumulation, promoting hydroxyl radical production and causing protein carbonylation.

Chronic CORT treatment may directly promote ROS production, which induces protein sulfenylation and carbonylation by Txnip/Trx independent pathways. Mitochondria (complex I and III) are recognized as a principal origin of ROS production. Impairment in transferring electrons through mitochondrial respiratory chain exacerbates generation of ROS [189]. It has been

found that chronic restraint stress inhibited activities of mitochondrial electron transport chain complexes I, II and III in rat brain [92]. Research has also shown that chronic unpredictable inhibited activities of mitochondrial complexes I, III and IV in rat cerebellum and cerebral cortex [93]. It has been found that activity of mitochondrial complex I was reduced in PC12 cells treated with dexamethasone at 125 μM for 24 hours [87]. These results indicate that chronic stress and CORT treatment may induce mitochondrial dysfunction and increase ROS production, which increases protein sulfenylation and carbonylation.

NADPH oxidase is another source for ROS production. It has been shown that chronic restraint stress elevated NADPH oxidase activity in rat cerebral cortex [90]. Chronic restraint stress and chronic CORT treatment were also found to increase NADPH oxidase subunits, p67phox and p47phox protein levels in mouse hippocampus [89]. It has been reported that prefrontal cortex of rats subjected to chronic mild stress for seven weeks resulted in increase of mRNA levels of NADPH oxidase 2 [185]. These results indicate that chronic stress and chronic CORT treatment may activate NADPH oxidase, increasing ROS production and promoting protein sulfenylation and carbonylation.

Many studies also reported that chronic stress and chronic CORT treatment elevated lipid peroxidation, reduced activities of antioxidant enzymes including superoxide dismutase, glutathione peroxidase and catalase, and inhibited total antioxidant capacity in rodent brain and cultured neuronal cells [94, 98, 190-193]. End products of lipid peroxidation including MDA and 4-HNE can form adducts with protein and introduce carbonylated groups to proteins. Inhibition of antioxidant enzymes can cause ROS accumulation that causes protein sulfenylation and carbonylation. Therefore, chronic stress and chronic CORT treatment may cause elevation in lipid peroxidation and decrease in antioxidant defense, promoting protein sulfenylation and

carbonylation.

In summary, we observed that 5 days treatment with CORT elevated sulfenylated protein levels and carbonylated protein levels in primary cultured mouse cerebral cortical cells. These results suggest that chronic CORT treatment promotes protein sulfenylation and carbonylation. Since chronic CORT treatment upregulates Txnip and Txnip facilitates oxidative stress, Txnip may mediate chronic CORT treatment - elevated protein sulfenylation and carbonylation.

4.3 Chronic CORT treatment has no effect on ASK1 apoptotic signaling

ASK1 apoptotic signaling can be activated by different stimuli such as ROS, endoplasmic reticulum stress, cytokines and others. ASK1 activation can result in phosphorylation and activation of JNK and p38, and promote apoptosis and release cytokines [194]. Under normal physiological conditions, Trx can interact with ASK1 N-terminal domain and result in formation of Trx/ASK1 complex. Trx/ASK1 complex inhibits ASK1 activity and prevents initiation of ASK1 apoptotic signaling pathways [137]. In the presence of Txnip, Txnip forms Txnip/Trx complex, and then ASK1 dissociates from Trx. Unbound ASK1 becomes phosphorylated and initiates apoptosis cascade [153]. In the current study, we found that treatment of primary cultured neurons with 1μM CORT for 5 days did not affect total ASK1 protein levels and ratio of phosphorylated ASK1/ total ASK1 protein levels. This result suggest that chronic CORT treatment has no effect on ASK1 phosphorylation. We also found that although rotenone and antimycin A (used as a complex I and complex III inhibitor respectively) reduced cell viability, 1μM CORT for 5 days did not affect cell viability in primary cultured mouse cerebral cortical neurons. According to the results of this study, it can be concluded that chronic CORT treatment does not affect ASK1 apoptotic signaling in primary cultured mouse cortical neurons.

4.4 Txnip mediates CORT-impaired neurite outgrowth

In this current study, we observed that treatment with CORT at 1μM from 7 DIV-12 DIV for 5 days significantly decreased primary neurite length and branches and total neurite length and branches in primary cultured mouse cerebral cortical neurons, suggesting chronic CORT treatment impairs neurite outgrowth.

Ability of the brain to adapt its function and structure in response to external and internal stimuli is recognized as a brain plasticity [27]. Alteration in neuronal connectivity is crucial factor in brain plasticity. Changes in dendritic length and branching can have a significant impact on neuroplasticity [195]. In primary cultured rodent neurons, neurons extend neurite and differentiate to mature neurons during 1 DIV-7 DIV. Then extended neurites start to form synaptic connections during 7 DIV-14 DIV. Between 14 DIV-25 DIV, extensive network of neurons is fromed. After 25 DIV, neurons start to degenerate [196, 197]. Since cultured neurons were treated with CORT from 7 DIV-12 DIV, our result also suggests that chronic CORT treatment may inhibit neuronal outgrowth which may ultimately result in synaptic connection impairment.

To explore the role of Txnip in CORT-impaired neurite outgrowth, we knocked down Txnip in primary cultured mouse cerebral cortical neurons using CRISPR/Cas9/Txnip sgRNA. Our result showed that knocking down Txnip gene prevented chronic CORT treatment-reduced neurite number and length of primary and total neurite branches. Our result suggests that chronic CORT treatment may impair neurite outgrowth by upregulating Txnip.

Previously, research has shown that ROS can induce impairment of neuronal growth. Morphological observation has shown that treatment of rat PC12 cells with 200 μM H_2O_2 for 6 hours diminished neurites [198]. Also, 24-hour treatment of PC12 cells with 150 μM H_2O_2 caused

reduction in the length and number of primary neurites [199]. Treatment with 30 μM H_2O_2 for 24 hours has been found to decrease total neurite length in primary cultured rat cerebral cortical neurons [200]. Also, significant reduction has been observed in length of neurite in primary cultured cortical neurons treated with H_2O_2 at concentration of 100 μM for 120 minutes [201]. Research has also shown that incubation of PC12 cells with NGF promoted neurite length, but treatment of PC12 cells with 10 μM H_2O_2 for 72 hours inhibited NGF-increased neurite length [202]. Taken together, it is suggested that CORT-induced overexpression of Txnip protein levels leads to overproduction of ROS by preventing Trx function. Excessive levels of ROS may lead to impairment in neurite outgrowth.

Neurotrophic factor BDNF is involved in neuronal differentiation, neuronal survival, synaptic plasticity and nerve growth. Expression of BDNF is regulated by binding of phosphorylated transcription factor CREB to the cAMP response element on the promoter of BDNF gene [47-49]. Studies have shown that chronic stress can interrupt CREB/BDNF signaling. For example, research showed that stress induced by separation of neonatal rats from their dam at day 2 of postnatal for 7 days caused significant reduction in phosphorylated CREB levels in hippocampus [203]. It has also been found that chronic mild stress for 4 weeks decreased mRNA levels of CREB and BDNF in mouse hippocampus [204]. Similarly, chronic restraint stress resulted in reduction of BDNF mRNA and protein levels in rat hippocampus [205, 206]. Further, it has been observed that chronic CORT treatment decreased phosphorylated CREB levels, and BDNF mRNA and protein levels in rodent brain [57, 58]. Administration of GR agonist dexamethasone at 10 μM over 3 days led to decrease in BDNF-induced neurite outgrowth in primary cultured rat hippocampal neurons [207]. Therefore, these findings indicate that chronic stress or chronic and excessive

CORT treatment downregulates CREB/BDNF neurotrophic signaling and further impairs neurite outgrowth.

ROS can suppress CREB/BDNF neurotrophic signaling. It has been reported in rat PC12 cells that treatment with H_2O_2 at 400 μM reduced phosphorylated CREB levels and morphological observation of neurites showed that H_2O_2 caused shortened neurites [208]. Treatment with H_2O_2 at 400 and 800 μM was also found to reduce neurite number and length in ventral spinal cord neuron X mouse neuroblastoma VSC4.1 hybrid cells [209]. Our laboratory also discovered that treatment of SH-SY5Y human neuroblastoma cells with 150 and 300 μM H_2O_2 caused reduction in phosphorylated CREB levels [157]. These findings suggest that ROS may damage neurons by targeting CREB/BDNF signaling. Recently, our laboratory also found that CREB cysteine residues can be oxidized and CREB oxidation attenuates phosphorylation of CREB [157], suggesting that H_2O_2-induced impairment of neurite outgrowth may be mediated by CREB oxidation. Trx can promote neurite outgrowth. Research showed that treatment with 1μM recombinant Trx for 2 days elevated neurite outgrowth in PC12 cells. Trx-induced neurite outgrowth is as effective as NGF-induced neurite outgrowth [156]. Previously our laboratory also found that knocking down Trx gene decreased length and number of dendritic branches in primary cultured mouse cerebral cortical neurons [157]. Since Txnip acts as an endogenous inhibitor for Trx, these findings together indicate that chronic stress or chronic CORT treatment may upregulate Txnip, subsequently inhibiting Trx and facilitating CREB oxidation, resulting in downregulating CREB/BDNF signaling and impairing neurite outgrowth.

Overall, we found that chronic CORT treatment decreased primary neurite length and branches and total neurite length and branches in primary cultured mouse cerebral cortical neurons; and that knocking down Txnip gene using Txnip sgRNA prevented chronic CORT treatment-reduced

neurite number and length of primary and total neurite branches. Our result indicates that chronic CORT treatment impairs neurite outgrowth and that Txnip may mediate chronic CORT treatment-impaired neurite outgrowth. Because we also observed that chronic CORT treatment increases Txnip expression and oxidative protein damage, our results indicate that chronic CORT treatment may elevate Txnip, promoting oxidative damage and further impairing neurite outgrowth. Since Trx can produce neurotrophic effect and ROS can interrupt CREB/BDNF neurotrophic signaling, our results may also indicate that CORT-upregulated Txnip inhibits Trx activity and elevates ROS formation, further damaging CREB/BDNF neurotrophic signaling and neurite outgrowth.

5 CHAPTER 5: SUMMARY, LIMITATION AND FUTURE STUDIES

5.1 Summary

Firstly, we veified that although treatment with CORT 1 μM at 7 DIV for 5 days had no effect on Trx, this treatment elevated Txnip levels in primary cultured mouse cerebrocortical neurons. Further we found that treatment with CORT at concentrations of 0.01, 0.1 and 1 μM dose-dependently increase Txnip protein levels in cultured neurons. We also verified that treatment of HT22 mouse hippocampal cells with H_2O_2 elevated sulfenylated protein levels and carbonylated protein levels, and treatment of these cells with NO donor GSNO led to elevation in nitrosylated protein levels. We also found that chronic treatment with CORT elevated sulfenylated protein levels and carbonylated protein levels, but it did not affect nitrosylated protein levels in primary cultured mouse cerebrocortical neurons. We also found that chronic CORT treatment did not affect ASK1 phosphorylation and cell viability in cultured neurons. Since Txnip acts as an endogenous Trx inhibitor protein, our results indicate that chronic CORT treatment may upregulate Txnip, inhibit Trx reducing activity and promote oxidative protein modification such as protein sulfenylation and protein carbonylation, but have no effect on ASK1 apoptotic signaling.

Second, we found that treatment with CORT 1 μM at 7 DIV for 5 days reduced the length and number of primary neurite branches and the length and number of total neurite branches in primary cultured mouse cerebrocortical neurons. By utilizing CRISPR/Cas9/Txnip sgRNA technique we further found that although chronic CORT treatment decreased the number and length of primary and total neurite branches in scrambled sgRNAs transfected neurons, CORT treatment had no effect on the length and number of primary and total neurite branches in Txnip sgRNA transfected

neurons. This result suggests that knocking down Txnip gene could prevent chronic CORT treatment-reduced neurite outgrowth.

As shown in Figure 21, our results suggest that chronic CORT treatment elevates Txnip, inhibits Trx reducing activity, resulting in increased protein oxidative modifications that impair neurite outgrowth. Because chronic stress is considered a major risk factor in developing depression and other psychiatric disorders, our findings also recommend that Txnip can be a potential target in treatment of psychiatric disorders.

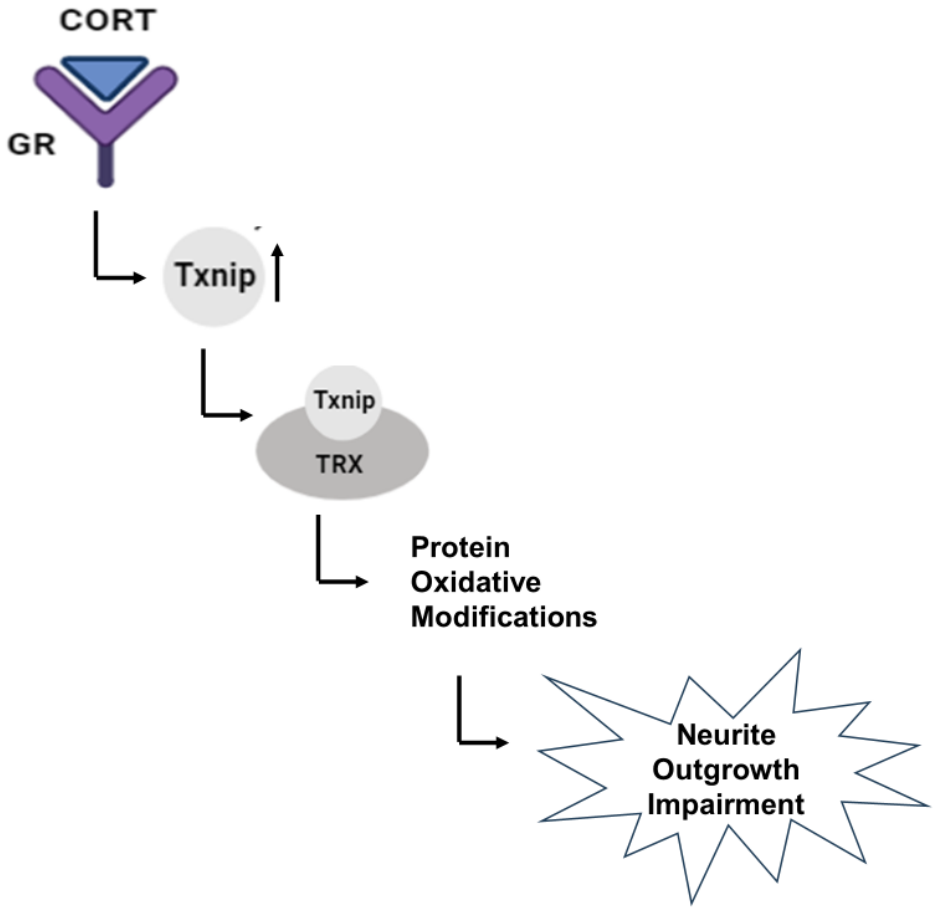

Figure 21. Potential role of thioredoxin-interacting protein in corticosterone-mediated protein oxidative damage and neurite outgrowth impairment. Chronic treatment with CORT can upregulate Txnip which inhibits Trx activity, further promoting protein cysteine oxidations and ultimately resulting in neurite outgrowth impairment.
GR: Glucocorticoid receptor, CORT: Corticosterone, Txnip: Thioredoxin interacting protein Trx, Thioredoxin. (Created by using www.biorender.com)

5.2 Limitation and future studies

Several limitations need to be acknowledged concerning the present study.

First, nitrosylation and sulfenylation of thiol group in cysteine residues of proteins are reversible oxidative modifications that may return to their reduced form during experiments. This makes the assessment of these oxidative modifications difficult. However, we tried to reduce the risks by incubation in blocking buffer for a longer time and running western blot the same day as isolating proteins. Mass spectrometry (MS) method can be also employed to identify protein nitrosylation and sulfenylation.

Second, in this research, we measured neurite outgrowth using immunocytochemistry with MAP2 antibody. MAP2 is predominantly found in dendrites, so we did not measure axonal growth. Studies have shown that primary cultured neurons develop neuronal polarity, with axons and dendrites having different structural organization and specific protein expression [210-212]. Axonal growth can be assessed by performing immunocytochemistry using anti-tau antibody to stain axons (Tau is a protein that is associated with microtubules and it is found in axons) [213]. Future research should be undertaken to explore the effect of CORT on axonal growth for better understanding of Txnip's role in CORT-impaired neuronal development.

Third, our cultured neurons were derived from cerebral cortical of embryonic mice. However, it is not very clear whether chronic CORT treatment affects other brain regions related to stress responses. In future, we will analyze the effect of chronic CORT treatment on Txnip and oxidative protein modification in hippocampus and amygdala. In addition, neuronal differentiation and development in the brain are influenced by other cell types such as astrocytes and microglia, while

in our study we only focused on cerebral cortical neurons. Future studies could be carried out to understand the effects of chronic CORT treatment on astrocytes and microglia.

Fourth, Txnip gene in primary cultured cortical neurons was knocked down by CRISPR/Cas9 technology. CRISPR/Cas9 technology may lead to the occurrence of off-target effects and target other genes. In this study, we did not investigate off-target of CRISPR/Cas9 system. It is needed to conduct further research to detect unwanted or unintended gene editing by whole genome sequencing (WGS), GUIDE-seq and CIRCLE-seq [214-216].

Fifth, our research only focused on *in vitro* studies, however conducting *in vivo* studies and behavioral research provides us with a comprehensive understanding of Txnip's role in mediating CORT-induced adverse effects in the brain. Previously in our lab we showed that chronic stress upregulated Txnip in mouse frontal cortex and hippocampus and induced depressive-like behaviors [163], suggesting that Txnip may be involved in chronic stress-induced damaging effects to the brain. In the future, we will investigate behavioral changes in mice following systemic administration of CORT including behavioral despair in the forced swim test, anhedonia in the sucrose preference test, anxiety-like behaviors in the open field test [163, 217] and cognitive dysfunction in the novel object recognition test [218].

References

1. Sheng, J.A., et al., The Hypothalamic-Pituitary-Adrenal Axis: Development, Programming Actions of Hormones, and Maternal-Fetal Interactions. Front Behav Neurosci, 2020. 14: p. 601939.
2. McEwen, B.S., et al., Mechanisms of stress in the brain. Nat Neurosci, 2015. 18(10): p. 1353-63.
3. Marin, M.F., et al., Chronic stress, cognitive functioning and mental health. Neurobiol Learn Mem, 2011. 96(4): p. 583-95.
4. Ströhle, A. and F. Holsboer, Stress responsive neurohormones in depression and anxiety. Pharmacopsychiatry, 2003. 36 Suppl 3: p. S207-14.
5. Makino, S., K. Hashimoto, and P.W. Gold, Multiple feedback mechanisms activating corticotropin-releasing hormone system in the brain during stress. Pharmacol Biochem Behav, 2002. 73(1): p. 147-58.
6. Maniam, J., C. Antoniadis, and M.J. Morris, Early-Life Stress, HPA Axis Adaptation, and Mechanisms Contributing to Later Health Outcomes. Front Endocrinol (Lausanne), 2014. 5: p. 73.
7. Smith, S.M. and W.W. Vale, The role of the hypothalamic-pituitary-adrenal axis in neuroendocrine responses to stress. Dialogues Clin Neurosci, 2006. 8(4): p. 383-95.
8. Vandenborne, K., et al., Corticosterone-induced negative feedback mechanisms within the hypothalamo-pituitary-adrenal axis of the chicken. J Endocrinol, 2005. 185(3): p. 383-91.
9. Gjerstad, J.K., S.L. Lightman, and F. Spiga, Role of glucocorticoid negative feedback in the regulation of HPA axis pulsatility. Stress, 2018. 21(5): p. 403-416.
10. Keller-Wood, M., Hypothalamic-Pituitary--Adrenal Axis-Feedback Control. Compr Physiol, 2015. 5(3): p. 1161-82.
11. Ramamoorthy, S. and J.A. Cidlowski, Corticosteroids: Mechanisms of Action in Health and Disease. Rheum Dis Clin North Am, 2016. 42(1): p. 15-31, vii.
12. Althaher, A.R., An Overview of Hormone-Sensitive Lipase (HSL). ScientificWorldJournal, 2022. 2022: p. 1964684.
13. Silverman, M.N. and E.M. Sternberg, Glucocorticoid regulation of inflammation and its functional correlates: from HPA axis to glucocorticoid receptor dysfunction. Ann N Y Acad Sci, 2012. 1261: p. 55-63.
14. Munhoz, C.D., et al., Glucocorticoids exacerbate lipopolysaccharide-induced signaling in the frontal cortex and hippocampus in a dose-dependent manner. J Neurosci, 2010. 30(41): p. 13690-8.
15. Merk, V.M., et al., Glucocorticoids are differentially synthesized along the murine and human respiratory tree. Allergy, 2023.
16. Vandewalle, J., et al., Therapeutic Mechanisms of Glucocorticoids. Trends Endocrinol Metab, 2018. 29(1): p. 42-54.
17. Koning, A., et al., Glucocorticoid and Mineralocorticoid Receptors in the Brain: A Transcriptional Perspective. J Endocr Soc, 2019. 3(10): p. 1917-1930.
18. Juszczak, G.R. and A.M. Stankiewicz, Glucocorticoids, genes and brain function. Prog Neuropsychopharmacol Biol Psychiatry, 2018. 82: p. 136-168.
19. Madalena, K.M. and J.K. Lerch, The Effect of Glucocorticoid and Glucocorticoid Receptor Interactions on Brain, Spinal Cord, and Glial Cell Plasticity. Neural Plast, 2017. 2017: p. 8640970.

20. Bamberger, C.M., H.M. Schulte, and G.P. Chrousos, Molecular determinants of glucocorticoid receptor function and tissue sensitivity to glucocorticoids. Endocr Rev, 1996. 17(3): p. 245-61.
21. Oakley, R.H. and J.A. Cidlowski, The biology of the glucocorticoid receptor: new signaling mechanisms in health and disease. J Allergy Clin Immunol, 2013. 132(5): p. 1033-44.
22. Saklatvala, J., Glucocorticoids: do we know how they work? Arthritis Res, 2002. 4(3): p. 146-50.
23. Newton, R. and N.S. Holden, Separating transrepression and transactivation: a distressing divorce for the glucocorticoid receptor? Mol Pharmacol, 2007. 72(4): p. 799-809.
24. Cruz-Topete, D. and J.A. Cidlowski, One hormone, two actions: anti- and pro-inflammatory effects of glucocorticoids. Neuroimmunomodulation, 2015. 22(1-2): p. 20-32.
25. Zenz, R., et al., Activator protein 1 (Fos/Jun) functions in inflammatory bone and skin disease. Arthritis Res Ther, 2008. 10(1): p. 201.
26. Liu, T., et al., NF-κB signaling in inflammation. Signal Transduct Target Ther, 2017. 2: p. 17023-.
27. Mateos-Aparicio, P. and A. Rodríguez-Moreno, The Impact of Studying Brain Plasticity. Front Cell Neurosci, 2019. 13: p. 66.
28. Forrest, M.P., E. Parnell, and P. Penzes, Dendritic structural plasticity and neuropsychiatric disease. Nat Rev Neurosci, 2018. 19(4): p. 215-234.
29. Cramer, S.C., et al., Harnessing neuroplasticity for clinical applications. Brain, 2011. 134(Pt 6): p. 1591-609.
30. Sasmita, A.O., J. Kuruvilla, and A.P.K. Ling, Harnessing neuroplasticity: modern approaches and clinical future. Int J Neurosci, 2018. 128(11): p. 1061-1077.
31. Frankfurt, M. and V. Luine, The evolving role of dendritic spines and memory: Interaction(s) with estradiol. Horm Behav, 2015. 74: p. 28-36.
32. Picard, K., et al., Neuroendocrine, neuroinflammatory and pathological outcomes of chronic stress: A story of microglial remodeling. Neurochem Int, 2021. 145: p. 104987.
33. Li, N., et al., Glutamate N-methyl-D-aspartate receptor antagonists rapidly reverse behavioral and synaptic deficits caused by chronic stress exposure. Biol Psychiatry, 2011. 69(8): p. 754-61.
34. Radley, J.J., et al., Repeated stress induces dendritic spine loss in the rat medial prefrontal cortex. Cereb Cortex, 2006. 16(3): p. 313-20.
35. Fraga, D.B., et al., Ketamine, but not fluoxetine, rapidly rescues corticosterone-induced impairments on glucocorticoid receptor and dendritic branching in the hippocampus of mice. Metab Brain Dis, 2021. 36(8): p. 2223-2233.
36. Yu, Z., et al., Neuroprotective effects of macamide from maca (Lepidium meyenii Walp.) on corticosterone-induced hippocampal impairments through its anti-inflammatory, neurotrophic, and synaptic protection properties. Food Funct, 2021. 12(19): p. 9211-9228.
37. Wang, G., et al., Corticosterone Impairs Hippocampal Neurogenesis and Behaviors through p21-Mediated ROS Accumulation. 2024. 14(3): p. 268.
38. Magariños, A.M., M. Orchinik, and B.S. McEwen, Morphological changes in the hippocampal CA3 region induced by non-invasive glucocorticoid administration: a paradox. Brain Res, 1998. 809(2): p. 314-8.

39. Agnihotri, S.K., et al., PINK1 deficiency is associated with increased deficits of adult hippocampal neurogenesis and lowers the threshold for stress-induced depression in mice. Behav Brain Res, 2019. 363: p. 161-172.
40. Swanson, A.M., et al., Glucocorticoid receptor regulation of action selection and prefrontal cortical dendritic spines. Commun Integr Biol, 2013. 6(6): p. e26068.
41. Bromberg, K.D., R. Iyengar, and J.C. He, Regulation of neurite outgrowth by G(i/o) signaling pathways. Front Biosci, 2008. 13: p. 4544-57.
42. Greene, L.A. and A.S. Tischler, Establishment of a noradrenergic clonal line of rat adrenal pheochromocytoma cells which respond to nerve growth factor. Proc Natl Acad Sci U S A, 1976. 73(7): p. 2424-8.
43. Xie, D., et al., The cellular model for Alzheimer's disease research: PC12 cells. Front Mol Neurosci, 2022. 15: p. 1016559.
44. Terada, K., et al., Inhibition of nerve growth factor-induced neurite outgrowth from PC12 cells by dexamethasone: signaling pathways through the glucocorticoid receptor and phosphorylated Akt and ERK1/2. PLoS One, 2014. 9(3): p. e93223.
45. Li, M., et al., Transcriptome profiles of corticosterone-induced cytotoxicity reveals the involvement of neurite growth-related genes in depression. Psychiatry Research, 2019. 276: p. 79-86.
46. McAllister, A.K., L.C. Katz, and D.C. Lo, Neurotrophins and synaptic plasticity. Annu Rev Neurosci, 1999. 22: p. 295-318.
47. Gao, L., et al., Brain-derived neurotrophic factor in Alzheimer's disease and its pharmaceutical potential. Transl Neurodegener, 2022. 11(1): p. 4.
48. Nieto, R., M. Kukuljan, and H. Silva, BDNF and schizophrenia: from neurodevelopment to neuronal plasticity, learning, and memory. Front Psychiatry, 2013. 4: p. 45.
49. Nair, A. and V.A. Vaidya, Cyclic AMP response element binding protein and brain-derived neurotrophic factor: molecules that modulate our mood? J Biosci, 2006. 31(3): p. 423-34.
50. Jeon, S.J., et al., Oroxylin A increases BDNF production by activation of MAPK-CREB pathway in rat primary cortical neuronal culture. Neurosci Res, 2011. 69(3): p. 214-22.
51. Pugazhenthi, S., et al., Downregulation of CREB expression in Alzheimer's brain and in Aβ-treated rat hippocampal neurons. Mol Neurodegener, 2011. 6: p. 60.
52. Koga, Y., et al., Roles of Cyclic AMP Response Element Binding Activation in the ERK1/2 and p38 MAPK Signalling Pathway in Central Nervous System, Cardiovascular System, Osteoclast Differentiation and Mucin and Cytokine Production. Int J Mol Sci, 2019. 20(6).
53. Mayr, B. and M. Montminy, Transcriptional regulation by the phosphorylation-dependent factor CREB. Nat Rev Mol Cell Biol, 2001. 2(8): p. 599-609.
54. Hazra, S., et al., Reversion of BDNF, Akt and CREB in Hippocampus of Chronic Unpredictable Stress Induced Rats: Effects of Phytochemical, Bacopa Monnieri. Psychiatry Investig, 2017. 14(1): p. 74-80.
55. Xiao, L., et al., Effects of different CMS on behaviors, BDNF/CREB/Bcl-2 expression in rat hippocampus. Biomedicine & Aging Pathology, 2011. 1(3): p. 138-146.
56. Di Liberto, V., et al., Anxiolytic effects of muscarinic acetylcholine receptors agonist oxotremorine in chronically stressed rats and related changes in BDNF and FGF2 levels in the hippocampus and prefrontal cortex. Psychopharmacology (Berl), 2017. 234(4): p. 559-573.
57. Dwivedi, Y., H.S. Rizavi, and G.N. Pandey, Antidepressants reverse corticosterone-mediated decrease in brain-derived neurotrophic factor expression: differential regulation

of specific exons by antidepressants and corticosterone. Neuroscience, 2006. 139(3): p. 1017-29.
58. Gourley, S.L., et al., Acute hippocampal brain-derived neurotrophic factor restores motivational and forced swim performance after corticosterone. Biol Psychiatry, 2008. 64(10): p. 884-90.
59. Tang, Y., et al., Berberine exerts antidepressant effects *in vivo* and *in vitro* through the PI3K/AKT/CREB/BDNF signaling pathway. Biomed Pharmacother, 2024. 170: p. 116012.
60. Lee, W.J., et al., Taurine and Ginsenoside Rf Induce BDNF Expression in SH-SY5Y Cells: A Potential Role of BDNF in Corticosterone-Triggered Cellular Damage. Molecules, 2020. 25(12).
61. Pandya, C., et al., Glucocorticoid regulates TrkB protein levels via c-Cbl dependent ubiquitination: a decrease in c-Cbl mRNA in the prefrontal cortex of suicide subjects. Psychoneuroendocrinology, 2014. 45: p. 108-18.
62. Juszczyk, G., et al., Chronic Stress and Oxidative Stress as Common Factors of the Pathogenesis of Depression and Alzheimer's Disease: The Role of Antioxidants in Prevention and Treatment. Antioxidants (Basel), 2021. 10(9).
63. Herbet, M., et al., Chronic Variable Stress Is Responsible for Lipid and DNA Oxidative Disorders and Activation of Oxidative Stress Response Genes in the Brain of Rats. Oxid Med Cell Longev, 2017. 2017: p. 7313090.
64. Bello-Medina, P.C., et al., Oxidative stress, the immune response, synaptic plasticity, and cognition in transgenic models of Alzheimer disease. Neurologia (Engl Ed), 2022. 37(8): p. 682-690.
65. Halliwell, B. and J.M. Gutteridge, Free radicals in biology and medicine. 2015: Oxford university press, USA.
66. Kühlbrandt, W., Structure and function of mitochondrial membrane protein complexes. BMC Biol, 2015. 13: p. 89.
67. Liu, Y., G. Fiskum, and D. Schubert, Generation of reactive oxygen species by the mitochondrial electron transport chain. J Neurochem, 2002. 80(5): p. 780-7.
68. Muller, F.L., Y. Liu, and H. Van Remmen, Complex III releases superoxide to both sides of the inner mitochondrial membrane. J Biol Chem, 2004. 279(47): p. 49064-73.
69. Cash, T.P., Y. Pan, and M.C. Simon, Reactive oxygen species and cellular oxygen sensing. Free Radical Biology and Medicine, 2007. 43(9): p. 1219-1225.
70. Pitkanen, S. and B.H. Robinson, Mitochondrial complex I deficiency leads to increased production of superoxide radicals and induction of superoxide dismutase. J Clin Invest, 1996. 98(2): p. 345-51.
71. Pastor, N., et al., A detailed interpretation of OH radical footprints in a TBP-DNA complex reveals the role of dynamics in the mechanism of sequence-specific binding. J Mol Biol, 2000. 304(1): p. 55-68.
72. Spiers, J.G., et al., Activation of the hypothalamic-pituitary-adrenal stress axis induces cellular oxidative stress. Front Neurosci, 2014. 8: p. 456.
73. Nayernia, Z., V. Jaquet, and K.H. Krause, New insights on NOX enzymes in the central nervous system. Antioxid Redox Signal, 2014. 20(17): p. 2815-37.
74. Le Belle, J.E., et al., Proliferative neural stem cells have high endogenous ROS levels that regulate self-renewal and neurogenesis in a PI3K/Akt-dependant manner. Cell Stem Cell, 2011. 8(1): p. 59-71.

75. Kim, Y.E. and J. Kim, ROS-Scavenging Therapeutic Hydrogels for Modulation of the Inflammatory Response. ACS Appl Mater Interfaces, 2021.
76. Phaniendra, A., D.B. Jestadi, and L. Periyasamy, Free radicals: properties, sources, targets, and their implication in various diseases. Indian J Clin Biochem, 2015. 30(1): p. 11-26.
77. Schrader, M. and H.D. Fahimi, Peroxisomes and oxidative stress. Biochim Biophys Acta, 2006. 1763(12): p. 1755-66.
78. Liang, J., et al., Reactive oxygen species and ovarian diseases: Antioxidant strategies. Redox Biol, 2023. 62: p. 102659.
79. Valko, M., et al., Free radicals and antioxidants in normal physiological functions and human disease. Int J Biochem Cell Biol, 2007. 39(1): p. 44-84.
80. Stevenson, J.R., et al., Oxytocin prevents dysregulation of the acute stress response and glucocorticoid-induced oxidative stress in chronically isolated prairie voles. Psychoneuroendocrinology, 2023. 153: p. 106121.
81. Spiers, J.G., et al., Dysregulation of stress systems and nitric oxide signaling underlies neuronal dysfunction in Alzheimer's disease. Free Radic Biol Med, 2019. 134: p. 468-483.
82. Liu, T., et al., A Meta-Analysis of Oxidative Stress Markers in Depression. PLoS One, 2015. 10(10): p. e0138904.
83. Ba, X. and I. Boldogh, 8-Oxoguanine DNA glycosylase 1: Beyond repair of the oxidatively modified base lesions. Redox Biol, 2018. 14: p. 669-678.
84. Maher, P. and D. Schubert, Signaling by reactive oxygen species in the nervous system. Cell Mol Life Sci, 2000. 57(8-9): p. 1287-305.
85. Di Domenico, F., A. Tramutola, and D.A. Butterfield, Role of 4-hydroxy-2-nonenal (HNE) in the pathogenesis of alzheimer disease and other selected age-related neurodegenerative disorders. Free Radic Biol Med, 2017. 111: p. 253-261.
86. Zhang, W., S. Xiao, and D.U. Ahn, Protein oxidation: basic principles and implications for meat quality. Crit Rev Food Sci Nutr, 2013. 53(11): p. 1191-201.
87. Tang, V., et al., Glucocorticoids increase protein carbonylation and mitochondrial dysfunction. 2013: p. 709-715.
88. Wang, Y., et al., Protective effects of ginsenoside Rg1 on chronic restraint stress induced learning and memory impairments in male mice. Pharmacol Biochem Behav, 2014. 120: p. 73-81.
89. Seo, J.S., et al., NADPH oxidase mediates depressive behavior induced by chronic stress in mice. J Neurosci, 2012. 32(28): p. 9690-9.
90. Pérez-Nievas, B.G., et al., Corticosterone as a marker of susceptibility to oxidative/nitrosative cerebral damage after stress exposure in rats. Psychoneuroendocrinology, 2007. 32(6): p. 703-11.
91. Zhang, Y., et al., Effects of hydrogen-rich water on depressive-like behavior in mice. Sci Rep, 2016. 6: p. 23742.
92. Madrigal, J.L., et al., Glutathione depletion, lipid peroxidation and mitochondrial dysfunction are induced by chronic stress in rat brain. Neuropsychopharmacology, 2001. 24(4): p. 420-9.
93. Rezin, G.T., et al., Inhibition of mitochondrial respiratory chain in brain of rats subjected to an experimental model of depression. Neurochem Int, 2008. 53(6-8): p. 395-400.
94. Sato, H., et al., Glucocorticoid Generates ROS to Induce Oxidative Injury in the Hippocampus, Leading to Impairment of Cognitive Function of Rats. J Clin Biochem Nutr, 2010. 47(3): p. 224-32.

95. da Silva Souza, S.V., et al., Effects of cholecalciferol on behavior and production of reactive oxygen species in female mice subjected to corticosterone-induced model of depression. Naunyn Schmiedebergs Arch Pharmacol, 2020. 393(1): p. 111-120.
96. You, J.M., et al., Mechanism of glucocorticoid-induced oxidative stress in rat hippocampal slice cultures. Can J Physiol Pharmacol, 2009. 87(6): p. 440-7.
97. Mutsaers, H.A. and R. Tofighi, Dexamethasone enhances oxidative stress-induced cell death in murine neural stem cells. Neurotox Res, 2012. 22(2): p. 127-37.
98. Che, Y., et al., Chronic unpredictable stress impairs endogenous antioxidant defense in rat brain. Neurosci Lett, 2015. 584: p. 208-13.
99. Khan, K., A.K. Najmi, and M. Akhtar, A Natural Phenolic Compound Quercetin Showed the Usefulness by Targeting Inflammatory, Oxidative Stress Markers and Augment 5-HT Levels in One of the Animal Models of Depression in Mice. Drug Res (Stuttg), 2019. 69(7): p. 392-400.
100. Salehpour, F., et al., Near-infrared photobiomodulation combined with coenzyme Q(10) for depression in a mouse model of restraint stress: reduction in oxidative stress, neuroinflammation, and apoptosis. Brain Res Bull, 2019. 144: p. 213-222.
101. McIntosh, L.J., K.E. Hong, and R.M. Sapolsky, Glucocorticoids may alter antioxidant enzyme capacity in the brain: baseline studies. Brain Res, 1998. 791(1-2): p. 209-14.
102. Silva, M.C., et al., Evidence for protective effect of lipoic acid and desvenlafaxine on oxidative stress in a model depression in mice. Prog Neuropsychopharmacol Biol Psychiatry, 2016. 64: p. 142-8.
103. Lopes, I.S., et al., Riparin II ameliorates corticosterone-induced depressive-like behavior in mice: Role of antioxidant and neurotrophic mechanisms. Neurochem Int, 2018. 120: p. 33-42.
104. Cvijić, G., et al., The effect of glucocorticoids on the activity of monoamine oxidase, copper-zinc superoxide dismutase and catalase in the rat hypothalamus. Funct Neurol, 1995. 10(4-5): p. 175-81.
105. Jin, W., et al., Protective effect of pig brain polypeptides against corticosterone-induced oxidative stress, inflammatory response, and apoptosis in PC12 cells. Biomedicine & Pharmacotherapy, 2019. 115: p. 108890.
106. Chiu, J.-H., et al., Protective effects of camellia oil and gac oil against corticosterone-induced neurotoxicity in Neuro-2a cells. Food Bioscience, 2023. 56: p. 103225.
107. Zafir, A. and N. Banu, Modulation of *in vivo* oxidative status by exogenous corticosterone and restraint stress in rats. Stress, 2009. 12(2): p. 167-77.
108. Aboul-Fotouh, S., Coenzyme Q10 displays antidepressant-like activity with reduction of hippocampal oxidative/nitrosative DNA damage in chronically stressed rats. Pharmacol Biochem Behav, 2013. 104: p. 105-12.
109. Camargo, A., et al., Cholecalciferol counteracts depressive-like behavior and oxidative stress induced by repeated corticosterone treatment in mice. Eur J Pharmacol, 2018. 833: p. 451-461.
110. Watson, W.H., et al., Thioredoxin and its role in toxicology. Toxicol Sci, 2004. 78(1): p. 3-14.
111. Yang, B., et al., Thioredoxin (Trx): A redox target and modulator of cellular senescence and aging-related diseases. Redox Biol, 2024. 70: p. 103032.
112. Choi, E.H. and S.J. Park, TXNIP: A key protein in the cellular stress response pathway and a potential therapeutic target. Exp Mol Med, 2023. 55(7): p. 1348-1356.

113. Weichsel, A., et al., Crystal structures of reduced, oxidized, and mutated human thioredoxins: evidence for a regulatory homodimer. Structure, 1996. 4(6): p. 735-751.
114. Watson, W.H., et al., Redox potential of human thioredoxin 1 and identification of a second dithiol/disulfide motif. J Biol Chem, 2003. 278(35): p. 33408-15.
115. Mitchell, D.A. and M.A. Marletta, Thioredoxin catalyzes the S-nitrosation of the caspase-3 active site cysteine. Nat Chem Biol, 2005. 1(3): p. 154-8.
116. Casagrande, S., et al., Glutathionylation of human thioredoxin: a possible crosstalk between the glutathione and thioredoxin systems. Proc Natl Acad Sci U S A, 2002. 99(15): p. 9745-9.
117. Bauer, H., S.M. Kanzok, and R.H. Schirmer, Thioredoxin-2 but not thioredoxin-1 is a substrate of thioredoxin peroxidase-1 from Drosophila melanogaster: isolation and characterization of a second thioredoxin in D. Melanogaster and evidence for distinct biological functions of Trx-1 and Trx-2. J Biol Chem, 2002. 277(20): p. 17457-63.
118. Hasan, A.A., et al., The Thioredoxin System of Mammalian Cells and Its Modulators. Biomedicines, 2022. 10(7).
119. Qayyum, N., et al., Role of Thioredoxin-Interacting Protein in Diseases and Its Therapeutic Outlook. Int J Mol Sci, 2021. 22(5).
120. Hwang, J., et al., Crystal structure of fully oxidized human thioredoxin. Biochem Biophys Res Commun, 2015. 467(2): p. 218-22.
121. Hwang, J., et al., The structural basis for the negative regulation of thioredoxin by thioredoxin-interacting protein. Nat Commun, 2014. 5: p. 2958.
122. Wang, Y., J. Yang, and J. Yi, Redox sensing by proteins: oxidative modifications on cysteines and the consequent events. Antioxid Redox Signal, 2012. 16(7): p. 649-57.
123. Gu, L. and R.A. Robinson, Proteomic approaches to quantify cysteine reversible modifications in aging and neurodegenerative diseases. Proteomics Clin Appl, 2016. 10(12): p. 1159-1177.
124. Brandes, N., S. Schmitt, and U. Jakob, Thiol-based redox switches in eukaryotic proteins. Antioxid Redox Signal, 2009. 11(5): p. 997-1014.
125. Wang, Y., et al., Protein cysteine S-nitrosylation inhibits vesicular uptake of neurotransmitters. Neuroscience, 2015. 311: p. 374-81.
126. Abrams, A.J., A. Farooq, and G. Wang, S-nitrosylation of ApoE in Alzheimer's disease. Biochemistry, 2011. 50(17): p. 3405-7.
127. Wang, Y., et al., Upregulation of Thioredoxin-Interacting Protein in Brain of Amyloid-β Protein Precursor/Presenilin 1 Transgenic Mice and Amyloid-β Treated Neuronal Cells. J Alzheimers Dis, 2019. 72(1): p. 139-150.
128. Li, H., et al., Small changes huge impact: the role of thioredoxin 1 in the regulation of apoptosis by S-nitrosylation. Acta Biochim Biophys Sin (Shanghai), 2013. 45(3): p. 153-61.
129. Li, Y.R., H. Zhu, and I. Danelisen, Role of Peroxiredoxins in Protecting Against Cardiovascular and Related Disorders. Cardiovasc Toxicol, 2020. 20(5): p. 448-453.
130. Rhee, S.G., et al., Peroxiredoxin functions as a peroxidase and a regulator and sensor of local peroxides. J Biol Chem, 2012. 287(7): p. 4403-10.
131. Chae, H.Z., T.B. Uhm, and S.G. Rhee, Dimerization of thiol-specific antioxidant and the essential role of cysteine 47. Proc Natl Acad Sci U S A, 1994. 91(15): p. 7022-6.
132. Chae, H.Z., S.J. Chung, and S.G. Rhee, Thioredoxin-dependent peroxide reductase from yeast. J Biol Chem, 1994. 269(44): p. 27670-8.

133. Song, I.K., et al., Degradation of Redox-Sensitive Proteins including Peroxiredoxins and DJ-1 is Promoted by Oxidation-induced Conformational Changes and Ubiquitination. Sci Rep, 2016. 6: p. 34432.
134. Ichijo, H., et al., Induction of apoptosis by ASK1, a mammalian MAPKKK that activates SAPK/JNK and p38 signaling pathways. Science, 1997. 275(5296): p. 90-4.
135. Gotoh, Y. and J.A. Cooper, Reactive oxygen species- and dimerization-induced activation of apoptosis signal-regulating kinase 1 in tumor necrosis factor-alpha signal transduction. J Biol Chem, 1998. 273(28): p. 17477-82.
136. Nishitoh, H., et al., ASK1 is essential for endoplasmic reticulum stress-induced neuronal cell death triggered by expanded polyglutamine repeats. Genes Dev, 2002. 16(11): p. 1345-55.
137. Saitoh, M., et al., Mammalian thioredoxin is a direct inhibitor of apoptosis signal-regulating kinase (ASK) 1. Embo j, 1998. 17(9): p. 2596-606.
138. Nishida, K. and K. Otsu, The role of apoptosis signal-regulating kinase 1 in cardiomyocyte apoptosis. Antioxid Redox Signal, 2006. 8(9-10): p. 1729-36.
139. Tobiume, K., et al., ASK1 is required for sustained activations of JNK/p38 MAP kinases and apoptosis. EMBO Rep, 2001. 2(3): p. 222-8.
140. Zhang, R., et al., Thioredoxin-2 inhibits mitochondria-located ASK1-mediated apoptosis in a JNK-independent manner. Circ Res, 2004. 94(11): p. 1483-91.
141. Liu, Y. and W. Min, Thioredoxin promotes ASK1 ubiquitination and degradation to inhibit ASK1-mediated apoptosis in a redox activity-independent manner. Circ Res, 2002. 90(12): p. 1259-66.
142. Tobiume, K., M. Saitoh, and H. Ichijo, Activation of apoptosis signal-regulating kinase 1 by the stress-induced activating phosphorylation of pre-formed oligomer. J Cell Physiol, 2002. 191(1): p. 95-104.
143. Matsuzawa, A., et al., ROS-dependent activation of the TRAF6-ASK1-p38 pathway is selectively required for TLR4-mediated innate immunity. Nat Immunol, 2005. 6(6): p. 587-92.
144. Song, J., et al., Apoptosis signal regulating kinase 1 (ASK1): potential as a therapeutic target for Alzheimer's disease. Int J Mol Sci, 2014. 15(2): p. 2119-29.
145. Hayakawa, R., et al., Therapeutic targets in the ASK1-dependent stress signaling pathways. Proc Jpn Acad Ser B Phys Biol Sci, 2012. 88(8): p. 434-53.
146. Argyrou, A. and J.S. Blanchard, Flavoprotein Disulfide Reductases: Advances in Chemistry and Function, in Progress in Nucleic Acid Research and Molecular Biology. 2004, Academic Press. p. 89-142.
147. Lu, J. and A. Holmgren, The thioredoxin antioxidant system. Free Radic Biol Med, 2014. 66: p. 75-87.
148. Williams, C.H., et al., Thioredoxin reductase two modes of catalysis have evolved. Eur J Biochem, 2000. 267(20): p. 6110-7.
149. Lu, J. and A. Holmgren, Selenoproteins*. Journal of Biological Chemistry, 2009. 284(2): p. 723-727.
150. Holmgren, A. and J. Lu, Thioredoxin and thioredoxin reductase: current research with special reference to human disease. Biochem Biophys Res Commun, 2010. 396(1): p. 120-4.
151. Jastrząb, A. and E. Skrzydlewska, Thioredoxin-dependent system. Application of inhibitors. J Enzyme Inhib Med Chem, 2021. 36(1): p. 362-371.

152. Sun, H., et al., An update on the role of thioredoxin-interacting protein in diabetic kidney disease: A mini review. Front Med (Lausanne), 2023. 10: p. 1153805.
153. Pan, M., et al., TXNIP: A Double-Edged Sword in Disease and Therapeutic Outlook. Oxid Med Cell Longev, 2022. 2022: p. 7805115.
154. Chutkow, W.A. and R.T. Lee, Thioredoxin regulates adipogenesis through thioredoxin-interacting protein (Txnip) protein stability. J Biol Chem, 2011. 286(33): p. 29139-29145.
155. Bai, J., et al., Critical roles of thioredoxin in nerve growth factor-mediated signal transduction and neurite outgrowth in PC12 cells. J Neurosci, 2003. 23(2): p. 503-9.
156. Horstkorte, R., et al., N-Propionylmannosamine-induced over-expression and secretion of thioredoxin leads to neurite outgrowth of PC12 cells. Biochem Biophys Res Commun, 2010. 395(3): p. 296-300.
157. Alejandra Llanes-Cuesta, M., et al., Redox Protein Thioredoxin Mediates Neurite Outgrowth in Primary Cultured Mouse Cerebral Cortical Neurons. Neuroscience, 2024. 537: p. 165-173.
158. Zhang, X., et al., Trx-1 ameliorates learning and memory deficits in MPTP-induced Parkinson's disease model in mice. Free Radic Biol Med, 2018. 124: p. 380-387.
159. Hirota, K., et al., Nucleoredoxin, glutaredoxin, and thioredoxin differentially regulate NF-kappaB, AP-1, and CREB activation in HEK293 cells. Biochem Biophys Res Commun, 2000. 274(1): p. 177-82.
160. Kong, L., et al., Neuroprotective effect of overexpression of thioredoxin on photoreceptor degeneration in Tubby mice. Neurobiol Dis, 2010. 38(3): p. 446-55.
161. Song, Y., et al., Perilla aldehyde attenuates CUMS-induced depressive-like behaviors via regulating TXNIP/TRX/NLRP3 pathway in rats. Life Sci, 2018. 206: p. 117-124.
162. Kim, M.H. and Y.H. Leem, Neurogenic effect of exercise via the thioredoxin-1/ extracellular regulated kinase/β-catenin signaling pathway mediated by β2-adrenergic receptors in chronically stressed dentate gyrus. J Exerc Nutrition Biochem, 2019. 23(3): p. 13-21.
163. Zhou, H., et al., Increased thioredoxin-interacting protein in brain of mice exposed to chronic stress. Prog Neuropsychopharmacol Biol Psychiatry, 2019. 88: p. 320-326.
164. Bharti, V., et al., Glucocorticoid Upregulates Thioredoxin-interacting Protein in Cultured Neuronal Cells. Neuroscience, 2018. 384: p. 375-383.
165. Wang, J.F., J.E. Azzam, and L.T. Young, Valproate inhibits oxidative damage to lipid and protein in primary cultured rat cerebrocortical cells. Neuroscience, 2003. 116(2): p. 485-9.
166. Hensley, K., Detection of protein carbonyls by means of biotin hydrazide-streptavidin affinity methods. Methods Mol Biol, 2009. 536: p. 457-62.
167. Kaja, S., et al., Quantification of Lactate Dehydrogenase for Cell Viability Testing Using Cell Lines and Primary Cultured Astrocytes. Curr Protoc Toxicol, 2017. 72: p. 2.26.1-2.26.10.
168. Kumar, S. and A.C. Mondal, Neuroprotective, Neurotrophic and Anti-oxidative Role of Bacopa monnieri on CUS Induced Model of Depression in Rat. Neurochem Res, 2016. 41(11): p. 3083-3094.
169. Liu, D., et al., Resveratrol reverses the effects of chronic unpredictable mild stress on behavior, serum corticosterone levels and BDNF expression in rats. Behavioural Brain Research, 2014. 264: p. 9-16.
170. Jin, P., et al., Antidepressant-like effects of oleoylethanolamide in a mouse model of chronic unpredictable mild stress. Pharmacol Biochem Behav, 2015. 133: p. 146-54.

171. Chhillar, R. and D. Dhingra, Antidepressant-like activity of gallic acid in mice subjected to unpredictable chronic mild stress. Fundam Clin Pharmacol, 2013. 27(4): p. 409-18.
172. Dhingra, D. and A. Bhankher, Behavioral and biochemical evidences for antidepressant-like activity of palmatine in mice subjected to chronic unpredictable mild stress. Pharmacological Reports, 2014. 66(1): p. 1-9.
173. Wang, Z., et al., Thioredoxin-interacting protein (txnip) is a glucocorticoid-regulated primary response gene involved in mediating glucocorticoid-induced apoptosis. Oncogene, 2006. 25(13): p. 1903-13.
174. He, X. and Q. Ma, Redox regulation by nuclear factor erythroid 2-related factor 2: gatekeeping for the basal and diabetes-induced expression of thioredoxin-interacting protein. Mol Pharmacol, 2012. 82(5): p. 887-97.
175. Minn, A.H., C. Hafele, and A. Shalev, Thioredoxin-interacting protein is stimulated by glucose through a carbohydrate response element and induces beta-cell apoptosis. Endocrinology, 2005. 146(5): p. 2397-405.
176. Stoltzman, C.A., et al., Glucose sensing by MondoA:Mlx complexes: a role for hexokinases and direct regulation of thioredoxin-interacting protein expression. Proc Natl Acad Sci U S A, 2008. 105(19): p. 6912-7.
177. Yu, F.X., et al., Adenosine-containing molecules amplify glucose signaling and enhance txnip expression. Mol Endocrinol, 2009. 23(6): p. 932-42.
178. Martín-Hernández, D., et al., Modulation of the antioxidant nuclear factor (erythroid 2-derived)-like 2 pathway by antidepressants in rats. Neuropharmacology, 2016. 103: p. 79-91.
179. Abuelezz, S.A. and N. Hendawy, Insights into the potential antidepressant mechanisms of cilostazol in chronically restraint rats: impact on the Nrf2 pathway. Behav Pharmacol, 2018. 29(1): p. 28-40.
180. Mendez-David, I., et al., Nrf2-signaling and BDNF: A new target for the antidepressant-like activity of chronic fluoxetine treatment in a mouse model of anxiety/depression. Neurosci Lett, 2015. 597: p. 121-6.
181. Spindel, O.N., C. World, and B.C. Berk, Thioredoxin interacting protein: redox dependent and independent regulatory mechanisms. Antioxid Redox Signal, 2012. 16(6): p. 587-96.
182. Chong, C.R., et al., Thioredoxin-interacting protein: pathophysiology and emerging pharmacotherapeutics in cardiovascular disease and diabetes. Cardiovasc Drugs Ther, 2014. 28(4): p. 347-60.
183. Zhou, J. and W.J. Chng, Roles of thioredoxin binding protein (TXNIP) in oxidative stress, apoptosis and cancer. Mitochondrion, 2013. 13(3): p. 163-9.
184. Kwatra, M., et al., Lipopolysaccharide exacerbates chronic restraint stress-induced neurobehavioral deficits: Mechanisms by redox imbalance, ASK1-related apoptosis, autophagic dysregulation. J Psychiatr Res, 2021. 144: p. 462-482.
185. Paladini, M.S., et al., Behavioral and molecular effects of the antipsychotic drug blonanserin in the chronic mild stress model. Pharmacol Res, 2021. 163: p. 105330.
186. Giles, N.M., et al., Metal and redox modulation of cysteine protein function. Chem Biol, 2003. 10(8): p. 677-93.
187. Møller, I.M., A. Rogowska-Wrzesinska, and R.S. Rao, Protein carbonylation and metal-catalyzed protein oxidation in a cellular perspective. J Proteomics, 2011. 74(11): p. 2228-42.

188. Zhang, X., et al., Mechanisms Underlying H2O2-Evoked Carbonyl Modification of Cytoskeletal Protein and Axon Injury in PC-12 Cells. Cell Physiol Biochem, 2018. 48(3): p. 1088-1098.
189. Lenaz, G., The mitochondrial production of reactive oxygen species: mechanisms and implications in human pathology. IUBMB Life, 2001. 52(3-5): p. 159-64.
190. Abelaira, H.M., et al., Effects of lamotrigine on behavior, oxidative parameters and signaling cascades in rats exposed to the chronic mild stress model. Neurosci Res, 2013. 75(4): p. 324-30.
191. Mohammadi, H.S., et al., Chronic administration of quercetin prevent spatial learning and memory deficits provoked by chronic stress in rats. Behav Brain Res, 2014. 270: p. 196-205.
192. Wang, C., et al., Oxidative parameters in the rat brain of chronic mild stress model for depression: relation to anhedonia-like responses. J Membr Biol, 2012. 245(11): p. 675-81.
193. Lucca, G., et al., Effects of chronic mild stress on the oxidative parameters in the rat brain. Neurochem Int, 2009. 54(5-6): p. 358-62.
194. Kawarazaki, Y., H. Ichijo, and I. Naguro, Apoptosis signal-regulating kinase 1 as a therapeutic target. Expert Opin Ther Targets, 2014. 18(6): p. 651-64.
195. Conrad, C.D., What is the functional significance of chronic stress-induced CA3 dendritic retraction within the hippocampus? Behav Cogn Neurosci Rev, 2006. 5(1): p. 41-60.
196. Lesuisse, C. and L.J. Martin, Long-term culture of mouse cortical neurons as a model for neuronal development, aging, and death. J Neurobiol, 2002. 51(1): p. 9-23.
197. Dong, W., et al., Mitochondrial dysfunction in long-term neuronal cultures mimics changes with aging. Med Sci Monit, 2011. 17(4): p. Br91-6.
198. Xiao, X.Q., J.W. Yang, and X.C. Tang, Huperzine A protects rat pheochromocytoma cells against hydrogen peroxide-induced injury. Neurosci Lett, 1999. 275(2): p. 73-6.
199. Khodagholi, F., et al., 3-Thiomethyl-5,6-(dimethoxyphenyl)-1,2,4-triazine improves neurite outgrowth and modulates MAPK phosphorylation and HSPs expression in H2O2-exposed PC12 cells. Toxicol In Vitro, 2012. 26(6): p. 907-14.
200. Kim, H., et al. Gongjin-Dan Enhances Neurite Outgrowth of Cortical Neuron by Ameliorating H2O2-Induced Oxidative Damage via Sirtuin1 Signaling Pathway. Nutrients, 2021. 13, DOI: 10.3390/nu13124290.
201. He, W., et al., Sonic hedgehog promotes neurite outgrowth of cortical neurons under oxidative stress: Involving of mitochondria and energy metabolism. Exp Cell Res, 2017. 350(1): p. 83-90.
202. Nagashima, D., et al., Effect of Coriander on H2O2-induced Oxidative Stress in PC12 Cells. J Clin Med Res, 2022. 4(3): p. 1-10.
203. Huang, L.T., et al., Maternal deprivation stress exacerbates cognitive deficits in immature rats with recurrent seizures. Epilepsia, 2002. 43(10): p. 1141-8.
204. Song, L., et al., Impairment of the spatial learning and memory induced by learned helplessness and chronic mild stress. Pharmacol Biochem Behav, 2006. 83(2): p. 186-93.
205. Murakami, S., et al., Chronic stress, as well as acute stress, reduces BDNF mRNA expression in the rat hippocampus but less robustly. Neurosci Res, 2005. 53(2): p. 129-39.
206. Xu, H., et al., Synergetic effects of quetiapine and venlafaxine in preventing the chronic restraint stress-induced decrease in cell proliferation and BDNF expression in rat hippocampus. Hippocampus, 2006. 16(6): p. 551-9.

207. Kumamaru, E., et al., Glucocorticoid prevents brain-derived neurotrophic factor-mediated maturation of synaptic function in developing hippocampal neurons through reduction in the activity of mitogen-activated protein kinase. Mol Endocrinol, 2008. 22(3): p. 546-58.
208. Bie, N., et al., The Protective Effect of Docosahexaenoic Acid on PC12 Cells in Oxidative Stress Induced by H(2)O(2) through the TrkB-Erk1/2-CREB Pathway. ACS Chem Neurosci, 2021. 12(18): p. 3433-3444.
209. Chen, J., et al., Oxidative stress disrupts the cytoskeleton of spinal motor neurons. Brain Behav, 2023. 13(2): p. e2870.
210. Dotti, C.G., C.A. Sullivan, and G.A. Banker, The establishment of polarity by hippocampal neurons in culture. J Neurosci, 1988. 8(4): p. 1454-68.
211. Kollins, K.M., et al., Dendrites differ from axons in patterns of microtubule stability and polymerization during development. Neural Dev, 2009. 4: p. 26.
212. Banker, G., The Development of Neuronal Polarity: A Retrospective View. J Neurosci, 2018. 38(8): p. 1867-1873.
213. Kempf, M., et al., Tau binds to the distal axon early in development of polarity in a microtubule- and microfilament-dependent manner. J Neurosci, 1996. 16(18): p. 5583-92.
214. Tsai, S.Q., et al., GUIDE-seq enables genome-wide profiling of off-target cleavage by CRISPR-Cas nucleases. Nat Biotechnol, 2015. 33(2): p. 187-197.
215. Tsai, S.Q., et al., CIRCLE-seq: a highly sensitive *in vitro* screen for genome-wide CRISPR-Cas9 nuclease off-targets. Nat Methods, 2017. 14(6): p. 607-614.
216. Guo, C., et al., Off-target effects in CRISPR/Cas9 gene editing. Front Bioeng Biotechnol, 2023. 11: p. 1143157.
217. Mehta, V., A. Parashar, and M. Udayabanu, Quercetin prevents chronic unpredictable stress induced behavioral dysfunction in mice by alleviating hippocampal oxidative and inflammatory stress. Physiol Behav, 2017. 171: p. 69-78.
218. Antunes, M. and G. Biala, The novel object recognition memory: neurobiology, test procedure, and its modifications. Cogn Process, 2012. 13(2): p. 93-110.